Title

Heterogeneity in Ribosomal RNA Base Modifications Modulate Lipid Metabolic Flux to Maintain a Tumor Suppressive Program

Author

Contreras, Adrian

Publication Date

2016

Peer reviewed|Thesis/dissertation

Heterogeneity in Ribosomal RNA Base Modifications Modulate Lipid Metabolic Flux to Maintain a Tumor Suppressive Program

by

Adrian Reynol Contreras

DISSERTATION

Submitted in partial satisfaction of the requirements for the degree of

DOCTOR OF PHILOSOPHY

in

Biochemistry and Molecular Biology

in the

GRADUATE DIVISION

of the

UNIVERSITY OF CALIFORNIA, SAN FRANCISCO

Acknowledgements

This work could not have been done without the support of countless people, some of whom I would like to thank here. First and foremost, I would like to thank my graduate advisor, **Dr. Davide Ruggero**, for years of support, mentorship, and scientific training. I joined Davide's lab during my second year of graduate school after I decided to switch labs in order to pursue cancer research. Davide's dedication and excitement for science were evident and contagious the first time I met him, and his support and diligence for science has never wavered over the years. Among the numerous things that I admire and appreciate from Davide is his constant support and guidance towards my research and graduate training. Davide is always motivating me to think bigger, ask novel questions that will expand and contribute to the current research filed, but most importantly to do good quality science and think critically about my data. Any scientific success that I may have in the future will be due to the years that I spent under his mentorship. Working with Davide gave me the great opportunity to collaborate with **Dr. Maria Barna**. Maria's deep scientific knowledge and critical thinking have been invaluable in helping to direct my research project. Working alongside with Davide and Maria has given me a clear example of the tremendous impact two passionate and dedicated people can have when they work together to solve a problem.

Being in Davide's lab gave me the opportunity to work with a tremendous group of intelligent, passionate, dedicated and hardworking scientist. Every member of the Ruggero lab that I had the pleasure to know during my time in the lab has contributed directly or indirectly to my graduate training and project. In particular I would like to acknowledge **Cristian Bellodi** and **Mary McMahon**, for going the extra mile with the amount of

mentorship and guidance they have giving me. Their passion, creativity, tenacity, and kindness have always motivated me to be a better scientist. I also want to thank **Craig Stumpf** and **Tom Cunningham** for always taking time to discuss my research and provide valuable guidance. In addition, I am grateful for the opportunity to work with and interact with **Craig Forester** and **Andrew Hsieh**, and for always reminding me about the positive impact that our science can have in the lives of patients. I would also like to thank **Morgan Truitt** and **Xiaming Pang** for helpful and enjoyable discussions about science and life in general. Finally, I would like to express my gratitude to **Kimhouy Tong** and **Christine Milentis** for all their hard work and help with fellowships and administrative support which allowed me to focus on science.

I must also thank the members of my thesis committee, **Dr. Kevan Shokat** and **Dr. Robert Blelloch**, who have given me invaluable guidance and support during my graduate training, which was critical for my success. I also want to express my gratitude to **Dr. Jayanta Debnath** and **Dr. David Morgan** for believing in me and always making sure I was advancing in my graduate studies. In addition, I am grateful for the wonderful support staff of the Tetrad program. In particular **Danny Dam**, **Billy Luh**, **Rachel Mozesson**, and **Toni Hurley** for making my life as a graduate student easier and helping with multiple issues such as housing and thesis requirements. They are like an oasis in the desert for a stressed graduate student.

Finally, I would like to thank my beautiful family. There are so many things I can say about the positive impact they have had in my life that will exceed the pages of this dissertation. Therefore, I will keep it short by simply saying that my parents and my siblings have always been my ultimate role models. Their passion, hard work, tenacity, and

wisdom have always motivated me to give my best in life. My family has always kept my mind and my heart healthy, brave, and positive. Everything that is good in me is a reflection of their love.

Contributions

The abstract, chapter 2, and chapter 4 are in part taken form a manuscript I co-authored with C. Bellodi, M. McMahon, D. Juliano, N. Kopmar, T. Nakamura, D. Maltby, A. Burlingame, A. Savage, A. Shimamura, and D. Ruggero published in *Cell Reports*. C. Bellodi and M. McMahon contributed equally to this work. C. Bellodi and M. McMahon designed and performed research, analyzed data, and wrote the manuscript. A. Contreras, D. Juliano, N. Kopmar, T. Nakamura, D. Maltby, designed and performed research, and analyzed data. A. Burlingame, A. Savage, A. Shimamura, and D. Ruggero desinged research and wrote the manuscript.

> Bellodi, C., McMahon, M., Contreras, A., Juliano, D., Kopmar, N., Nakamura, T., Maltby, D., Burlingame, A., Savage, S.A., Shimamura, A*., et al.* (2013). H/ACA Small RNA Dysfunctions in Disease Reveal Key Roles for Noncoding RNA Modifications in Hematopoietic Stem Cell Differentiation. Cell Rep *3*, 1493-1502.

Chapter 1 is adapted from a review I co-authored with M. McMahon and D. Ruggero published in *Wiley Interdisciplinary Reviews.*

> McMahon, M., Contreras, A., and Ruggero, D. (2015). Small RNAs with big implications: new insights into H/ACA snoRNA function and their role in human disease. Wires Rna *6*, 173-189.

The Abstract, Chapter 3, and Chapter 4 are in part taken from a manuscript currently in preparation for publication entitled “Heterogeneity in Ribosomal RNA base modifications modulates lipid metabolic flux to maintain a tumor suppressive program”. A. Contreras and M. McMahon designed and performed research, analyzed data, and wrote the manuscript. G. Byeon designed and performed research, and analyzed data. C. Forester designed and performed research, and analyzed data. G. Ryan analyzed and diagnosed tissue specimens.

M. Barna designed research, analyzed data, and wrote the manuscript. D. Ruggero designed research, analyzed data, and wrote the manuscript.

Adrian Contreras, Mary McMahon, Gun Byeon, Craig Forester, Ryan Gill, Maria Barna, and Davide Ruggero. Heterogeneity in Ribosomal RNA base modifications modulates lipid metabolic flux to maintain a tumor suppressive program. (Manuscript in preparation).

Abstract

It is now appreciated that both coding and non-coding RNAs contain a large variety of post-transcriptional nucleotide modifications that change the chemical composition of RNA. However, since the discovery of the first RNA nucleotide modification more than fifty years ago, the function of these modifications remains poorly understood. The RNA component of the ribosome, ribosomal RNA (rRNA) is the most abundant type of RNA in all domain of life and contains the highest amount of base modifications, however the function of these modifications and whether they are subject to regulation remains poorly understood. Interestingly, both the complexity of the machinery required to modify rRNA and the number of modifications found within rRNA have significantly increased from Achaea to eukaryotes suggesting that these nucleotide modifications may have evolved additional roles within eukaryotic ribosomes. Intriguingly, several studies demonstrate that both the enzyme responsible for modifying rRNA and the small non-coding RNAs implicated in guiding nucleotide modifications at specific sites are altered in numerous developmental disorders and cancer. These interesting findings raise the question as to whether base modifications within specific clusters of the ribosome harbor previously uncharacterized regulatory potential within the ribosome to mediate various cellular functions in higher eukaryotes.

Pseudouridine (Ψ), the most abundant nucleotide modification on rRNA, is guided by a class of intron-encoded non-coding RNAs termed H/ACA small nucleolar RNAs (snoRNAs) in association with a protein complex harboring the pseudouridine synthase, dyskerin. The *DKC1* gene, encoding dyskerin, is mutated in the multisystem disorder X-linked Dyskeratosis Congenita (X-DC). A central question is whether *DKC1* mutations affect

the stability of H/ACA RNPs including those modifying rRNA. We carried out comprehensive profiling of dyskerin-associated H/ACA RNPs, revealing remarkable heterogeneity in the expression and function of subsets of H/ACA small RNAs in X-DC patient cells. Using a novel mass spectrometry approach, we uncovered single-nucleotide perturbations in dyskerin-guided rRNA Ψ modifications, providing functional readouts of small RNA dysfunction in X-DC. In addition, we identified that, strikingly, the catalytic activity of dyskerin is required for accurate hematopoietic stem cell differentiation. Altogether, these findings reveal that small noncoding RNA dysfunctions may contribute to the pleiotropic manifestation of human disease.

The observation that only specific Ψ residues are affected in X-DC suggests that the position of these nucleotides modification within the ribosome may be important for its activity. Thus, an outstanding question is whether individual pseudouridine modifications influence the ability of the ribosome to translate the transcriptome and more importantly whether the pattern of Ψ modifications on rRNA is differentially regulated. To this end we sought to determine the landscape of H/ACA snoRNA expression during the earliest cellular responses to oncogenic insult such as DNA damage. Unexpectedly, upon profiling H/ACA small RNAs in primary human fibroblasts, we observed coordinated regulation of specific subsets of H/ACA snoRNAs guiding modifications within similar regions of rRNA following DNA damage. The observed coordinated regulation in H/ACA snoRNA expression is functionally important as we observed a corresponding change in site-specific rRNA Ψ modifications within specific regions of the ribosome. Furthermore, we uncovered that loss of function of one snoRNA, SNORA24, and inhibition of its target rRNA Ψ modifications alters the translation of mRNAs implicated in lipid metabolism both *in vitro* and *in vivo* to

maintain senescence, a stress response that acts as a critical barrier against cellular transformation. Rewired lipid metabolism results in increased lipid synthesis allowing for bypass of senescence in response to DNA damage in primary human fibroblasts and upon activation of oncogenic N-Ras^{V12} in mouse liver. We further probed whether increased lipid synthesis upon loss of SNORA24 contributes to cellular transformation and tumor development. Strikingly, we observe that loss of function of SNORA24 cooperates with oncogenic N-Ras^{V12} to develop hepatocellular carcinoma with significant accumulation of lipid droplets. These exciting findings provide the first evidence that the pattern of RNA base modifications within the ribosome are dynamically regulated in response to oncogenic insult and suggests a new layer of ribosome-mediated control in safeguarding the genome against cellular transformation.

Table of Contents

List of Figures

Chapter Figures

Supplementary Figures

List of Tables

Chapter Tables

Supplementary Tables

Chapter 1: Introduction

The RNA component of the ribosome, ribosomal RNA (rRNA), undergoes numerous site-specific post-transcriptional nucleotide modifications, several of which are located within functionally important regions of the ribosome (Decatur and Fournier, 2002; Maden, 1990). Two predominant types of rRNA modifications involve the addition of a methyl group to the 2'-hydroxyl group of a ribose residue (2'-O-methylation) and the isomerization of uridine to pseudouridine (Ψ), a process known as pseudouridylation. In eukaryotes, both types of modifications occur in the nucleolus and require hundreds of small nucleolar RNAs (snoRNAs) (Maxwell and Fournier, 1995), ranging in length from 60-300 nucleotides, as well as multicomponent protein complexes, collectively referred to as small nucleolar ribonucleoprotein (snoRNP) complexes (Balakin et al., 1996; Kiss, 2001). Importantly, snoRNP-guided nucleotide modifications are extremely conserved and present in two domains of life, archaea and eukaryotes (Watkins and Bohnsack, 2012). The highly conserved box C/D snoRNAs, first described in the late 1980's (Tyc and Steitz, 1989), guide 2'-O-methylation at specific sites on rRNA (Kiss-Laszlo et al., 1996) together with the methyltransferase fibrillarin (Reichow et al., 2007; Tollervey et al., 1991; Watkins et al., 2000). A different highly conserved snoRNP complex, consisting of the pseudouridine synthase dyskerin, additional core proteins including NOP10, NHP2 and GAR1, and small ncRNAs known as box H/ACA snoRNAs, guide pseudouridine modifications at specific sites on rRNA (Ganot et al., 1997a; Lafontaine et al., 1998; Ni et al., 1997; Watkins et al., 1998). There is now a growing appreciation that nucleotide modifications on rRNA may impart regulatory potential to the ribosome, and although the precise function of distinct types of rRNA modifications is not fully understood, there is now a growing realization that the

machinery required for site-specific rRNA modifications is necessary for normal development and is altered in numerous human diseases, particularly cancer (He et al., 2002; Heiss et al., 1998; Marcel et al., 2013; Newton et al., 2003; Valleron et al., 2012a; Valleron et al., 2012b; Williams and Farzaneh, 2012). Together, these findings suggest an important yet perhaps unappreciated functional role of snoRNAs in cellular physiology that, when deregulated, may directly contribute to disease.

Architecture of H/ACA snoRNAs and Their Function in Guiding rRNA Pseudouridine Modifications

H/ACA snoRNAs are distinctly classified from the other major class of snoRNAs, C/D snoRNAs, according to both sequence and structural features (Balakin et al., 1996). The evolutionarily conserved sequences within H/ACA snoRNAs include box H and box ACA motifs and structural elements, such as hairpin structures and pseudouridylation pockets (Balakin et al., 1996; Ganot et al., 1997a; Ganot et al., 1997b) (Figure 1.1). The secondary structure of H/ACA snoRNAs typically consists of 60 to 75 nucleotide-long hairpins that contain a region referred to as a pseudouridylation pocket, where isomerization of the target uridine residue on the substrate RNA occurs (Bortolin et al., 1999). Recently, it has been demonstrated in human cells that the pseudouridine synthase dyskerin, the enzyme responsible for converting uridine to pseudouridine within the H/ACA snoRNP, has a strong preferential association to the H box motif of H/ACA snoRNAs (Kishore et al., 2013). Indeed, these findings support the notion that the H box motif represents a protein recognition signal for H/ACA snoRNP-associated proteins and is required for H/ACA

snoRNA stability as well as biogenesis of a functionally active H/ACA snoRNP complex (Ganot et al., 1997b). In addition, the ACA triplet, located approximately three nucleotides from the 3' end of the RNA, also appears to be necessary for H/ACA snoRNA stability (Balakin et al., 1996; Ganot et al., 1997b). The selection of a uridine residue for modification on substrate RNA is achieved by base pairing of the H/ACA snoRNA with 3-10 nucleotides on either side of the target uridine, with the exception of one nucleotide adjacent to the target uridine (Figure 1.1). Several questions arise as to why such distinct secondary structures are required for the function of H/ACA snoRNAs in RNA-guided modifications. One possibility is that the unique spatial arrangement between the guide H/ACA snoRNA and the substrate RNA is required for isomerization of target uridines.

The H/ACA snoRNP protein components, together with H/ACA snoRNAs, are responsible for guiding up to 100 pseudouridine modifications on mammalian rRNAs; rRNA is thus often referred to as the canonical substrate of H/ACA snoRNAs. In eukaryotes, the base-pairing interaction between H/ACA snoRNAs and rRNAs allows the H/ACA snoRNP complex to isomerize distinct uridine residues to pseudouridine (Kiss et al., 2004; Ni et al., 1997). Each H/ACA snoRNP consists of a single guide H/ACA snoRNA, a protein complex comprised of the pseudouridine synthase dyskerin and other core snoRNP components NOP10, NHP2, and GAR1. The association of dyskerin, NOP10, and NHP2 with H/ACA snoRNAs appears to be essential for the biogenesis and formation of a catalytically active H/ACA snoRNP complex. For a comprehensive account of the structural and functional organization of H/ACA snoRNPs, please refer to (Duan et al., 2009; Hamma and Ferre-D'Amare, 2010; Hamma et al., 2005; Kiss et al., 2006; Li and Ye, 2006; Rashid et al., 2006). Interestingly, the same snoRNP protein complex, along with another class of H/ACA

small RNAs, termed H/ACA small cajal body RNAs (scaRNAs), modify uridine residues on small nuclear RNAs (snRNA) that are required for RNA splicing (Darzacq et al., 2002; Terns and Terns, 2006). In addition to a role in RNA-guided modifications, it has also been demonstrated that one H/ACA snoRNA, U17/E1, is required for the cleavage and processing of pre-rRNA with no detectable role in guiding rRNA pseudouridylation (Atzorn et al., 2004; Morrissey and Tollervey, 1993). Although it has not been formally proven, it is also possible that additional H/ACA snoRNAs may be involved in nucleolytic processing of rRNA, or alternatively, that H/ACA snoRNA U17 may function in nucleolytic processing of additional classes of RNAs. Therefore, it is evident that while one specific H/ACA snoRNA is directly involved in the nucleolytic processing of rRNA, the most well characterized role for the overwhelming majority of H/ACA snoRNAs is in guiding pseudouridine modifications within the ribosome.

The presence of pseudouridine is thought to confer unique properties to rRNA that may modulate its structure and function. Interestingly, it has been proposed that the presence of an additional hydrogen bond donor site on pseudouridine (Figure 1.2) confers unique properties to the RNA backbone, such as enhanced rigidity (Charette and Gray, 2000; Kierzek et al., 2014; Newby and Greenbaum, 2002). Consistent with the hypothesis that pseudouridine residues on tRNA restrict the mobility of the RNA backbone, thus stabilizing the RNA (Yarian et al., 1999), recent findings in human cells suggest that pseudouridine residues within 28S rRNA may play a conserved role in stabilizing rRNA (Sumita et al., 2005). For example, pseudouridine residues within helix 69 (H69) of human 28S rRNA appear to affect RNA stability and structure within this functionally important region of the ribosome (Sumita et al., 2005). Overall, it seems likely that specific

conformational changes in the tertiary structure of rRNA, imposed by pseudouridine modifications, may stabilize rRNA, thereby potentially impacting the structure, protein composition, and function of the ribosome. Broadening our knowledge of the mechanisms governing H/ACA snoRNA expression and H/ACA snoRNP biogenesis will undoubtedly prove invaluable in understanding the role of pseudouridine modifications within the ribosome. Furthermore, understanding whether H/ACA snoRNA expression and function may be modulated in a cell and tissue specific manner will provide significant insights into the role of this abundant RNA modification in maintaining normal cellular physiology.

Biogenesis and regulation of H/ACA snoRNPs involved in rRNA pseudouridine modifications

The biogenesis of catalytically active H/ACA snoRNPs is a complex process that requires the orchestrated expression, assembly, and nuclear transport of H/ACA snoRNP components, in addition to a number of chaperone proteins (Filipowicz and Pogacic, 2002; Kiss et al., 2006). One of the first steps required for H/ACA snoRNP biogenesis is the coordinated expression and association of H/ACA snoRNAs with H/ACA snoRNP proteins, namely dyskerin, NHP2, and NOP10. Intriguingly, the majority of H/ACA snoRNA genes appear to lack detectable transcriptional regulatory elements and are located within intronic regions of protein coding genes that are often referred to as H/ACA snoRNA 'host' genes (Dieci et al., 2009; Kiss, 2002). The apparent lack of a detectable, independent promoter element in the majority of H/ACA snoRNAs implies that their expression may inevitably be regulated by the transcription of their host gene. Indeed, human H/ACA

snoRNAs are processed from the excised and debranched host gene intron by exonucleases (Kiss and Filipowicz, 1995), and the association of core H/ACA snoRNP proteins such as dyskerin with H/ACA snoRNA motifs define the termini of mature H/ACA snoRNAs (Ganot et al., 1997b). The binding of H/ACA snoRNP proteins to H/ACA snoRNAs also appears to be critical for their processing, stability, and nucleolar localization. One striking observation is that in contrast to C/D snoRNAs, processing of human H/ACA snoRNAs does not appear to be coupled with host gene splicing (Richard et al., 2006). Instead, the recognition of intronic H/ACA snoRNAs and assembly of pre-snoRNPs appear to occur during transcription elongation and, in the case of one H/ACA snoRNA (U64), correct processing and nuclear localization are dependent on RNA polymerase II (RNAPII) transcription of the snoRNA precursor (Richard et al., 2006). Thus, it seems likely that the processing and assembly of H/ACA snoRNPs may be regulated by some components of the RNAPII machinery. In addition to coupling the expression of H/ACA snoRNAs with their binding to protein components of H/ACA snoRNPs, several chaperone proteins (for example, NAF1 and SHQ1) are also implicated in modulating the stepwise assembly and nuclear targeting of mature H/ACA snoRNPs (Darzacq et al., 2006; Grozdanov et al., 2009; Walbott et al., 2011). Indeed, it appears that a hierarchy of component assembly must occur in order to achieve a functionally active H/ACA snoRNP complex in the nucleolus. A detailed account of H/ACA snoRNA processing and the stepwise assembly and biogenesis of H/ACA snoRNPs can be found in (Filipowicz and Pogacic, 2002; Kiss et al., 2006).

An important and poorly understood question is whether the formation of a catalytically active H/ACA snoRNP is regulated in response to cellular cues, for instance upon increased demands for cell growth. Evidence suggesting that some steps in the

biogenesis of H/ACA snoRNPs may indeed be regulated is supported by the observation that, in most cases, H/ACA snoRNA host genes encode proteins implicated in ribosome biogenesis and function (Lestrade and Weber, 2006). These findings suggest that H/ACA snoRNA expression and H/ACA snoRNP biogenesis may be innately regulated in response to increased demands for protein synthesis. In support of this hypothesis, it is interesting to note that several H/ACA snoRNA host genes including DKC1, encoding the pseudouridine synthase dyskerin, are direct targets of the well-characterized oncogene and transcription factor Myc (Alawi and Lee, 2007; van Riggelen et al., 2010). As Myc plays an essential role in controlling cell growth and protein synthesis (van Riggelen et al., 2010), it is reasonable to speculate that modulation of Myc transcriptional activity may also regulate H/ACA snoRNP biogenesis in order to accommodate increased demands for protein synthesis. Additionally, it remains poorly understood whether the biogenesis of catalytically active H/ACA snoRNPs, comprised of H/ACA snoRNAs that guide modifications at specific sites on rRNA, are differentially regulated for example, during development or upon oncogenic activation. Some evidence suggesting that H/ACA snoRNPs, comprised of distinct H/ACA snoRNAs, may be differentially modulated is supported by findings that H/ACA snoRNAs display a tissue-specific expression pattern and/or are variably expressed amongst different human tissues (Castle et al., 2010; Cavaille et al., 2000). Additional findings that the expression of subsets of H/ACA snoRNAs may be modulated by components of the RNAPII machinery also suggest that the biogenesis of distinct H/ACA snoRNPs targeting different sites on rRNA may be tightly regulated. For instance, a post-translational modification in the carboxy-terminal domain (CTD) of RNAPII in mammalian cells facilitates the expression of distinct RNAs, including

subsets of H/ACA snoRNAs known to guide pseudouridine modifications on 18S rRNA (e.g., H/ACA SNORA55 and SNORA74) (Sims et al., 2011). This fascinating observation opens up the exciting and intriguing possibility that H/ACA snoRNPs comprised of distinct H/ACA snoRNAs may differentially guide pseudouridine modifications on rRNA in mammalian cells and challenges the notion that pseudouridine modifications within the ribosome are uniform. Based on recent findings demonstrating that altered expression of specific subsets of H/ACA snoRNAs manifest in several hematological diseases and malignancies, it is of particular interest to understand whether the corresponding pseudouridine sites on rRNA, guided by these subsets of H/ACA snoRNAs, are also deregulated in human disease.

Role for H/ACA snoRNA-guided rRNA pseudouridine modifications in translational control

Ribosomes from organisms in all domains of life contain pseudouridine modifications, and in most cases, pseudouridine residues are located within conserved and functionally important regions of rRNA (Lane et al., 1995). Notably, the number of uridine residues converted to pseudouridine has increased throughout evolution (Piekna-Przybylska et al., 2008), as has the complexity of the machinery necessary for performing pseudouridine modifications. These findings indicate that perhaps in higher organisms an increase in pseudouridine modifications provides an additional regulatory layer in modulating post-transcriptional gene expression mediated by the ribosome. Support for this hypothesis is evident from findings that an apparent lack of pseudouridine modifications within bacterial ribosomes does not adversely affect growth or the overall rate of protein synthesis

(Ofengand, 2002), while in eukaryotes loss of rRNA pseudouridine synthases is not compatible with life (He et al., 2002; Jiang et al., 1993). Remarkably, approximately 8-10% of total uridine residues on human 28S and 18S rRNA are converted to pseudouridine (Lestrade and Weber, 2006), indicating that this process is highly selective for specific uridine residues. An outstanding question that arises is why are specific uridine residues selectively modified on rRNA? One clue as to the functional importance of pseudouridine modifications on rRNA is that pseudouridine residues tend to cluster within regions of rRNA critical for modulating ribosome activity, namely the decoding center and peptidyl transferase center (PTC). In fact, a role for rRNA pseudouridine modifications in affecting specific aspects of ribosome function is evident from findings in yeast, mouse, and human cells demonstrating that rRNA pseudouridine modifications influence translational fidelity, stop codon recognition, and ribosome-ligand interactions (Baudin-Baillieu et al., 2009; Jack et al., 2011; King et al., 2003; McMahon et al., 2013). Therefore, alterations in rRNA pseudouridylation levels may have profound effects on the ribosome's ability to accurately and efficiently translate mRNA. These observations add to and support a growing body of evidence that structural components of the ribosome modulate specific aspects of protein synthesis.

In line with the observations that rRNA pseudouridylation plays a conserved role in regulating specific aspects of ribosome function, it is not surprising that a global decrease in rRNA pseudouridine modifications has no apparent overall effect on ribosome biogenesis or the global rate of protein synthesis (Yoon et al., 2006). Indeed, deregulation of the pseudouridine synthase dyskerin, for instance, leads to defects in the translation of specific mRNAs (Bellodi et al., 2010a; Montanaro et al., 2010b; Yoon et al., 2006).

Importantly, mRNAs found to be sensitive to changes in rRNA pseudouridylation harbor *cis*-regulatory elements in their 5' untranslated regions, such as internal ribosome entry site (IRES) elements. IRES elements are structured RNAs of variable length, originally identified in picornavirus RNAs, that directly engage with the 40S ribosomal subunit during translation initiation (Hellen and Sarnow, 2001; Jang et al., 1988; Pelletier and Sonenberg, 1988). Intriguingly, rRNA pseudouridine modifications play an evolutionarily conserved role in modulating the ability of ribosomes to bind to RNAs harboring IRES elements (Jack et al., 2011). IRES-dependent translation is an important RNA-based mode of translation initiation that effectively modulates gene expression during specific cellular events, for instance, mitosis, quiescence, hypoxia, nutrient deprivation, and apoptosis (Hellen and Sarnow, 2001; Holcik and Sonenberg, 2005; Lewis and Holcik, 2005). Therefore, it is tempting to speculate that rRNA pseudouridine modifications may be particularly important for the temporal translation of distinct subsets of mRNAs. In line with this hypothesis, impairments in the translation of distinct mRNAs known to harbor IRES elements, including the tumor suppressor p53, have been identified upon dyskerin deregulation during oncogenic activation (Bellodi et al., 2010a). Thus, pseudouridine modifications may impart a dynamic regulatory role to the ribosome, critical for control of gene expression at the translation level.

An interesting question arises as to whether distinct pseudouridine residues located at specific sites on rRNA guided by H/ACA snoRNAs may also modulate the translation of selective mRNAs in mammalian cells. For example, it is possible that modulating the pattern of rRNA pseudouridylation may provide an adaptive mechanism to control cell fate by regulating the translation of specific mRNAs. This is a particularly important question to

address in light of recent observations demonstrating that subsets of H/ACA snoRNAs are deregulated in several human diseases. Overall, although historically thought to exert a housekeeping function in the cytoplasm, emerging evidence suggests that ribosomes exhibit tremendous regulatory potential in modulating gene expression post-transcriptionally (Xue and Barna, 2012), and rRNA pseudouridylation appears to play an important role in this process.

Expanding cellular roles of H/ACA snoRNAs

Pseudouridine modifications on rRNA mediated by H/ACA snoRNAs are emerging as evolutionarily conserved and important regulators of ribosome function. Intriguingly, the continuous identification of mammalian H/ACA snoRNA genes from both computational and experimental approaches (Gu et al., 2005; Kishore et al., 2013; Schattner et al., 2006) raises the exciting possibility that the number of novel rRNA target sites is rapidly expanding and that non-canonical RNA substrates of H/ACA snoRNAs likely exist. In fact, the recent discovery that the repertoire of RNA species containing pseudouridine modifications is far greater than previously thought (Carlile et al., 2014; Schwartz et al.), suggests that H/ACA snoRNA-guided modifications may likely occur on mRNAs as well as on additional ncRNAs. Furthermore, tremendous advancements in small RNA deep sequencing have aided the identification of seemingly abundant and conserved small ncRNAs derived from H/ACA snoRNAs in eukaryotes (Ender et al., 2008; Taft et al., 2009). Is it possible that H/ACA snoRNAs may have evolved additional regulatory roles in eukaryotes that may provide a new layer of complexity in control of gene expression?

Exploring the functional diversity of H/ACA snoRNAs in eukaryotes will undoubtedly ignite several new avenues of research and identify perhaps previously uncharacterized functions of H/ACA snoRNAs.

New RNA substrates for pseudouridine modifications

Since its discovery in 1957 (Davis and Allen, 1957), pseudouridine modifications have traditionally thought to occur on non-coding regulatory RNAs, namely tRNA, rRNA, and snRNA. However, exciting new studies have uncovered that mRNAs, snoRNAs, and lncRNAs also contain pseudouridine modifications (Carlile et al., 2014; Schwartz et al.). Importantly, some pseudouridine modifications found on mRNA are dependent on the pseudouridine synthase dyskerin (Carlile et al., 2014; Schwartz et al.), thereby indicating that H/ACA snoRNAs associated with dyskerin and known to guide modifications on rRNA, may also be responsible for modifying specific uridine residues on distinct mRNAs. These findings raise several intriguing questions regarding the putative role of H/ACA snoRNP-guided pseudouridine modifications on novel RNA substrates. Although the functional consequence of pseudouridine modifications on mRNAs has yet to be resolved, an intriguing possibility is that pseudouridylation may have broad effects on the life of an mRNA, potentially affecting mRNA stability, localization, and/or translation. Furthermore, other recent findings have demonstrated that targeted pseudouridylation of stop codons by a synthetic H/ACA snoRNA leads to recognition of pseudouridylated stop codons by aminoacyl-tRNAs in yeast (Fernandez et al., 2013; Karijolich and Yu, 2011), suggesting that mRNA pseudouridylation may change the coding potential of mRNAs (Karijolich and Yu, 2011). Therefore, it is evident that H/ACA snoRNP-guided pseudouridine modifications on

diverse RNA species such as rRNA and mRNA may have profound implications for post-transcriptional gene expression regulation by modulating RNA fate and function. In addition to predictions that H/ACA snoRNAs with defined rRNA targets may guide modifications on novel RNA substrates, it is also possible that orphan H/ACA snoRNAs, so-called because their putative RNA targets are not known (Vitali et al., 2003), may guide isomerization of select uridine residues on rRNA and non-canonical RNA substrates, including mRNAs. Likewise, it is also conceivable that a recently identified class of H/ACA small RNAs termed AluACA RNAs (Jady et al., 2012) may participate in pseudouridylation of diverse RNA species.

Potential role for H/ACA snoRNAs in chromatin remodeling

In addition to the well-characterized role of H/ACA snoRNAs in rRNA pseudouridine modifications from archaea to eukaryotes (Terns and Terns, 2002), recent evidence opens up the possibility that subsets of H/ACA snoRNAs may also play a role in chromatin biology in eukaryotes. Findings that C/D and H/ACA snoRNAs are enriched in chromatin-associated RNAs (caRNAs) from human and drosophila cells (Schubert et al., 2012), independent of snoRNP proteins, suggest a conserved and previously uncharacterized role for H/ACA snoRNAs in chromatin remodeling. For example, in human fibroblasts several H/ACA snoRNAs (U64, U23, and ACA44) that guide modifications on rRNA, were found to be associated with chromatin. Although the precise function of H/ACA snoRNAs on chromatin was not assessed, the association of C/D snoRNAs with a drosophila chromatin binding protein (Df31) was shown to play a role in maintaining open chromatin structure (Schubert et al., 2012). Whether this unanticipated function occurs in human cells and

whether H/ACA snoRNAs can directly modulate chromatin structure remains to be investigated.

H/ACA snoRNA-derived RNAs (sdRNAs) and snoRNA-like miRNAs

Recently, a number of small RNAs containing snoRNA features has been identified in eukaryotes. One class of small RNAs ranging in length from 20-24 nucleotides, supposedly derived from H/ACA snoRNAs, has been designated H/ACA snoRNA-derived RNAs (sdRNAs) and snoRNA-like miRNAs (Ender et al., 2008; Scott et al., 2009; Taft et al., 2009). Interestingly, computational analyses indicate that these RNAs are located within and may be processed from H/ACA snoRNA and orphan H/ACA snoRNA genomic regions (Scott et al., 2009). These findings suggest that H/ACA snoRNAs involved in rRNA modifications may serve as precursors of novel small RNAs. Surprisingly, H/ACA sdRNAs and snoRNA-like miRNAs appear to be regulated by or associated with components of the RNAi pathway, such as DICER1 (Taft et al., 2009), AGO1 and AGO2 (Ender et al., 2008). Although the function of H/ACA snoRNA-derived small RNAs has not been assessed, one snoRNA-like miRNA derived from an H/ACA scaRNA (designated ACA45 small RNA) was found to play a role in post-transcriptional gene silencing in a manner similar to that of miRNAs (Ender et al., 2008). Together these findings provide a previously uncharacterized connection between H/ACA snoRNAs, components of the RNA silencing machinery, and miRNAs. It remains to be addressed whether H/ACA sdRNAs and/or snoRNA-like miRNAs merely represent non-functional degradation products of H/ACA snoRNAs or whether they hold novel regulatory potential *in vivo.*

In summary, although the function of H/ACA snoRNA derivatives and ncRNAs with H/ACA snoRNA features remains completely unknown, based on the recent discoveries described above, it is reasonable to envision that these ncRNAs may hold novel regulatory potential in modulating chromatin state or controlling gene expression in a manner similar to that described for miRNAs and lncRNAs. Is it possible that H/ACA snoRNA derivatives and ncRNAs with H/ACA snoRNA features may have evolved to provide an additional regulatory step in decoding the genetic template in higher eukaryotes? As these hypothetical regulatory ncRNAs have not yet been identified in eubacteria or archaea, it is possible that they may provide an additional step in controlling gene expression in multicellular organisms such as mammals, where temporal and spatial gene expression regulation is critical during development and, when deregulated, may lead to human disease.

Deregulation of H/ACA snoRNAs in human disease

ncRNAs control critical cellular processes and are emerging as key players in human disease (Esteller, 2011; Taft et al., 2010). Increasing studies suggest that H/ACA snoRNAs that guide pseudouridine modifications at distinct sites on rRNA are frequently altered in hematological disorders and solid tumors (Table 1.1). Although their contribution to disease remains largely unexplored, one of the most intriguing and puzzling aspects of H/ACA snoRNA deregulation in disease is that only specific subsets of H/ACA snoRNAs appear to be altered. Moreover, the observation that deregulation of H/ACA snoRNA expression in several malignancies is often independent of host gene transcription (Mei et

al., 2012; Ronchetti et al., 2013; Ronchetti et al., 2012) reinforces the notion that this is not simply a global phenomenon and, rather, indicates that H/ACA snoRNA deregulation may be directly implicated in disease. Furthermore, findings that mutations in several genes encoding protein components of H/ACA snoRNPs have been identified in cancer and congenital bone marrow failure syndromes (Bellodi et al., 2010b; Cerami et al., 2012; Forbes et al., 2011; Heiss et al., 1998; Knight et al., 1999; Taylor et al., 2010; Vulliamy et al., 2008; Walne et al., 2007; Zhong et al., 2011) suggest that functional perturbations of H/ACA snoRNAs may, in fact, contribute to disease. In this section, we discuss and provide our perspective on the potential functional consequences of alterations in H/ACA snoRNA expression in human disease.

Hematological disorders

Alterations in specific subsets of H/ACA snoRNAs have been reported predominantly in hematological disorders, in particular acute myeloblastic and lymphoblastic leukemia, chronic lymphocytic leukemia, T-cell lymphoma, multiple myeloma and the cancer susceptibility and bone marrow failure syndrome X-linked dyskeratosis congenita (X-DC) (Bellodi et al., 2013; Ronchetti et al., 2013; Ronchetti et al., 2012; Teittinen et al., 2012; Valleron et al., 2012a; Valleron et al., 2012b). Intriguingly, as opposed to a global perturbation in H/ACA snoRNA expression in these diseases, only specific subsets of H/ACA snoRNAs appear to be altered. Importantly, the levels of most H/ACA snoRNAs found altered in hematological disorders, as well as many other diseases, appear to be decreased compared to control cells. For instance H/ACA SNORA15 and SNORA24 are two examples of H/ACA snoRNAs that are commonly downregulated in disease (Table 1.1). In

some cases, changes in H/ACA snoRNA expression do not correlate with host gene levels, suggesting that host gene transcriptional changes (Ronchetti et al., 2013; Ronchetti et al., 2012) are uncoupled from and cannot account for alterations in H/ACA snoRNA expression. Therefore, it seems likely that alterations in specific subsets of H/ACA snoRNAs may occur post-transcriptionally and may directly affect H/ACA snoRNP biogenesis and function. Intriguingly, nucleotide deletions or substitutions reported in H/ACA snoRNAs (Brecqueville et al., 2014; Lawrence et al., 2014) are located within structurally and functionally important regions of H/ACA snoRNAs that may in fact significantly alter the predicted structure of H/ACA snoRNAs (Figure 1.3) and may hinder their association with H/ACA snoRNP proteins as well as their ability to guide modifications on substrate RNAs. It is also interesting to note that epigenetic alterations involving deletion and hypermethylation of distinct H/ACA snoRNA loci have also been reported in cancer cells, including those of hematological origin (Ferreira et al., 2012). Collectively, these findings strongly indicate that deregulated expression of distinct subsets of H/ACA snoRNAs is emerging as a common feature of disease, particularly in those originating from hematopoietic tissue.

One evolutionarily conserved functional outcome of deregulated H/ACA snoRNA expression and biogenesis is impairment in rRNA pseudouridine modifications. Consistent with these findings, alterations in H/ACA snoRNA expression also lead to functional perturbations in H/ACA snoRNA-guided pseudouridylation at specific sites on rRNA in hematological diseases (Bellodi et al., 2013). For example, decreased expression of H/ACA SNORA15 results in a corresponding reduction in pseudouridine modifications at nucleotide U1367 on 18S rRNA in X-DC patient cells. X-DC, a congenital disorder

characterized by a wide range of defects, some of which include bone marrow failure, skin abnormalities, hematopoietic malignancies, and pulmonary fibrosis (Dokal, 2000), is caused by mutations in DKC1, the gene encoding the evolutionarily conserved pseudouridine synthase dyskerin. DKC1 mutations appear to affect the expression and function of unique subsets of H/ACA snoRNAs in modifying rRNA in X-DC (Bellodi et al., 2013) and are consistent with an evolutionarily conserved role of dyskerin and additional H/ACA snoRNP components in modulating H/ACA snoRNA expression and function (Alawi and Lin, 2011; Gu et al., 2008; Watkins et al., 1998). Although the downstream functional contribution of perturbations in H/ACA snoRNAs and site-specific rRNA pseudouridylation in disease remains relatively unexplored, it is likely that defects in the expression of specific subsets of H/ACA snoRNAs may lead to heterogeneous pools of ribosomes harboring unique differences in rRNA pseudouridine modifications. As mentioned previously, such heterogeneity in ribosome nucleotide modifications may have profound functional implications for translational regulation. Although not formally proven, it is tempting to speculate that a decrease in pseudouridine modifications at distinct sites on rRNA in cells of hematopoietic origin may impinge on the translation of specific mRNAs, such as those encoding important mediators of cell fate, including tumor suppressors and regulators of stem cell differentiation. Importantly, the enzymatic activity of dyskerin in catalyzing pseudouridine modifications on RNA was shown to rescue, to a large extent, hematopoietic stem cell differentiation defects in primary CD34+ hematopoietic progenitor cells from a patient harboring a DKC1 promoter mutation (Bellodi et al., 2013). These findings illuminate an important requirement for H/ACA snoRNA-guided RNA pseudouridine modifications in stem cell differentiation and may provide one explanation

for why H/ACA snoRNA deregulation is frequently reported in hematological disorders. Given that alterations in H/ACA scaRNAs involved in spliceosomal snRNA modifications are also perturbed in some hematological disorders and that the repertoire of pseudouridylated RNA species is rapidly expanding, it cannot be excluded that defective pseudouridine modifications on additional RNA species may also contribute to disease. Similarly, it is also possible that, although functionally uncharacterized, emerging non-canonical functions of H/ACA snoRNAs, H/ACA snoRNA derivatives, and ncRNAs with H/ACA snoRNA features may also be deregulated in diseases where alterations in H/ACA snoRNAs have been reported.

Solid tumors

It is also emerging that specific subsets of H/ACA snoRNAs are altered in solid tumors of distinct histological origin including prostate (Martens-Uzunova et al., 2012) and lung (Liao et al., 2010) (Table 1.1). Several mechanisms have been identified that may lead to dysfunction of H/ACA snoRNAs in solid tumors, including H/ACA snoRNA nucleotide deletions and substitutions (Lawrence et al., 2014). Importantly, the position of these nucleotide deletions and substitutions may have a dramatic impact on the structure, stability, and function of H/ACA snoRNAs as predicted for a nucleotide substitution of one H/ACA snoRNA found in head and neck cancer (Figure 1.3). Furthermore, CpG island hypermethylation associated with transcriptional silencing of H/ACA snoRNAs in cancer cell lines from colon and renal tumors (Ferreira et al., 2012) has also been reported. Intriguingly, although the overwhelming majority of H/ACA snoRNAs altered in disease appear to be decreased, a small subset of H/ACA snoRNAs appear to be increased, most

noticeably H/ACA snoRNA42. H/ACA snoRNA42 guides a pseudouridine modification on 18S rRNA and is commonly increased in a number of solid tumors as well as in X-DC patient cells. Interestingly, X-DC patients have a high incidence of solid tumors, particularly head and neck cancer (Alter et al., 2009). Therefore, it is possible that, although uncommon, increased expression of unique H/ACA snoRNAs may also contribute to disease. For instance, H/ACA snoRNA42 is found significantly upregulated in Non-Small Cell Lung Cancer (NSCLC), amongst other cancers (Table 1.1). SNORA42 is encoded within a chromosomal region commonly amplified in NSCLC, and high SNORA42 expression in NSCLC patients correlates with poor survival (Mei et al., 2012). Importantly, gain and loss of function studies suggest that increased H/ACA snoRNA42 expression may be pro-tumorigenic in the lung (Mei et al., 2012). However, whether the function of H/ACA snoRNA42 in modifying RNA is increased and may directly contribute to NSCLC *in vivo* remains to be determined. Likewise, elucidating whether the observed deregulation of additional H/ACA snoRNAs in solid tumors can directly promote tumorigenesis or is merely a secondary effect due to changes in proliferation or host gene transcription requires further investigation. As mentioned earlier, it seems likely that direct perturbations of distinct subsets of H/ACA snoRNAs in solid tumors may lead to the production of ribosomes harboring unique patterns of rRNA pseudouridine modifications. Is it possible that alterations in the pattern of rRNA pseudouridine modifications may contribute to tumorigenesis by modulating specific aspects of ribosome function? An emerging role for rRNA post-transcriptional modifications in modulating translational specificity and accuracy in cancer is supported by findings that rRNA ribose methylation plays a key role in regulating ribosome activity in breast cancer cells (Basu et al., 2011;

Marcel et al., 2013). Collectively, these studies highlight a functionally important role of H/ACA snoRNA-guided rRNA modifications in cellular physiology that, when deregulated, may directly contribute to human disease.

Figures

Figure 1.1. Schematic secondary structure of a box H/ACA snoRNA. Schematic representation of a box H/ACA snoRNA (blue) containing several evolutionarily conserved elements, including a box H (ANANNA) and box ACA motif and two pseudouridylation pockets. Pseudouridylation pockets are shown base pairing to the complementary sequence on substrate RNA (gray). The position of the target uridine modified to pseudouridine (Ψ) on substrate RNA is indicated by red arrow.

Figure 1.2. Pseudouridine is an isomer of uridine. Pseudouridine (Ψ) is an isomer of uridine (U) and is the only nucleotide to possess a carbon-carbon (C-C) glycosidic bond (C5, highlighted with a red arrowhead). Isomerization of uridine to pseudouridine involves the detachment of the uracil base at position N1 (red arrowhead) and rotation (180°) through the N3-C6 axis. The newly synthesized pseudouridine possesses an additional hydrogen bond donor site, highlighted in orange.

Figure 1.3. Predicted effect of a single nucleotide substitution on H/ACA snoRNA secondary structure. Sequence and predicted secondary structure of SNORA71C (a) and a

SNORA71C variant found in head and neck cancer, SNORA71 60A>G (Lawrence et al., 2014) (b). The position of the substituted nucleotide is indicated with an arrowhead. The nucleotide substitution appears to alter the predicted structure of the pseudouridylation pocket within SNORA71C (highlighted in green) and may likely inhibit base pairing to human 18S rRNA (blue, with position of pseudouridine highlighted in red). The box H and box ACA elements are boxed and shown in orange. Secondary structure predictions were obtained using RNAfold (Denman, 1993) and visual inspection.

Figure 1.1

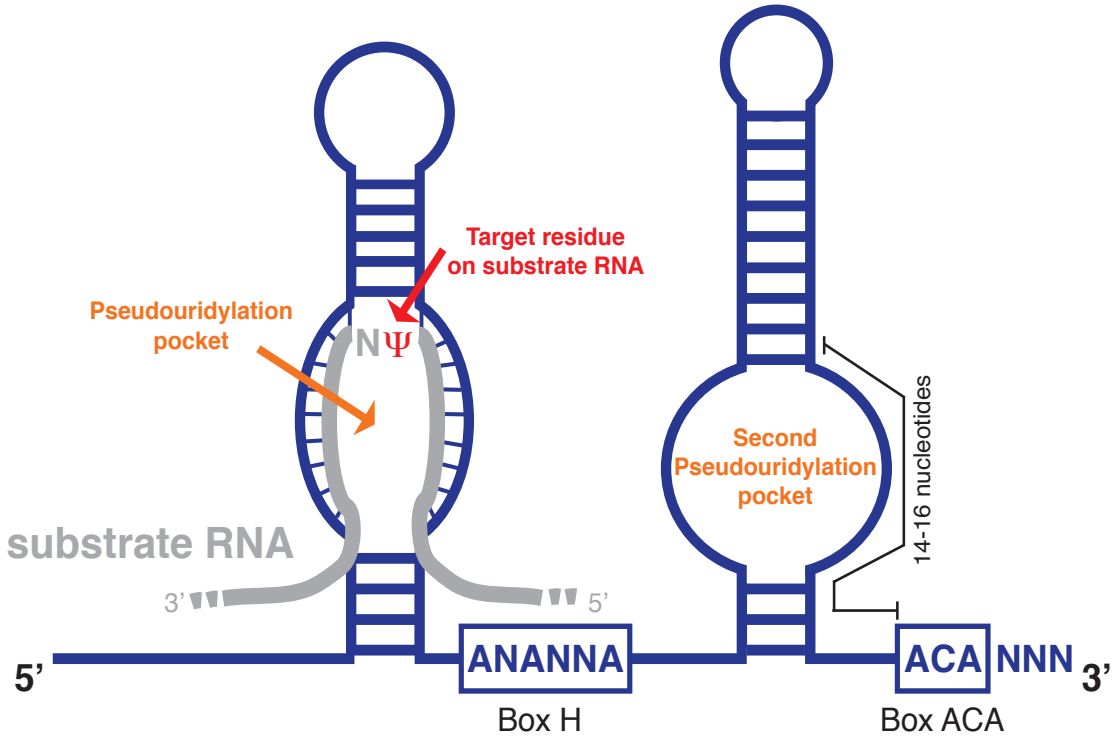

H/ACA snoRNA

Figure 1.2

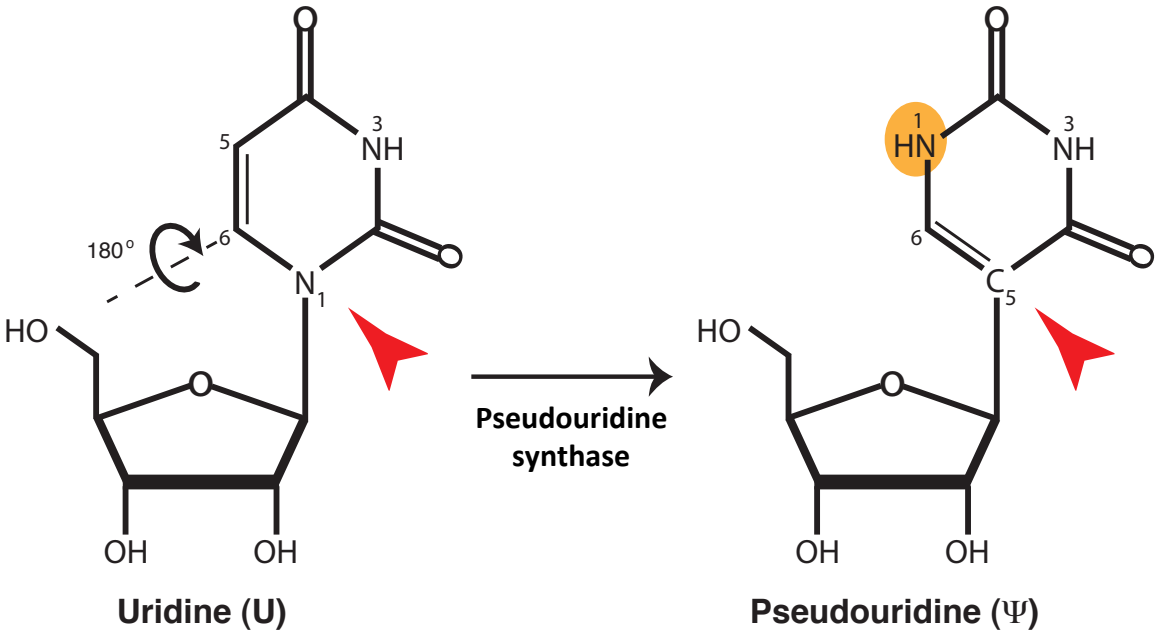
180°
HO
OH
OH
NH
HN
Pseudouridine synthase
Uridine (U)
Pseudouridine (Ψ)

Figure 1.3

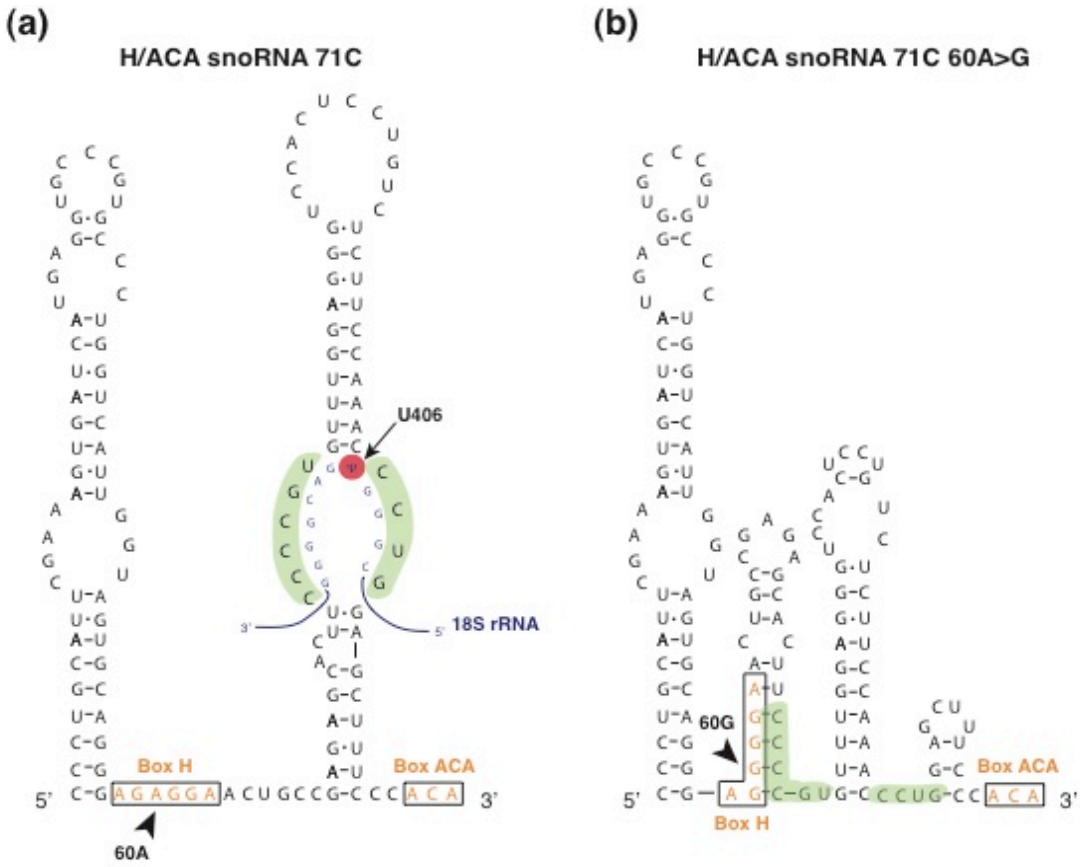
(a)
H/ACA snoRNA 71C
U406
18S rRNA
Box H
Box ACA
60A
5'
3'
(b)
H/ACA snoRNA 71C 60A>G
60G
Box H
Box ACA
5'
3'

Tables

Table 1.1. Illustrative list of H/ACA snoRNAs commonly altered in human disease

Table 1.1

			Expression Level		Genetic or Epigenetic Alteration		
Name	Locus	Substrate	Expression	Disease	Alteration	Disease	Reference
SNORA15	7p11	18S rRNA	Decrease	Acute myeloblastic leukemia			20
				Acute lymphoblastic leukemia			20
				Peripheral T-cell lymphoma			21
				X-linked dyskeratosis congenita			103
SNORA24	4q26	18S rRNA	Decrease	Acute myeloblastic leukemia			20
				Acute lymphoblastic leukemia			20
				Chronic lymphocytic leukemia			91
				Peripheral T-cell lymphoma			21
				X-linked dyskeratosis congenita			103
SNORA41	2q33	18S rRNA	Decrease	Acute myeloblastic leukemia	Nucleotide substitution and deletion	Endometrial cancer	20,105
				Acute lymphoblastic leukemia			20
SNORA48	17p13	28S rRNA	Decrease	Acute myeloblastic leukemia	Nucleotide substitution	Breast cancer	20,105
				Acute lymphoblastic leukemia			20
				Multiple myeloma			92
				X-linked dyskeratosis congenita			103
SNORA70C	9q33	18S rRNA	Decrease	Chronic lymphocytic leukemia	CpG island hyper-methylation	Leukemia cell line	91,107
				Colorectal cancer cell line		Colorectal cancer cell line	107
SNORA71C	20q11	18S rRNA	Decrease	Chronic lymphocytic leukemia	Gene deletion	Myelofibrosis	91,106
					Nucleotide substitution	Head and neck cancer	105
SNORA71D	20q11	18S rRNA	Decrease	Acute myeloblastic leukemia	Gene deletion	Myelofibrosis	20,106
				Peripheral T-cell lymphoma	Nucleotide substitution	Colorectal cancer	21,105
SNORA74A	5q31	28S rRNA	Increase	Chronic lymphocytic leukemia			91
		U3 snRNA		Multiple myeloma			92
				Prostate cancer			111
SNORA42	1q22	18S rRNA	Increase	Non-small cell lung cancer	Gene amplification	Non-small cell lung cancer	93,112
				Prostate cancer			111
				X-linked dyskeratosis congenita			103
SNORA64	16p13	28S rRNA	Increase	Multiple myeloma			92
				Prostate cancer			111
				X-linked dyskeratosis congenita			103

Chapter 2: H/ACA Small RNA Dysfunctions in Disease Reveal Key Roles for Noncoding RNA Modifications in Hematopoietic Stem Cell Differentiation

Background

H/ACA small RNAs are an evolutionarily conserved class of abundant noncoding RNAs (ncRNAs) involved in a diverse range of processes including post-transcriptional modifications of functional RNAs, pre-ribosomal RNA processing, and telomere maintenance (Baxter-Roshek et al., 2007; Lestrade and Weber, 2006; Matera et al., 2007; Reichow et al., 2007; Williams and Farzaneh, 2012). A central protein associated with all classes of H/ACA small RNAs is dyskerin, which is thereby at the nexus of controlling many diverse cellular processes (Lafontaine et al., 1998; Montanaro, 2010; Watkins et al., 1998). The largest subgroup of dyskerin-associated H/ACA small RNAs are small nucleolar RNAs (snoRNAs) that are responsible for modifying hundreds of specific nucleotides on the ribosome. The association of dyskerin with H/ACA snoRNAs is important for their stability and forms catalytically active ribonucleoprotein (RNP) complexes, which guide the site-specific conversion of uridine to pseudouridine (Ψ) residues on ribosomal RNA (rRNA)(Charette and Gray, 2000).

Importantly, the *DKC1* gene encoding for dyskerin is mutated in a number of cancers and inherited human syndromes including X-linked Dyskeratosis Congenita (X-DC) and the clinically severe variant of Dyskeratosis Congenita (DC) known as Hoyeraal-Hreidarsson (HH) syndrome (Bellodi et al., 2010b; Cerami et al., 2012; Forbes et al., 2011; Heiss et al.,

1998; Knight et al., 1999; Yip et al., 2012). These human syndromes are characterized by a wide range of defects including hematopoietic and cutaneous abnormalities (abnormal pigmentation, nail dysplasia, leukoplakia), increased risk of cancer, pulmonary fibrosis and liver disease, as well as severe congenital birth defects in brain development, growth, and the genitourinary system (Kirwan and Dokal, 2008). Among all H/ACA small RNAs, the telomerase RNA (TERC) is the most characterized and is widely employed as a prognostic molecular marker of DC (Alter et al., 2007; Mitchell et al., 1999). It remains largely unknown whether a multitude of small RNAs may be affected in human disease as a consequence of mutations in *DKC1*. In addition, a central unresolved question is whether the enzymatic activity of dyskerin is perturbed in and may contribute to some of the pathological features of diseases associated with mutations in *DKC1*. Interestingly, emerging evidence further suggests that specific subsets of dyskerin-associated H/ACA snoRNAs are deregulated in hematological disorders such as leukemia, lymphoma, and multiple myeloma (Ronchetti et al., 2012; Teittinen et al., 2012; Valleron et al., 2012a; Valleron et al., 2012b).

Here we sought to determine the landscape of H/ACA small RNA dysregulation in patients harboring *DKC1* mutations that may underlie the wide range of pathological features observed. Surprisingly, by carrying out an extensive profiling screen for these small RNAs, we observed unexpected heterogeneity in their expression levels in X-DC patient cells harboring distinct *DKC1* mutations. Thereby, these findings reveal unexpected complexity in the manifestation of impairments in small RNAs that may reflect an important genotype to phenotype relationship associated with human disease etiology. Strikingly, applying a novel and highly quantitative mass spectrometry approach, we

identified reductions in site-specific rRNA Ψ modifications, which correspond to the decreased expression of H/ACA snoRNAs guiding the modification of these residues. Thereby, the catalytic activity of RNP complexes is also directly affected in X-DC human disease. Moreover, we uncovered a critical role for dyskerin's catalytic activity towards hematopoietic differentiation. Altogether, these findings provide compelling evidence that the deregulated expression and function of H/ACA snoRNPs may underlie specific pathological features of human disease. Moreover, complex deregulations in the patterns of H/ACA small RNA expression may serve as important molecular markers of human health and disease.

Results

Heterogeneous defects in all classes of H/ACA small RNAs are present in X-DC patients harboring distinct DKC1 mutations

To uncover whether *DKC1* mutations affect functionally unique subsets of dyskerin-containing H/ACA small RNPs, we undertook a systematic expression analysis to examine a large panel of H/ACA small RNAs. First, we sought to examine the expression profiles of these small RNAs directly in highly purified CD34+ hematopoietic progenitor cells, as a common pathological feature and cause of lethality in X-DC patients is bone marrow failure (Dokal, 2011). To this end, we characterized patient cells harboring a mutation in the *DKC1* promoter, a C to G substitution at position -141 hereafter referred to as *DKC1*(c.-141 C>G) (Figure 2.1A, top), which produces a hypomorphic allele that significantly reduces *DKC1* transcript levels (Figure 2.1B). The same mutation in the putative Sp1 transcription

binding sites within the *DKC1* promoter has been previously reported (Knight et al., 2001; Salowsky et al., 2002). This patient presented at two years of age with several clinical features of DC including hematological defects, congenital anomalies involving the central nervous system and genitourinary system, and a family history of early onset colon and lung cancers (Figure 2.1A, bottom). Therefore, *DKC1*(c.-141 C>G) cells provide a very unique system to assess the impact of reducing the overall threshold of dyskerin activity.

We directly assessed the expression of functionally distinct H/ACA small RNAs in *DKC1*(c.-141 C>G) CD34+ cells, including 27 H/ACA snoRNAs, which are the most abundant class of dyskerin-associated small RNAs involved in site-specific rRNA pseudouridylation (Figure 2.1C, top row). In addition, the expression of small Cajal Body RNAs (scaRNAs), involved in pseudouridylation of spliceosomal small nuclear RNAs (snRNAs) (ACA12, U85, U93, and U109), as well as TERC, important for telomere function, was also examined. Unexpectedly, we observed differential reductions in the expression of distinct H/ACA small RNAs relative to matched healthy control CD34+ cells (Figure 2.1C, top row), which did not display significant variations in H/ACA small RNA levels (Figure S2.1A). Notably, the expression of H/ACA snoRNA15 and snoRNA67, which guide site-specific modifications of two consecutive Ψ residues on 18S rRNA (i.e. Ψ1367 and Ψ 1445), displayed the greatest reduction, up to a 60% decrease (Figure 2.1C). Interestingly, the levels of TERC remained unchanged in DKC1(c.-141 C>G) patient cells (Figure 2.1C) and consistently no significant difference in telomere length was observed (data not shown). These results suggest that missense mutations in DKC1 have a more profound effect on TERC levels (Batista et al., 2011; Walne et al., 2007) as compared to the DKC1 promoter mutation described in this study. For example, it is possible that missense mutations in dyskerin may

disrupt specific protein-protein interactions within the telomerase complex that may be important for TERC stability. These results indicate that distinct classes of dyskerin-associated H/ACA small RNAs may be differentially affected by this specific *DKC1* mutation.

In order to determine whether aberrant expression of H/ACA small RNAs is common among X-DC patients, we next extended our analysis to individuals harboring different *DKC1* mutations. In this respect, we performed unsupervised hierarchical clustering of H/ACA small RNA relative expression in *DKC1*(c.-141 C>G), *DKC1*(T66A), *DKC1*(ΔL37), and *DKC1*(A386T) patient cells (Figure 2.1C). We observed remarkable heterogeneity in the expression of H/ACA small RNAs amongst X-DC patient cells harboring different mutations that have similar histologic origins, relative to matched controls, which did not display significant variations in H/ACA small RNA levels (Figures S2.1B-S2.1C). Moreover, specific H/ACA small RNAs stratified according to their relative expression levels, cell type and nature of the *DKC1* mutation (Figure 2.1C dendrograms). For example, the expression of a group of four H/ACA snoRNAs (snoRNA48, E2, 22, and 75) is perturbed in *DKC1*(ΔL37) fibroblasts, but remains unaltered in *DKC1*(A386T) fibroblasts (Figure 2.1C). Similar variations in the expression of distinct H/ACA small RNAs were also observed amongst X-DC patient lymphoblasts harboring different *DKC1* mutations (Figure 2.1C). Furthermore, we also identified differences in H/ACA snoRNA expression in cells from different tissues (lymphoblasts versus fibroblasts) harboring the same *DKC1*(ΔL37) mutation (e.g. snoRNA31, 42, 15 and U85) (Figure 2.1C), suggesting that tissue-specific defects in H/ACA small RNA expression may at least in part underlie the specific pathological features present in X-DC patients. Common nodes of dysregulation in H/ACA small RNA expression are also evident. For example, six H/ACA small RNAs (snoRNA16, 52,

24, U93, ACA12 and TERC) display the most dramatic reductions in the majority of X-DC patient cells analyzed (Figure 2.1C). Moreover, we confirmed these findings by northern blot analysis (Figure S2.1D). Importantly, not all the H/ACA small RNAs are reduced in X-DC patient cells. In particular, H/ACA snoRNAs such as 28 and U64 do not display differences in expression levels, in agreement with previous reports (Figure 2.1C) (Batista et al., 2011; Mitchell et al., 1999). Interestingly, our observation that snoRNA42 expression is increased in *DKC1*(ΔL37) lymphocytes raises the possibility that certain snoRNAs may be selectively increased as a compensatory mechanism for perturbations in subsets of H/ACA small RNAs (Figure 2.1C). Strikingly, H/ACA sno/scaRNAs 24, U93, ACA12, 80, and 56 are decreased in the majority of X-DC patient cells, closely clustering with concomitant diminished TERC expression, and may therefore represent a central node of small RNA dysfunctions in human disease (Figure 2.1C). Importantly, the altered expression of H/ACA small RNAs in X-DC patients is highly specific, as a similar class of non-dyskerin associated small RNAs implicated in methyl modifications of rRNA, termed C/D snoRNAs (Bachellerie and Cavaille, 1997), are unaffected in X-DC patient cells (Figure 2.2).

To establish whether the specific pattern of reductions in H/ACA small RNAs in X-DC cells is directly caused by dyskerin dysfunction, we restored dyskerin expression close to normal levels in primary X-DC fibroblasts (Figure 2.2). Importantly, reintroduction of dyskerin specifically rescued, to a large extent, the expression of dyskerin-associated H/ACA small RNAs in *DKC1*(ΔL37) primary fibroblasts compared to controls (Figure 2.2). Taken together, these results uncover aberrant expression of functionally diverse classes of dyskerin-associated H/ACA small RNAs in patients harboring distinct *DKC1* mutations. Furthermore, these findings suggest that variations in the expression of specific H/ACA

small RNAs may underlie, at least in part, the wide range and degree of clinical features observed amongst X-DC patients.

Defects in site-specific and global rRNA pseudouridylation are present in X-DC patients

Currently, it remains unknown whether dysregulations in H/ACA small RNA expression translate into defects in specific cellular processes orchestrated by these small RNAs. In particular, H/ACA snoRNAs are assembled into catalytically active RNP complexes through their association with dyskerin, which catalyzes the conversion of ~100 uridine residues to Ψ in functionally important domains of rRNA (Ni et al., 1997). To ascertain the contribution of altered H/ACA snoRNA expression in X-DC patient cells on Ψ modifications at specific sites on the rRNA, we developed a novel highly sensitive mass spectrometry method for relative quantification of changes in Ψ residues on rRNA at nucleotide resolution (Figure 2.3A and experimental procedures for details). To our knowledge, this is the first technology that enables quantification of site-specific pseudouridine modifications on individual rRNA nucleotides. In this study we employed this novel technique to monitor the levels of site-specific Ψ modifications on 18S rRNA, as previously reported translational impairments upon dyskerin dysfunction are associated with defects involving the small ribosomal subunit (Bellodi et al., 2010a; Jack et al., 2011; Montanaro et al., 2006; Montanaro et al., 2010a). Total 18S rRNA isolated from control and X-DC patient cells was cleaved to generate a mixture of Ψ-containing rRNA oligonucleotides that were subsequently resolved by liquid chromatography tandem mass spectrometry (LC/MS/MS).

Briefly, Ψ modifications at specific sites on rRNA oligonucleotides (Figure S2.2A) were selected based on their *m/z* ratio and nucleotide sequence. The Ψ signal on each oligonucleotide was quantified and standardized to the amount of a non-Ψ containing oligonucleotide in the mixture (see experimental procedures for details). In particular, we employed two distinct X-DC patient cells including *DKC1*(ΔL37) primary fibroblasts and immortalized *DKC1*(T66A) cells. Utilizing this novel methodology, we detected reductions in the amount of Ψ residues at specific sites on rRNA in these X-DC patient cells (Figure 2.3B), which precisely correspond to reductions in H/ACA snoRNAs annotated to guide these modifications (Figure S2.2A) (Lestrade and Weber, 2006). For example, in *DKC1*(ΔL37) fibroblasts, pronounced reductions were observed in Ψ levels at Ψ119, Ψ1367, and Ψ1445 on 18S rRNA compared to control cells (Figure 2.3B and S2.2B). Conversely, no significant changes were detected at Ψ105 on 18S rRNA, in agreement with our findings that the expression of the corresponding guide H/ACA snoRNAs, 36A and 50, were not perturbed (Figure 2.1C). In *DKC1*(T66A) cells, heterogeneous defects in site-specific pseudouridylation on 18S rRNA (Figures 2.3B and S2.2C) were also observed, including perturbations in sites that were either reduced or unaltered in *DKC1*(ΔL37) fibroblasts. For example, Ψ1445 on 18S rRNA is similarly reduced in both *DKC1*(ΔL37) and *DKC1*(T66A) cells and this is consistent with decreased expression of the corresponding guide H/ACA snoRNA (snoRNA67) in both cell types (Figures 2.1C and 2.3B). By contrast, the site-specific reductions of Ψ105, Ψ1692, or Ψ218 are exclusively observed in either *DKC1*(T66A) or *DKC1*(ΔL37) cells, respectively (Figures 2.3B and 2.3C). Based on these findings, we have uncovered a direct role for impaired H/ACA snoRNA expression toward defective patterns of rRNA pseudouridylation in X-DC patient cells. We further confirmed

these findings by performing quantitative High Performance Liquid Chromatography (HPLC). Early passage *DKC1*(ΔL37) primary fibroblasts displayed significant reductions in total pseudouridine levels in both 18S and 28S rRNA (Figure 2.3D). Notably, no differences in the total amount of 18S or 28S rRNA were observed (data not shown). Moreover, significant reductions in the total pseudouridine levels from five different *DKC1* point mutations including *DKC1*(T70I), *DKC1*(K314R) *DKC1*(K390Q), *DKC1*(A353V) and *DKC1*(T66A) were also observed (Figure 2.3E). The reductions in the total amount of rRNA pseudouridylation ranging from 10-25% may reflect unique differences in specific patterns of modifications on rRNA as revealed by mass spectrometry. Together, these findings provide the first evidence that rRNA modification defects are common amongst X-DC patients. Moreover, the patterns of Ψ modifications are distinct and directly correlate with specific decreases in subsets of H/ACA snoRNAs originating from distinct *DKC1* point mutations.

The pseudouridine synthase capacity of dyskerin is important for hematopoietic stem cell function

As individual H/ACA small RNAs from diverse classes, including those implicated in ribosome, splicing, and telomerase functions, are diminished in X-DC patient cells, an outstanding question is whether impaired dyskerin enzymatic activity is required for some of the pathological features of the disease. This is an important question as dyskerin is able to associate with diverse H/ACA small RNAs to maintain their stability. However, dyskerin acts as a pseudouridine synthase in the context of only a subset of these small RNAs. For example, dyskerin's association with TERC serves to stabilize the telomerase complex;

however, its association with H/ACA scaRNAs and snoRNAs converts these RNP particles into catalytically active complexes guiding site-specific conversions of uridine to Ψ residues on snRNAs and rRNA, respectively (Meier, 2005). Given that bone marrow abnormalities are common and amongst the primary causes of early mortality in DC patients, we sought to determine the precise contribution of the pseudouridine synthase activity of dyskerin towards hematopoiesis. To this end, we employed *DKC1*(c.-141 C>G) primary CD34+ hematopoietic progenitor cells. The *DKC1*(c.-141 C>G) mutation is characterized by severe features of X-DC, including significant bone marrow hypoplasia and cytopenia (Figure 2.1A). We introduced expression constructs for wild type *DKC1* (designated *DKC1*^{WT}) or a catalytically inactive *DKC1* mutant, D125A (designated *DKC1*^{D125A}) so that they were both expressed at equivalent levels in *DKC1*(c.-141 C>G) CD34+ cells. *DKC1*^{D125A} harbors a mutation in a critical amino acid within the evolutionarily conserved TruB Ψ synthase domain that is essential for enzymatic activity (Figures 2.4A) (Hamma et al., 2005; Rashid et al., 2006; Zebarjadian et al., 1999). We next assessed hematopoietic progenitor colony formation on methylcellulose in the presence of a complete cocktail of cytokines that sustains the differentiation of progenitor cells into mature myeloid and erythroid cells (Figure 2.4B). *DKC1*(c.-141 C>G) CD34+ cells are greatly impaired in their capacity to differentiate and generate mature myeloid and erythroid colonies as compared to matched healthy human CD34+ cells (Figure 2.4B). Strikingly, the expression of *DKC1*^{WT} completely restored the ability of *DKC1*(c.-141 C>G) CD34+ progenitors to differentiate into mature myeloid and erythroid cells (Figure 2.4B). In contrast, introduction of the *DKC1*^{D125A} catalytic mutant failed to rescue the severe differentiation defect present in these cells (Figure 2.4B). These findings provide significant

insight into the molecular basis that may account for specific hematopoietic defects in X-DC patients and strongly implicate dyskerin's pseudouridine synthase enzymatic activity as a requirement for efficient hematopoiesis.

Figures

Figure 2.1. Characterization of dyskerin-associated H/ACA small RNAs in X-DC patient cells. (A) Schematic of the *DKC1*(c.-141C>G) mutation illustrating the position of the base pair substitution on the *DKC1* promoter (top). Clinical features of the *DKC1*(c.-141C>G) patient are shown (bottom). (B) Quantification of DKC1 mRNA levels in CD34+ cells from two healthy controls and *DKC1*(c.-141C>G) patient was measured by real-time qPCR. (C) Heatmap diagram displaying hierarchical clustering of 32 H/ACA small RNA relative expression levels in X-DC patient cells. The expression of H/ACA small RNAs was measured by real-time qPCR, relative to two type-matched control cells for each mutation, and normalized to the abundance of RN7SK small non-coding RNA from at least three independent experiments. Each row represents a different type of X-DC patient-derived cell. Each column illustrates the expression of individual H/ACA small RNAs relative to controls. The color bar indicates the color-coding of small RNA expression from +3 to -3 in $\log_2$ space (bottom). Only slight variation in the expression of H/ACA small RNAs was observed amongst controls either by real-time qPCR or northern blot analysis (Figure S2.1).

Figure 2.2. Expression of dyskerin rescues H/ACA small RNA expression levels in primary X-DC fibroblasts. Expression levels of different classes of small RNAs in control,

DKC1(ΔL37) primary fibroblasts, and *DKC1*(ΔL37) primary fibroblasts expressing exogenous wild type dyskerin ($DKC1^{WT}$) measured by real-time qPCR. Graphs show mean fold expression ± SEM relative to control and normalized to the abundance of RN7SK small non-coding RNA from three independent experiments. Western blot analysis of dyskerin expression is shown in control and *DKC1*(ΔL37) primary fibroblasts in the absence or presence of $DKC1^{WT}$ (top). β-actin was used as loading control. Statistical analysis was performed using the unpaired Student's *t*-test, $*P<0.05$ and $**P<0.01$.

Figure 2.3. Defective site-specific and global rRNA pseudouridylation manifest in X-DC patient cells. (A) Schematic representation of the mass spectrometry approach used to detect site-specific pseudouridine modifications on 18S rRNA from control and X-DC patient cells. *m/z* stands for mass-to-charge ratio. ESI is an abbreviation for electrospray ionization. (B) Site-specific quantification of Ψ levels in two controls and in *DKC1*(ΔL37) fibroblasts (top) and *DKC1*(T66A) lymphoblasts (bottom). Graph shows mean percentage Ψ reduction ± SEM relative to two controls at specific Ψ sites on 18S rRNA from three independent experiments. Quantification of all Ψ sites examined in this study is shown in Figures S3B-S3C. The accuracy of these measurements is well controlled for by performing calibration curves, demonstrating a linear response to different concentrations of synthetic Ψ-containing oligonucleotides within the range of Ψ values observed in patient samples (Figure S2.2D). The percentage reductions in Ψ measurements are relative and not absolute. (C) Venn diagram illustrates unique and commonly reduced Ψ sites in X-DC patient cells analyzed. (D) HPLC quantification of 18S and 28S rRNA Ψ levels in control and *DKC1*(ΔL37) primary fibroblasts. The graph shows mean Ψ to cytosine (Ψ/C) ratio ± SEM

relative to controls from two independent experiments. (E) HPLC quantification of 18S rRNA Ψ levels in six independent controls and five X-DC lymphoblast cell lines harboring distinct *DKC1* point mutations. The specific *DKC1* mutation is presented on each column. The graph shows mean Ψ to cytosine (Ψ/C) ratio ± SEM for each X-DC lymphoblast cell line relative to controls from at least three independent experiments. Statistical analysis was performed using the unpaired Student's *t*-test, **P*<0.05 and ***P*<0.01.

Figure 2.4. Dyskerin pseudouridylation activity is important for HSC differentiation. (A) Schematic presentation of dyskerin coding region highlighting evolutionary conservation of the TruB Ψ synthase domain across several species. A substitution of aspartic acid (D) with alanine (A) at position 125 abolishes dyskerin pseudouridylation activity and was employed as a catalytically inactive $DKC1^{(D125A)}$ mutant. (B) Hematopoietic colony forming assay was performed on CD34+ progenitor cells from a healthy control and *DKC1*(c.-141C>G) patient in the absence or presence of wild type $DKC1^{WT}$ or its catalytic mutant $DKC1^{D125A}$ using methylcellulose supplemented with complete cytokines cocktail sustaining the growth of all blood cell lineages. The total number of colonies formed was scored 10 days after plating. Graph shows the mean total percentage number of colonies ± SEM relative to controls from two independent experiments. Statistical analysis was performed using the unpaired Student's *t*-test, ***P*<0.01

Figure 2.1

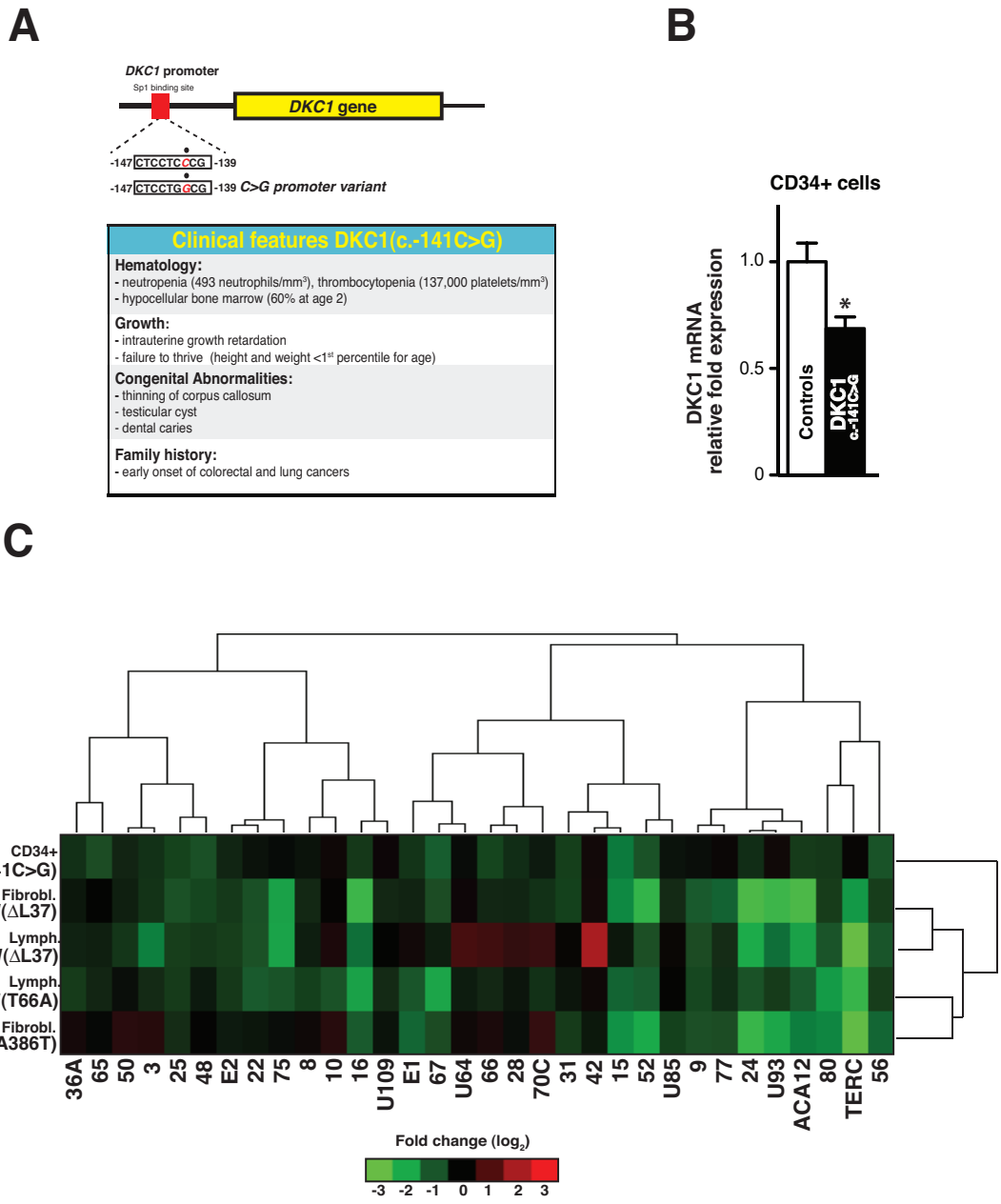
A
DKC1 promoter
Sp1 binding site
DKC1 gene
-147 CTCCTCCCG -139
-147 CTCCTGGCG -139 C>G promoter variant
Clinical features DKC1(c.-141C>G)
Hematology:
- neutropenia (493 neutrophils/mm3), thrombocytopenia (137,000 platelets/mm3)
- hypocellular bone marrow (60% at age 2)
Growth:
- intrauterine growth retardation
- failure to thrive (height and weight <1st percentile for age)
Congenital Abnormalities:
- thinning of corpus callosum
- testicular cyst
- dental caries
Family history:
- early onset of colorectal and lung cancers
B
CD34+ cells
DKC1 mRNA relative fold expression
1.0
0.5
0
Controls
DKC1 c.-141C>G
*
C
CD34+ DKC1(c.-141C>G)
Fibrobl. DKC1(ΔL37)
Lymph. DKC1(ΔL37)
Lymph. DKC1(T66A)
Fibrobl. DKC1(A386T)
36A 65 50 3 25 48 E2 22 75 8 10 16 U109 E1 67 U64 66 28 70C 31 42 15 52 U85 9 77 24 U93 ACA12 80 TERC 56
Fold change (log2)
-3 -2 -1 0 1 2 3

Figure 2.2

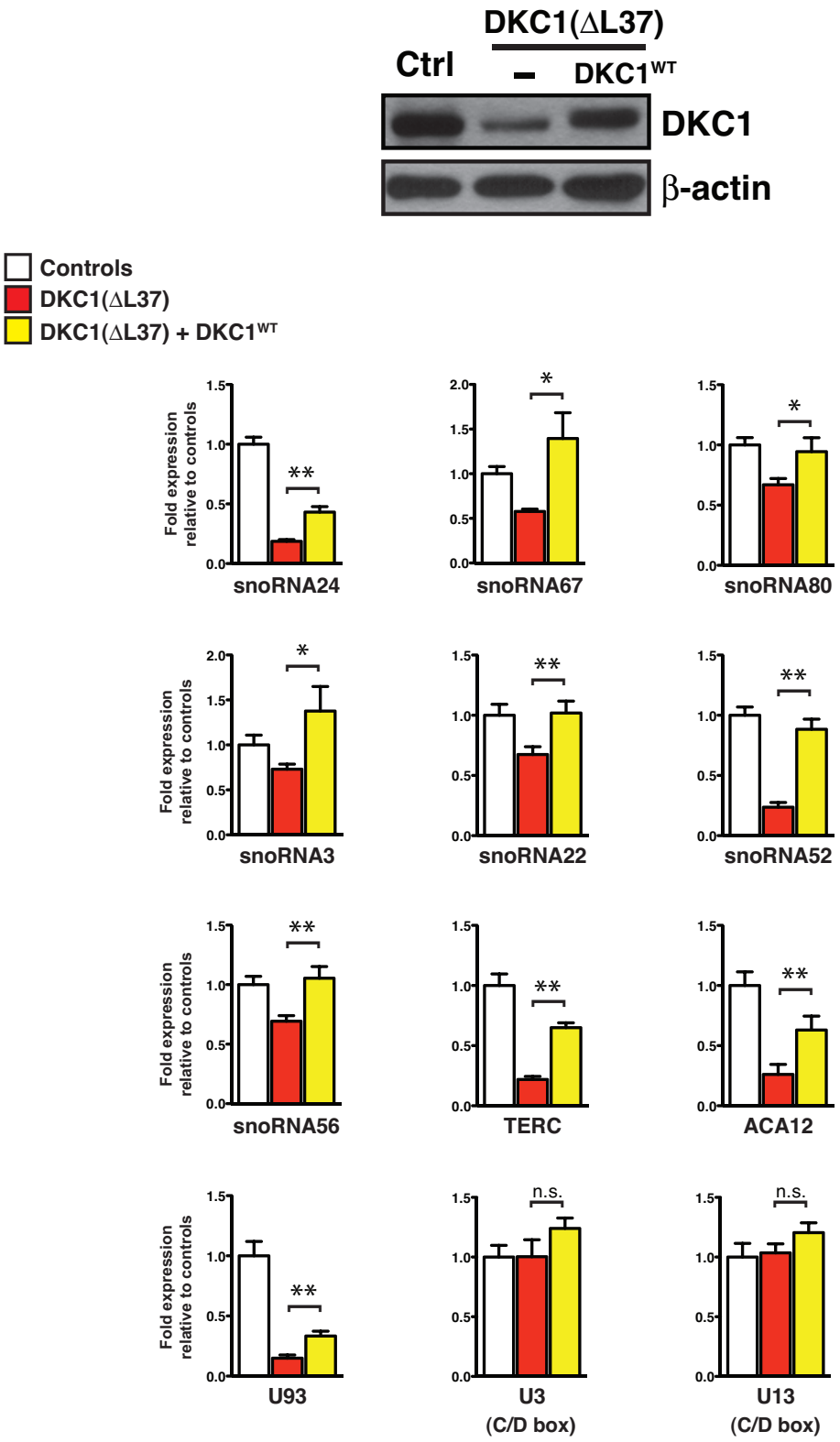
DKC1(ΔL37)
Ctrl
-
DKC1WT
DKC1
β-actin
Controls
DKC1(ΔL37)
DKC1(ΔL37) + DKC1WT
Fold expression relative to controls
snoRNA24
snoRNA67
snoRNA80
snoRNA3
snoRNA22
snoRNA52
snoRNA56
TERC
ACA12
U93
U3 (C/D box)
U13 (C/D box)
n.s.

Figure 2.3

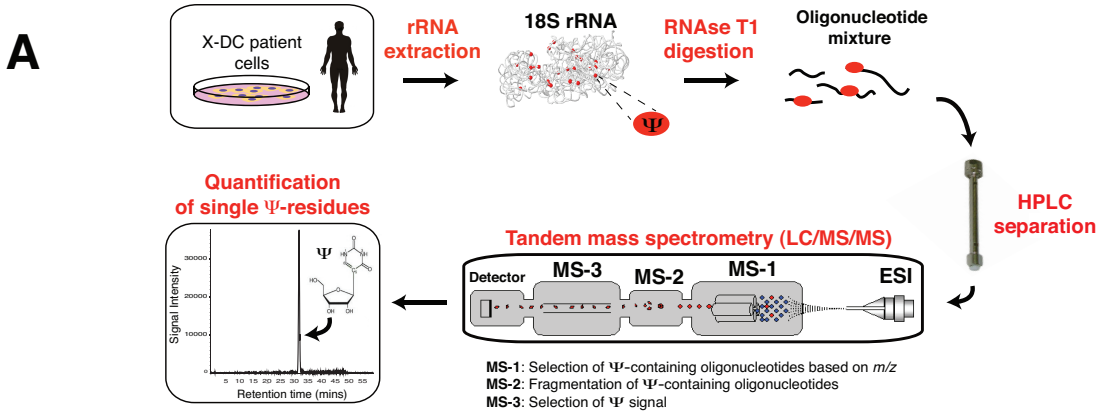
A
X-DC patient cells
rRNA extraction
18S rRNA
RNAse T1 digestion
Oligonucleotide mixture
HPLC separation
Tandem mass spectrometry (LC/MS/MS)
Detector
MS-3
MS-2
MS-1
ESI
Quantification of single Ψ-residues
Signal Intensity
Retention time (mins)
MS-1: Selection of Ψ-containing oligonucleotides based on m/z
MS-2: Fragmentation of Ψ-containing oligonucleotides
MS-3: Selection of Ψ signal

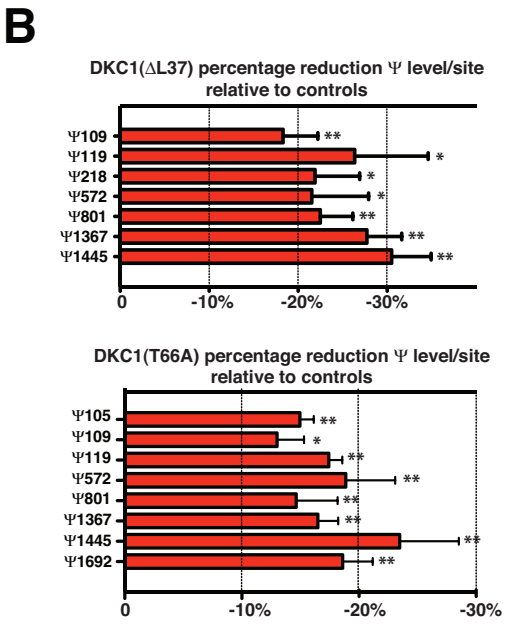
B
DKC1(ΔL37) percentage reduction Ψ level/site relative to controls
Ψ109
Ψ119
Ψ218
Ψ572
Ψ801
Ψ1367
Ψ1445
0
-10%
-20%
-30%
DKC1(T66A) percentage reduction Ψ level/site relative to controls
Ψ105
Ψ109
Ψ119
Ψ572
Ψ801
Ψ1367
Ψ1445
Ψ1692

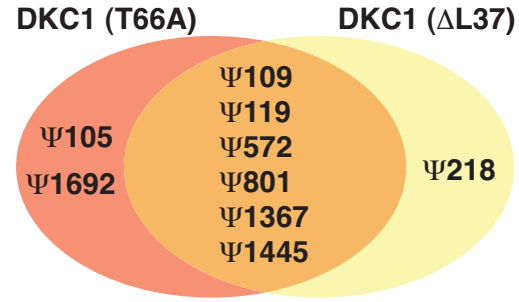
C
DKC1 (T66A)
DKC1 (ΔL37)
Ψ105
Ψ1692
Ψ109
Ψ119
Ψ572
Ψ801
Ψ1367
Ψ1445
Ψ218

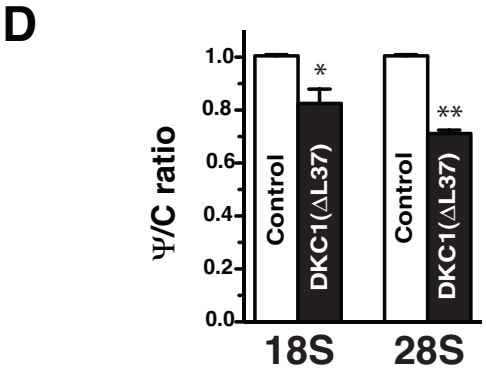
D
Ψ/C ratio
Control
DKC1(ΔL37)
Control
DKC1(ΔL37)
18S
28S

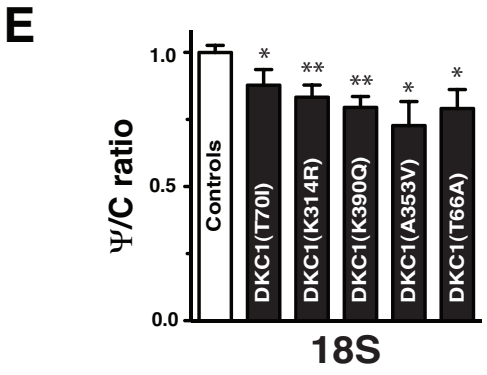
E
Ψ/C ratio
Controls
DKC1(T70I)
DKC1(K314R)
DKC1(K390Q)
DKC1(A353V)
DKC1(T66A)
18S

Figure 2.4

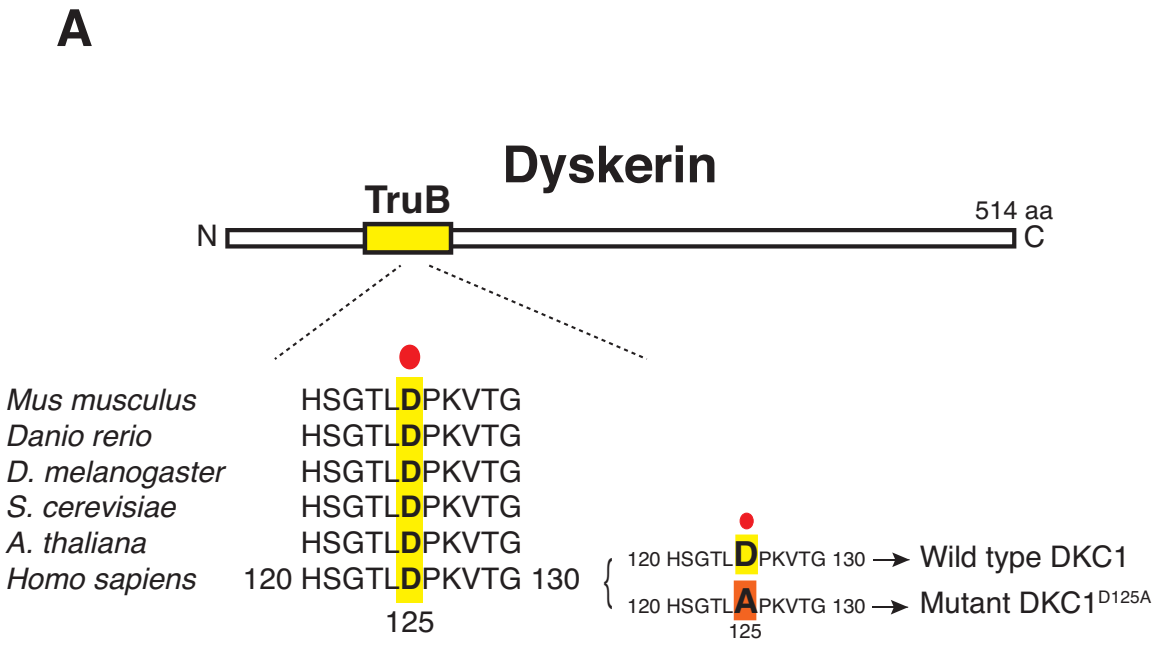
A
Dyskerin
TruB
N
514 aa
C
Mus musculus HSGTLDPKVTG
Danio rerio HSGTLDPKVTG
D. melanogaster HSGTLDPKVTG
S. cerevisiae HSGTLDPKVTG
A. thaliana HSGTLDPKVTG
Homo sapiens 120 HSGTLDPKVTG 130
125
120 HSGTLDPKVTG 130 → Wild type DKC1
120 HSGTLAPKVTG 130 → Mutant DKC1D125A
125

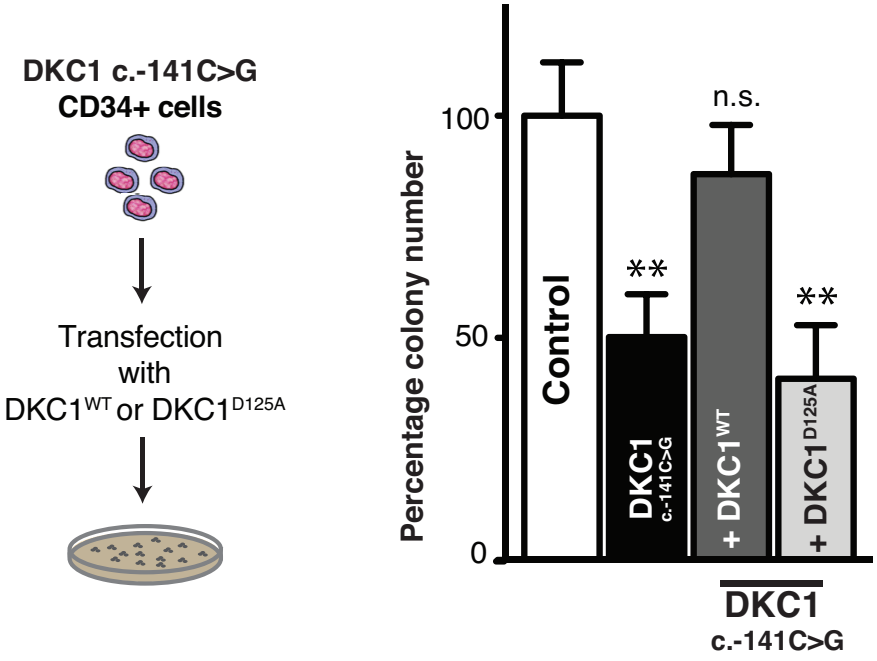
B
DKC1 c.-141C>G
CD34+ cells
Transfection
with
DKC1WT or DKC1D125A
Percentage colony number
100
50
0
Control
DKC1 c.-141C>G
+ DKC1WT
+ DKC1D125A
n.s.
**
**
DKC1
c.-141C>G

Supplemental Figure 2.1. H/ACA small RNAs expression levels in controls and X-DC patient cells. (A) Heatmap diagram showing hierarchical clustering of the mean relative expression of H/ACA small RNAs in two independent primary control and DKC1(c.–141C > G) CD34+ cells. (B) Heatmap diagram showing hierarchical clustering of the mean relative expression of H/ACA small RNAs in two independent controls and DKC1(T66A) lymphoblasts. (C) Heatmap diagram showing hierarchical clustering of the mean relative expression of H/ACA small RNAs in two independent controls and DKC1(DL37) primary fibroblasts. The expression of H/ACA small RNAs was measured by real-time qPCR from three independent experiments. Each row represents a control or X-DC patient-derived cells. Columns show individual H/ACA small RNA expression levels. The color bar indicates the color-coding of small RNA expression from +3 to -3 in log2 space. (D) Northern blot analysis of the indicated small RNAs in fibroblasts from two healthy control (Ctrl1 and Ctrl 2) and DKC1(DL37) patients, with RN7SK small ncRNA used as a loading control (top). The graph shows the mean ratio ±SEM of H/ACA snoRNA E2, snoRNA 24, and snoRNA 52 expression normalized to the levels of RN7SK in two controls and DKC1(DL37) fibroblasts from three independent experiments (bottom). Statistical analysis was performed using the unpaired Student's t test, *$p < 0.05$ and **$p < 0.01$.

Supplemental Figure 2.2. Site-Specific Ψ Quantifications on 18S rRNA. (A) The position of specific Ψ sites on 18S rRNA that were resolved and quantified by mass spectrometry as well as the corresponding guide H/ACA snoRNAs annotated to guide the modifications at these sites are shown. H/ACA snoRNAs analyzed in our study are highlighted in bold (see Figure 1C). (B) Site-specific quantification of Ψ levels in two

controls and in DKC1(DL37) fibroblasts. Individual graphs show the mean pseudouridylation levels ±SEM relative to two controls from three independent experiments. Statistical analysis was performed using the unpaired Student's t test, *p < 0.05 and **p < 0.01. (C) Site-specific Ψ quantifications in 18S rRNA from controls and DKC1(T66A) lymphoblasts. Individual graphs show the mean pseudouridylation levels ±SEM relative to two controls from three independent experiments. Statistical analysis was performed using the unpaired Student's t test, *p < 0.05 and **p < 0.01. (D) Calibration curves were generated by LC-MS/MS analysis of synthetic Ψ-containing oligonucleotide corresponding to sequences of human 18S rRNA. For each oligonucleotide the position of the Ψ residue is indicated: ΨUAUG (Ψ109), UmUΨACUUUG (Ψ801), and UCCACUΨUAAAmUCCUUUAACG (Ψ572). Graphs show MRM transition peak areas corresponding to concentrations ranging from 7.8 fmol to 1.0 pmol ofJ-containing oligonucleotides. Each data point is the average ±SEM of triplicate measurements. Data was fit to a linear regression function, were y represents slope and R2 is the correlation coefficient. All Ψ-containing oligonucleotides yielded linear calibration curves with high precision.

Figure S2.1

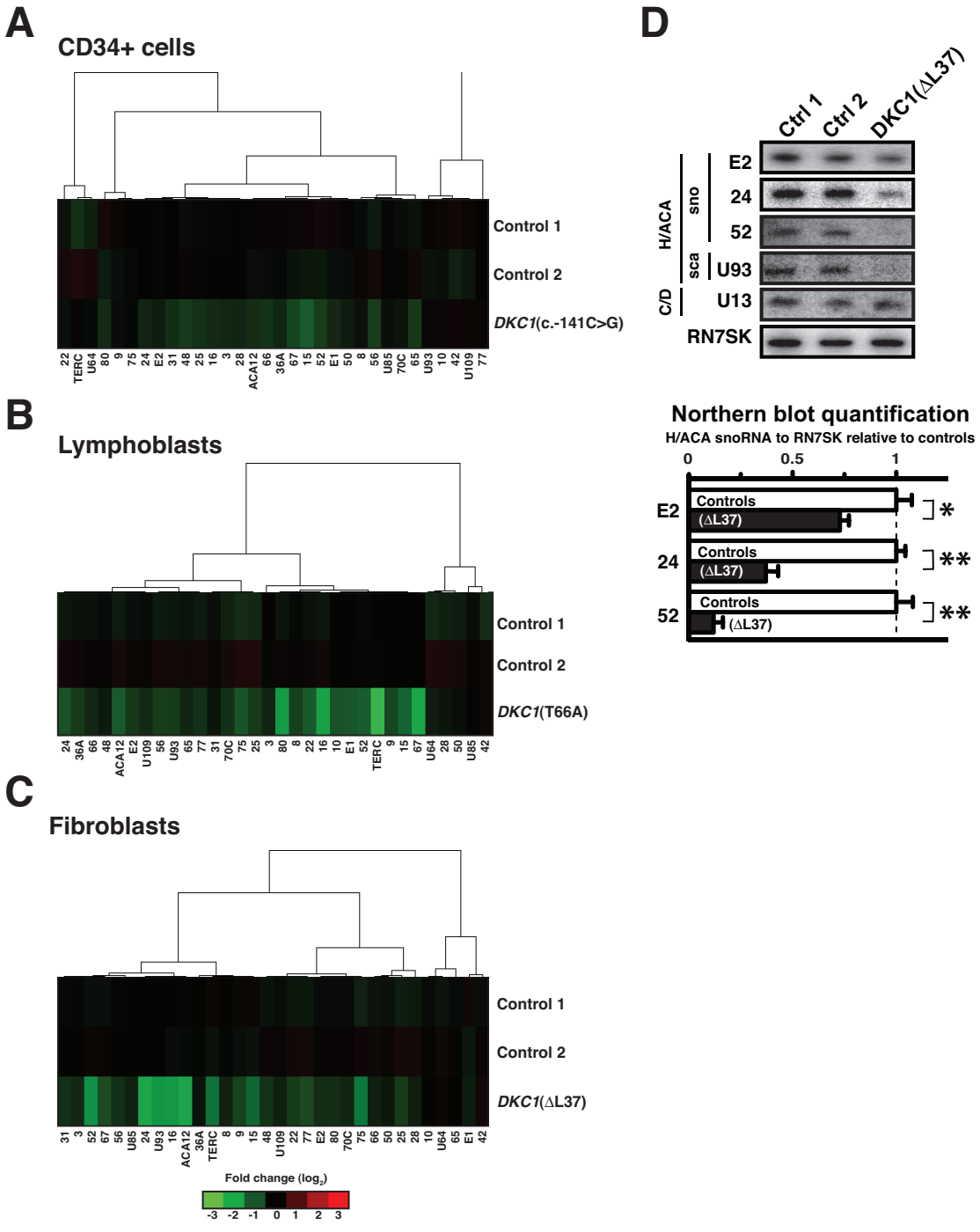
A
CD34+ cells
Control 1
Control 2
DKC1(c.-141C>G)
22 TERC U64 80 9 75 24 E2 31 48 25 16 3 28 ACA12 66 36A 67 15 52 E1 50 8 56 U85 70C 65 U93 10 42 U109 77
B
Lymphoblasts
Control 1
Control 2
DKC1(T66A)
24 36A 66 48 ACA12 E2 U109 56 U93 65 77 31 70C 75 25 3 80 8 22 16 10 E1 52 TERC 9 15 67 U64 28 50 U85 42
C
Fibroblasts
Control 1
Control 2
DKC1(ΔL37)
31 3 52 67 56 U85 24 U93 16 ACA12 36A TERC 8 9 15 48 U109 22 77 E2 80 70C 75 66 50 25 28 10 U64 65 E1 42
Fold change (log2)
-3 -2 -1 0 1 2 3
D
Ctrl 1
Ctrl 2
DKC1(ΔL37)
H/ACA
sno
sca
C/D
E2
24
52
U93
U13
RN7SK
Northern blot quantification
H/ACA snoRNA to RN7SK relative to controls
0
0.5
1
E2
24
52
Controls
(ΔL37)
*
**
**

Figure S2.2

A

Ψ site on 18S rRNA	Corresponding guide H/ACA snoRNAs
Ψ105	**snoRNA36A**, snoRNA36B, **snoRNA50**, snoRNA76
Ψ109	**snoRNA42, snoRNA80**, snoRNA80B
Ψ119	**snoRNA66**
Ψ218	**snoRNA31**
Ψ572	**snoRNA42, snoRNA80**, snoRNA80B
Ψ801	**snoRNA25**
Ψ1367	**snoRNA15**
Ψ1445	**snoRNA67**
Ψ1692	snoRNA70B, **snoRNA70C**, snoRNA70D, snoRNA70E, snoRNA70F, snoRNA70G

B

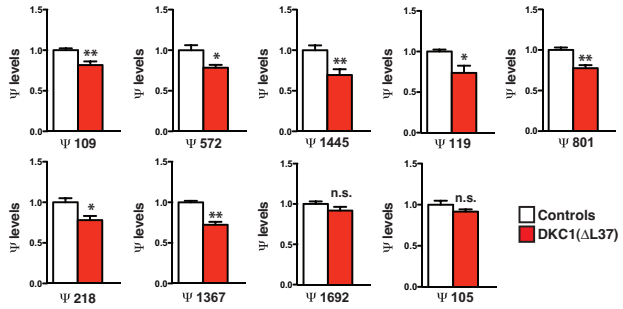

C

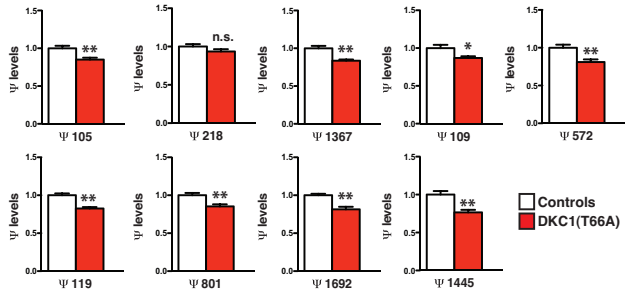

D

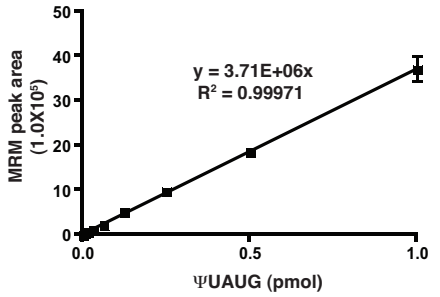

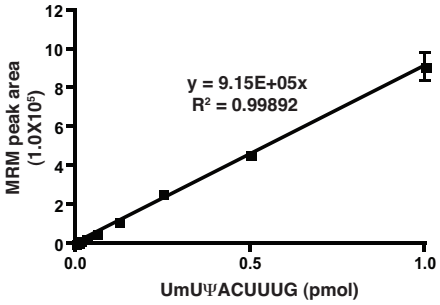

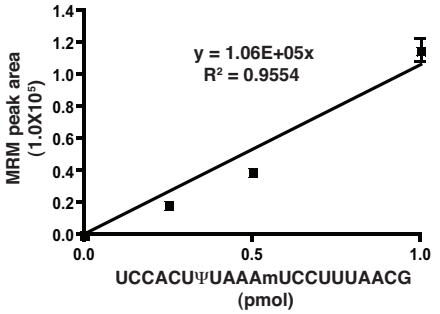

Supplemental Tables

Supplemental Table S2.1. List of Ψ-Containing Oligonucleotides and Their MRM Transitions Used in the Study.

Supplemental Table S2.2. Sequences of Primers Used in the Study.

Table S2.1

Ψ site on 18S rRNA	Oligonucleotide Sequence	m/z	RT (min)	Ψ Ion profile
Ψ105	CUCAmUUAAAΨCAG	692.6	39	207.04
Ψ109	ΨUAUG	535.7	24	165.0302
Ψ119	UUmCCΨUUmG	505	33	207.04
Ψ218	CAΨUUAUCAG	636	36	207.04
Ψ572	UCCACUΨUAAAmUCCUUUAACG	662	40	207.04
Ψ801	UmUΨACUUUG	568.5	34	207.04
Ψ1367	ΨUAAUUCCG	570.1	33	165.0302
Ψ1445	CCCCCAACUUmCUΨAGmAG	713.7	40	207.04
Ψ1692	CCCΨUUG	548	30	207.04

Normalization control on 18S rRNA

Oligonucleotide Sequence	m/z	RT (min)	Ion profile
AmAmCCUG	996	38	362

Table S2.2

SNORA3	Rev tggtgactgactgtgccataa
SNORA8	For GCATGGTATCTGCACTCAGC
SNORA8	Rev GAAAACCAACGATGCCAGAT
SNORA52	For GAGCACCCTAGAAGCCTCAC
SNORA52	Rev CTAGAAGTGCCCATGACGTG
E1	For CTCTGTCCAAGTGGCGTAGG
E1	Rev CGTTGTGGAAAGGGACTTGT
E2	For ACTGACTGGCCGATGAACTC
E2	Rev CCAGAGACCCTTGTGGTGTT
U64	For TCACCCGTGTGACTTTCGTA
U64	Rev ACCCCTCAAGGAAAGAGAGG
snoRNA67	For agcagcttggaatagaatctgg
snoRNA67	Rev ccaaggaaggcagaggaaata
TERC	For CTAACCCTAACTGAGAAGGGCGTA
TERC	Rev GGCGAACGGGCCAGCAGCTGACATT
ACA12	For TTCTCAAGGTGAAGATAACTCTTTG
ACA12	Rev CGACCCACCCTTTTTACTTG
U85	For GGCTGTTGTGATTCAGTTGG
U85	Rev CTGTATCGCCCACCAAGATT
U93	For GAGCACACCAGACTTGCAGA
U93	Rev CAGAGGAAAATTGCACATGG
U109	For GCATGTGGAAATGTCTGCTT
U109	Rev CAGCCCTGAGAACTCCTTTG
U3	For TTTTCTCCTGAGCGTGAAGC
U3	Rev TCCCCAATACGGAGAGAAGA
U13	For TTCATGAGCGTGATGATTGG
U13	Rev GTAATGTGCCCACGTCGTAA
RN7SK	For AGGGTTGATTCGGCTGATCT
RN7SK	Rev CTCTATCGGGGATGGTCGT
snord44	For CCTGGATGATGATAAGCAAATG
snord44	Rev GAGCTAATTAAGACCTTCATGTTCA
snord49A	For CACTAATAGGAAGTGCCGTCAG
snord49A	Rev CAGACAGGAGTAGTCTTCGTCAGT

Materials and Methods

NCI participant lymphocytes

The patients with T70I, K314R, A353V, and K390Q mutations in *DKC1* are participants in the Institutional Review Boards (IRBs)-approved longitudinal cohort study at the National Cancer Institute (NCI) entitled "Etiologic Investigation of Cancer Susceptibility in Inherited Bone Marrow Failure Syndromes" (www.marrowfailure.cancer.gov, NCI 02-C-0052, ClinicalTrials.gov Identifier: NCT00027274 (Alter et al., 2010). See Extended Experimental Procedures for detailed methods.

Commercially Available Healthy Controls and X-DC Cells

Controls (GM04390 and GM00730), X-DC fibroblasts DKC1 (A386T) (GM04646), and DKC1(ΔL37) (GM01774) (Passage 7-10) were obtained from Coriell Cell Repositories (Coriell Institution for Medical Research, Camden, NJ) and maintained in MEM as described (Bellodi et al., 2010a). Controls (GM11626, GM07544, GM03299, GM22674, GM22647, GM08814 and GM03329) and DKC1(T66A) (GM03195) lymphocytes were obtained from Coriell Cell Repositories and maintained in 20% RPMI as described (Bellodi et al., 2010a).

Primary bone marrow progenitor cells

Informed consent was obtained from the *DKC1*(c.-141 C>G) patient in accordance with a human subjects study protocol approved by the IRBs of the Seattle Children's Hospital and Fred Hutchinson Cancer Research Center. Anonymous healthy control bone marrow cells

were obtained from discarded bone marrow harvest screens as approved by the Fred Hutchinson Cancer Research Center IRB.

Plasmids

A plasmid encoding DKC1WT has previously been described (Bellodi et al., 2010b). The DKC1D125A mutant was generated using a site-directed mutagenesis kit (Stratagene) according to manufacturer's instructions.

Western Blot, Northern Blot, and qPCR Analysis

Western blot was performed using standard protocols and the following primary antibodies: dyskerin (1:1,000; Santa Cruz), FLAG (1:1,000; Sigma), and β-actin (1: 5,000; Sigma). Northern blot analysis was performed on total RNA (2 μg), isolated using TRIzol reagent (Invitrogen), using 32P end labeled oligonucleotides (Table S2.2) and quantification was performed using ImageQuant 5.2 software (Molecular Dynamics). For real-time qPCR analysis, total RNA was isolated using TRIzol Reagent and treated with Turbo DNA-free kit (Ambion). 1-2 μg of RNA was reverse transcribed using SuperScript II Reverse Transcriptase Kit (Invitrogen) and analysis was performed using iQ Sybr Green mix (Bio-Rad). The expression of H/ACA small RNAs was measured by real-time qPCR, relative to two type-matched control cells for each mutation, and normalized to the abundance of RN7SK small ncRNA from at least three independent experiments. Primer sequences are listed in Table S2.2. Selected H/ACA snoRNAs guide Ψ modifications within functionally important regions of both the small and large ribosomal subunits such as the

peptidyl transferase center (PTC), the decoding center (DC), as well as ribosome expansion segments.

HPLC and Mass Spectrometry quantification of human rRNA pseudouridylation

Global analysis of rRNA pseudouridine levels was performed by HPLC analysis on a C18 250x4.6 mm (particle size 5 μm) Reverse phase HPLC column (Agilent) as previously described (Jack et al., 2011). For quantifications of site-specific Ψ modifications all LC-MS/MS analyses were performed using an in-house packed capillary column (320 μm ID x 150 mm length, packed with Jupiter 4 μm Phenomenex Proteo 90 A material). The solvents used were as described with minor modifications (Apffel et al., 1997). A stock solvent solution was made consisting of 460 ml of HPLC grade water (Fisher Scientific), 42 ml of 1,1,1,3,3,3-hexafluoro-2-propanol (Fluka) and 1.2 ml of Triethylamine (Pierce). Solvent A was prepared by diluting the stock 1:1 V:V with HPLC grade water. Solvent B was prepared by diluting the stock 1:1 V:V with HPLC grade methanol (Fisher). The HPLC system consisted of an Eldex Micropro LC and a Dionex LC-Packings FAMOS auto sampler. The flow rate was 5 to 7 μl/min on a 45 min linear gradient from 0%–70% B. All samples and standards were dissolved in Solvent A prior to injection. Selected Ψ sites on human 18S rRNA (Figure S2.2A and Table S2.1) were determined by LC-MS/MS following RNase T1 (Roche) digestion using 10U/μg of gel purified 18S rRNA (0.2-1.0 μg) in 10 mM Tris-HCl, 1 mM EDTA, pH 7.4 on a Thermo LTQ Orbitrap Velos mass spectrometer using 90 min gradients and operated in negative ion detection mode. The IS voltage was set at 4.0 to 5.0 kV, with source temperature at 225°C and a sheath gas flow of 10. The instrument was run in a data dependent mode, using a survey scan from 400-1600, resolution 30,000, and with

a 2E6 AGC setting for full scan with one microscan of 250 ms (ms). After every survey scan, the top three most intense ions were selected for HCD fragmentation with 2E5 AGC setting, and 3 × 200 ms microscans. The HCD mass range was set at 100-2000. Ions selected for HCD were added to an exclusion list for the next 60 s. The data files were processed using Xcalibur software suite (Thermo Scientific). Extracted ion profiles for previously characterized Ψ ions at 165.0302 (when the Ψ is at the 5′ end of an oligo) and 207.0400 (when elsewhere in the oligo) (Pomerantz and McCloskey, 2005) were created for all data files and were used to locate and map distinct Ψ-containing oligonucleotides from purified human 18S rRNA. The HCD spectrum was manually interpreted with the aid of Ariadne (Nakayama et al., 2009) and the Mongo Oligo Mass Calculator program (http://rna-mdb.cas.albany.edu/RNAmods/masspec/mongo.htm). The identifications of Ψ-containing oligonucleotides were facilitated by the accurate masses (±5 ppm) obtained from the Velos instrument in both full scan and HCD scan mode. In total nine oligonucleotides containing one unique Ψ residue from human 18S rRNA were selected and the sequence of the oligonucleotides with the position of the pseudouridine highlighted in bold were the following: ΨUAUG (Ψ109), CCCΨUUG (Ψ1692), UUmCCΨUUmG (Ψ119), CAΨUUAUCAG (Ψ218), UmUΨACUUUG (Ψ801), ΨUAAUUCCG (Ψ1367), CUCAmUUAAAΨCAG (Ψ105), CCCCCAACUUmCUΨAGmAG (Ψ1445), UCCACUΨUAAAmUCCUUUAACG (Ψ572). Upon identification of specific Ψ sites, relative quantitation was obtained by MRM using an ABSciex QTRAP 4000 mass spectrometer and using the same HPLC conditions described above. The appropriate parent mass determined by the Velos HCD experiments was selected for MRM analysis. The QTRAP was operated in negative ion mode, using the Turbo IonSpray source with a spray voltage of −4.5 kV, ion source gas one value of 15 and a

source temperature of 50°C. The instrument was operated in LOW/LOW resolution setting for these analyses. The dwell time for each transition was set to 50 ms and the collision energy was set at 65V. The Analyst 1.5 software was used to determine the peak area for each transition. To ascertain that the MRM response of the Ψ-containing oligonucleotides was linear over the range of areas detected in patient samples, a standard curve of areas against amount injected was generated for three synthetic Ψ-containing oligonucleotides (Figure S2.2D). The 996 (2+ ion) to 362 transition (362 is the y1 ion for this oligo) of a non-Ψ containing oligonucleotide (AmAmCCUG) was selected as a normalization control in the analysis. The transitions used for MRM experiments and retention times for each oligonucleotide are shown in Table S2.1. Using this method, for a given oligonucleotide, only the presence of a Ψ ion can be determined and not the amount of the corresponding oligonucleotide devoid of Ψ. Therefore, Ψ quantification measurements are relative and not absolute. Using the experimental conditions described above, we were unable to quantify single Ψ residues present on oligonucleotides that coeluted under our HPLC conditions or on oligonucleotides containing more than one Ψ residue. However, resolution of additional Ψ sites on 18S rRNA may be achieved by employing RNA nucleases other than RNAase T1 (such as RNase A and/or U2) and/or by altering the HPLC conditions.

Methylcellulose Colony Forming Assays

CD34+ hematopoietic progenitors were purified from total bone marrow mononuclear (BMCs) cells aspirates using CD34+ microbeads (Miltenyi Biotech) according to the manufacturer instructions. After purification, flow cytometry confirmed that the isolated cells were greater than 85% CD34+. Cells were cultured in StemSpan SFEM serum-free

media (StemCell Technologies) supplemented with 100ng/ml of the following cytokines; stem cell factor (SCF), Flt3 ligand, thrombopoietin (TPO), and interleukin-6 (IL-6) and incubate overnight at 37°C. Healthy control and X-DC patient purified CD34+ cells were transfected with control, DKC1WT or DKC1D125 expression vectors using the human CD34+ Amaxa nucleofection kit (Amaxa Biosystems). Transfected CD34+ progenitor cells were cultured as described above and plated in methylcellulose medium (Methocult H4434, StemCell Technologies) supplemented with SCF, GM-CSF, interleukin-3 (IL-3) and erythropoietin (EPO) after 12 hr. Cells were seeded at 500 cells/dish in duplicate and maintained at 37°C. Colonies containing more than 20 cells were scored using an inverted light microscope (Leica) after 10 days. All cytokines were purchased from Peprotech.

Acknowledgements

We thank M. Barna for critical discussion and reading of this manuscript; K. Tong for editing the manuscript; the Fujimori laboratory for technical support and equipment; J. Johl for technical assistance and Lizette Caballero and the UCSF BMT Laboratory for their generous assistance. We also thank Drs. B. P. Alter, and N. Giri at the National Cancer Institute, for clinical characterization of patients and biospecimen collection. We are grateful to the patients for their valuable contributions to this study. C.B. is a fellow of the Leukemia & Lymphoma Society and Aplastic Anemia & MDS International Foundation. D.R. is a Leukemia & Lymphoma Society Scholar. This work was supported, in part, by the intramural research program of the Division of Cancer Epidemiology and Genetics, National Cancer Institute, National Institutes of Health (S.S.). This work is supported by NIH

R01DK098057-06A1 (D.R.), NIH R01HL085572 (D.R.), NIH 3R01HL085572-05S1 (D.R.), NIH NIGMS 8P41GM103481 (A.B.) and NIH NIGMS 8P41GM103481 (A.B.).

Chapter 3: Heterogeneity in Ribosomal RNA base modifications modulate lipid metabolic flux to maintain a tumor suppressive program

Background

The field of epitranscriptomics has illuminated that both coding and non-coding RNAs contain a large variety of post-transcriptional nucleotide modifications that change the chemical composition of RNA. However, since the discovery of the first RNA nucleotide modification more than fifty years ago, the function of these modifications remains poorly understood. The RNA component of the ribosome, ribosomal RNA (rRNA) is the most abundant type of RNA in all domain of life and contains the highest amount of base modifications. Ribosomes are complex cellular ribonucleoprotein machines responsible for translating mRNA to protein. A common evolutionary conserved feature of all ribosomes is that they are decorated with nucleotide modifications, however the function of these modifications and whether they are subject to regulation remains poorly understood. Interestingly, both the complexity of the machinery required to modify rRNA and the number of modifications found within rRNA have significantly increased from Achaea to eukaryotes suggesting that these nucleotide modifications may have evolved additional roles within eukaryotic ribosomes (McMahon et al., 2013). Intriguingly, several studies demonstrate that not all, but distinct groups of small non-coding RNAs implicated in guiding nucleotide modifications at specific sites on rRNA are altered in numerous developmental disorders and cancer (Bellodi et al., 2013; He et al., 2002; Heiss et al., 1998;

Marcel et al., 2013; Newton et al., 2003; Valleron et al., 2012a; Valleron et al., 2012b; Williams and Farzaneh, 2012). These interesting findings raise the question as to whether base modifications within specific clusters of the ribosome harbor previously uncharacterized regulatory potential within the ribosome to mediate various cellular functions in higher eukaryotes.

Pseudouridine (Ψ), the most abundant nucleotide modification on rRNA, is guided by a class of intron-encoded non-coding RNAs termed H/ACA small nucleolar RNAs (snoRNAs) in association with a protein complex harboring the pseudouridine synthase, dyskerin (Ganot et al., 1997a; Lafontaine et al., 1998; Ni et al., 1997; Watkins et al., 1998). The specificity of this reaction is determined by direct base pairing of the H/ACA snoRNAs to specific regions of rRNA, thus guiding the conversion of distinct uridine residues to pseudouridine. The observation that only specific uridine residues are converted to pseudouridine suggests that the position of these nucleotides modification within the ribosome may be important for its activity. Thus, an outstanding question is whether individual pseudouridine modifications influence the ability of the ribosome to translate the transcriptome and more importantly whether the pattern of Ψ modifications on rRNA is differentially regulated. To gain insights into the putative role of H/ACA snoRNAs and site-specific pseudouridine modifications within the ribosome in response to distinct cellular stimuli, we sought to determine the landscape of H/ACA snoRNA expression during the earliest cellular responses to oncogenic insult such as DNA damage.

Unexpectedly, upon profiling H/ACA small RNAs in primary human fibroblasts, we observed coordinated regulation of specific subsets of H/ACA snoRNAs guiding modifications within similar regions of rRNA following DNA damage. The observed

coordinated regulation in H/ACA snoRNA expression is functionally important as we observed a corresponding change in site-specific rRNA Ψ modifications within specific regions of the ribosome. Furthermore, we uncovered a critical role for one snoRNA, SNORA24, towards regulating lipid metabolism both *in vitro* and *in vivo* to maintain senescence, a stress response that acts as a critical barrier against cellular transformation. Specifically, we found that loss of function of H/ACA SNORA24 and inhibition of its target rRNA Ψ modifications alters the translation of mRNAs implicated in lipid metabolism. Rewired lipid metabolism results in increased lipid synthesis allowing for bypass of senescence in response to DNA damage in primary human fibroblasts and upon activation of oncogenic N-Ras^{V12} in mouse liver. Importantly, excessive lipid content in human cancers is now considered a hallmark of disease aggressiveness (Abramczyk et al., 2015; Beloribi-Djefaflia et al., 2016; Bozza and Viola, 2010; de Gonzalo-Calvo et al., 2015; Yue et al., 2014). Therefore, we further probed whether increased lipid synthesis upon loss of SNORA24 contributes to cellular transformation and tumor development. Strikingly, we observe that loss of function of SNORA24 not only leads to bypass of senescence upon activation of oncogenic N-Ras^{V12} but also resulted in the development of hepatocellular carcinoma with significant accumulation of lipid droplets. These exciting findings provide the first evidence that the pattern of RNA base modifications within the ribosome are dynamically regulated in response to oncogenic insult and suggests a new layer of ribosome-mediated control in safeguarding the genome against cellular transformation.

Results

Dynamic regulation of H/ACA snoRNAs and specific Ψ sites within rRNA upon oncogenic insult

It remains incompletely understood whether single Ψ modifications within the ribosome have an impact on gene expression at the post-transcriptional level. Furthermore, an outstanding question is whether the expression and biogenesis of H/ACA snoRNAs are differentially regulated to alter the pattern of Ψ modifications. To investigate whether H/ACA snoRNAs and rRNA Ψ-modifications are altered in response to specific cellular stimuli, we analyzed the expression of a large panel of H/ACA snoRNAs in primary human fibroblasts during the earliest cellular responses to oncogenic insult such as DNA damage. Upon DNA damage primary cells dynamically regulate gene expression programs to repair DNA damage and counteract oncogenic transformation in a process known as senescence (di Fagagna, 2008). In fact, cellular senescence is a critical and cell autonomous anti-tumor barrier that restrains the proliferation of cells carrying potentially oncogenic genomic alterations. However, in this somewhat 'quiescent' state cells remain metabolically active and upon acquiring subsequent oncogenic lesions bypass senescence and are fully transformed. Surprisingly, analysis of a large number of H/ACA snoRNAs in primary human skin fibroblasts treated with gamma irradiation (10 Gy) revealed dynamic regulation of distinct H/ACA snoRNAs (Figure 3.1). For example, whereas no change in the expression of distinct H/ACA snoRNAs, such as snoRNA21 and snoRNA45, were observed upon DNA damage, other snoRNAs had either increased or decreased levels compared to non-

irradiated controls such as snoRNA24 and snoRNA64, respectively (Figure 3.1A). Unexpectedly, we observed a coordinated regulation of specific subsets of H/ACA snoRNAs guiding Ψ modifications within distinct clusters on both 18S and 28S rRNA as revealed by modeling sites of modification on the 3D structure of the ribosome (Figure 3.1). For example, snoRNAs displaying co-regulated expression such as snoRNA20, snoRNA24, snoRNA46, and snoRNA50 guide modifications within helix 3, 4, 18 and expansion segment 6 ($ES6^S$) in 18S rRNA (Figure 3.1A). Interestingly, helix 18 and $ES6^S$ have been shown to make direct contact with *cis*-acting RNA elements and eukaryotic initiation factor 3 (eIF3) respectively, thereby suggesting that regulation of Ψ modifications within this region may have important implications for translation regulation of gene expression (Hashem et al., 2013; Schuler et al., 2006; Weingarten-Gabbay et al., 2016). Furthermore, we also observe a down regulation in the expression of snoRNAs guiding Ψ modifications within a unique region of rRNA (Figure 2.1B), such as snoRNA37, snoRNA64, snoRNA17, and snoRNA33. These exciting results provide the first evidence that H/ACA snoRNAs are dynamically regulated in response to distinct cellular cues and suggest that the pattern of modifications within the ribosome may be subsequently be altered in response to oncogenic insult.

Currently, it remains unknown whether the pattern of RNA modifications on the ribosome are regulated or whether changes in H/ACA snoRNA expression influence their function in guiding Ψ modifications. To determine whether changes in snoRNA expression upon DNA damage may change the pattern of Ψ modifications we next investigate site-specific pseudouridylation of two residues within helix 18 and ES6. To this end, we employed a thin-layer chromatography based method that allows for the quantification of pseudouridine and uridine per site on rRNA, a precision that is currently not feasible with

recently described high throughput sequencing methods (Figure 3.2A) (Karijolich et al., 2010). Quantification of the amount of pseudouridine and uridine at individual sites revealed that, at steady state levels, there are differential levels of pseudouridylation within the ribosome (Figure 3.2B). For example, we noted significant difference in the amount of Ψ present at position 609 and position 863 on 18S rRNA. These exciting findings challenge the dogma that all sites within rRNA are uniformly pseudouridylated. Moreover, we observed a pronounce increase in Ψ levels at postion 609 and 863 on 18S rRNA upon DNA damage in agreement with our findings that the expression of the corresponding guide, snoRNA24, is increased (Figure 3.2B). Conversely, we found that a reduction of Ψ4659 on 28S rRNA is consistent with decreased expression of the corresponding guide, snoRNA17 following DNA damage Figure 3.2C). Altogether, although historically rRNA Ψ modifications and H/ACA snoRNA expression have been considered to be uniform, static, and not subject to regulation, our novel findings demonstrate that the pattern of modifications on rRNA is modulated following mitogenic signals. Furthermore, our observations that all sites on rRNA are not equally pseudouridylated indicating that cells may harbor populations of ribosomes displaying differential base-modification states. These findings provide a new way of thinking about the dynamic nature of rRNA modifications and suggest that Ψ modifications may impart a dynamic regulatory role to the ribosome in order to modulate gene expression programs.

DNA-damage induced senescence is impaired upon decreased expression of a single H/ACA snoRNA

Although important epigenetic and transcriptional changes have been described during senescence, currently it remains incompletely understood whether RNA modifications play a role in regulation of senescence. Our exciting findings that specific H/ACA snoRNAs are regulated in response to DNA damage prompted us to address whether distinct H/ACA snoRNAs and their function in modulating site-specific pseudouridylation, may impact senescence maintenance. Interestingly, among the snoRNAs displaying increased expression upon DNA damage, we found that expression of snoRNA24 was significantly downregulated across multiple cancers, suggesting that it may act as a tumor suppressor (Figure S3.1). Therefore, we functionally tested whether loss of function of snoRNA24 could alter the senescence response upon oncogenic insult, such as DNA damage. Firstly, we inhibited snoRNA24 expression using locked nucleic acids (LNAs) in primary human fibroblasts treated with gamma irradiation, which resulted in a 50% reduction in Ψ609 and Ψ863 (Figure S3.2A). Importantly, reduction of snoRNA24 did not affect ribosome biogenesis (Figure S3.2B), nor did it influence pseudouridine modifications at rRNA residues not guided by snoRNA24 (Figure S3.2A). Cell cycle profiles of LNA-control (LNA-Scrbl) treated primary fibroblasts following DNA damage exhibited a profound G2/M phase arrests following irradiation (Figure 3.3A). Unexpectedly, fibroblasts treated with LNAs against snoRNA24 (LNA-24) did not exhibit a profound G2/M phase arrest upon irradiation indicating that cells bypassed the cell cycle checkpoint associated with DNA damage. Next, we directly evaluated senescence in primary fibroblasts upon irradiation using a well-characterized marker for senescence known as β-galactosidase (Debacq-Chainiaux et al.,

2009). Interestingly, inhibition of snoRNA24 impairs DNA-damage induced senescence as demonstrated by a significant reduction in the number of β-galactosidase-positive cells (Figure 3.3B) compared to LNA-Scrbl. Furthermore, in contrast to LNA-Scrbl, inhibition of SNORA24 also lead to a dramatic increase in the clonogenic potential of primary fibroblasts upon DNA damage, indicated that these cells have not undergone an irreversible cell cycle arrest, a characteristic of senescent cells (Figure 3.3C). These findings indicate that loss of snoRNA24 cooperates with DNA damage to bypass senescence and strongly suggests that SNORA24 may act as a tumor suppressor, at least in part, through control of DNA damage-induced senescence.

Senescence is primarily characterized as a tumor suppressor mechanism in primary cells, however several studies demonstrate that cancer cells can also undergo senescence (Collado and Serrano, 2010; Perez-Mancera et al., 2014). Therefore, we also sought to address whether snoRNA24 could regulate senescence in an established cancer cell line competent of senescence, namely the human osteosarcoma U2OS cell line. Similar to what was observed in primary fibroblast, inhibition of snoRNA24 impairs DNA-damage induced senescence and lead to a dramatic increase in the clonogenic potential of U2OS cells when compared to LNA-control treated cells (Figure S3.3A, B). Altogether, these findings illuminate a previously uncharacterized role of H/ACA snoRNAs and pseudouridine modifications in safeguarding the genome against oncogenic insult.

H/ACA snoRNA24 modulates distinct gene expression programs upon DNA damage-induced senescence both transcriptionally and translationally

Although pseudouridine modifications within the ribosome are known to modulate specific aspects of ribosome function such as translational specificity and fidelity (Jack et al., 2011), the role of individual pseudouridine modifications guided by distinct H/ACA snoRNAs towards translational control remains unexplored. Based on our findings that the expression and function of H/ACA snoRNAs in guiding Ψ modifications is dynamically regulated upon DNA damage we hypothesize that altering the pattern of rRNA modifications can serve as a mechanism to modulate translational programs to maintain senescence. To understand whether and how changes in gene expression mediated by snoRNA24 lead to bypass of senescence we explored, on a genomic and transcriptomic wide scale, regulation of transcription and translation in primary human fibroblasts following DNA damage using RNA-seq and ribosome profiling. Libraries from three biological replicas were prepared from primary fibroblasts treated with LNA-24 or LNA-Scbl at 0, 38, and 72 hours post DNA damage in order to gain a snapshot of the earliest changes in gene expression.

Overall, our analysis identified predominant changes both at the level of transcription (FDR <0.001) and translation (FDR <0.01) in all conditions analyzed (Figure 3.4A). Firstly, ribosome profiling analysis indicates that a gene-specific translation program occurs following DNA damage in primary fibroblasts. Gene ontology analysis revealed that the most highly translated mRNAs attributed to DNA damage are predominantly implicated in transcription regulation, cell cycle, and kinase signaling whereas transcripts demonstrating lower than expected translation efficiently were involved in predominantly

RNA based cellular processes such as translation and splicing (Figure S3.4A, B) indicating that an overall decrease in post-transcriptional activity may occur in irradiated cells. Our findings are consistent with previous reports demonstrating that specific gene expression programs occur during senescence regulated at the translational level (Loayza-Puch et al., 2013).

Consistent with findings that a reduction in snoRNA24 did not affect ribosome biogenesis (Figure S3.2B), we did not observe dramatic changes in overall protein synthesis from our ribosome profiling analysis. Intriguingly, a reduction in snoRNA24 did however lead to statistically significant changes in the translational efficiency of specific transcripts upon DNA damage including enrichment of mRNA that stratify into unique functional categories involved in transcription regulation and RNA metabolism (Figure 3.4B).

To determine whether aberrant translation of factors involved in transcriptional regulation were functionally significant upon snoRNA24 reduction, we next interrogated our RNA expression datasets. We identified changes in RNA expression levels with statistically significance (FDR <0.001) (Figure 3.4A) upon loss of snoRNA24 during DNA damage. Interestingly, one of the most significantly enriched functional classes of genes affected by loss of snoRNA24 upon DNA damage includes genes involved in various aspects of fatty acid synthesis and lipid metabolism (Figure 3.4C). Particularly, genes involved in lipid and cholesterol synthesis were significantly increased, while genes involved in lipolysis and fatty acid oxidation were significantly decreased upon reduction in snoRNA24 at both 36 and 72 hours following DNA damage. Altogether, these findings indicated that upon DNA damage, loss of function of snoRNA24 alters gene expression programs that may

influence the ability of primary fibroblasts to regulate the synthesis and utilization of lipids and provides a new link between H/ACA snoRNAs and lipid metabolism.

Aberrant lipid metabolism upon loss of snoRNA24 leads to bypass of senescence upon DNA damage

Previous studies indicate that during senescence, although growth arrested, primary cells remain highly metabolic. In particular, senescence cells utilize cellular lipid stores to generate energy mainly through fatty acid oxidation (Aird and Zhang, 2014; Quijano et al., 2012). In contrast, transformed cells often upregulate lipid synthesis to maintain increased demands for cellular expenditure and abnormal proliferation rates (Santos and Schulze, 2012). Interestingly, lipid accumulation in tumor specimens is now considered a hallmark of cancer progression and is often associated with poor survival (Abramczyk et al., 2015; Beloribi-Djefaflia et al., 2016; Bozza and Viola, 2010; de Gonzalo-Calvo et al., 2015; Yue et al., 2014). However, the mechanism by which deregulated lipid metabolism contributed to cancer initiation and progression is poorly understood. To assess whether lipid metabolic rewiring may lead to bypass of senescence upon reduction in snoRNA24, we first visualized lipid stores in cells using a well-characterized fluorescence probe of lipids, Nile red. Interestingly, we observe a dramatic accumulation of lipids specifically upon snoRNA24 loss following DNA damage induced senescence (Figure 3.5A). To further dissect which arm of the lipid metabolic pathway was directly responsible for the bypass of senescence observed upon snoRNA24 knockdown, we treated primary fibroblasts upon snoRNA24 knockdown with specific inhibitors of fatty acid synthesis (C-75), cholesterol synthesis (Simvastatin), and phospholipases including PLC (U-73122) which is involved in the

synthesis of diacylglycerol and cPLA2α (525143) which is involved in eicosanoid synthesis. We monitored cell cycle and used G2/M phase arrest as readout for senescence following DNA damage. Surprisingly, while under steady state conditions, treatment with each lipid metabolic pathway inhibitor did not have a significant effect on cell cycle (data not shown), phospholipase inhibitors reversed the ability of LNA-24 treated cells to escape G2/M phase arrest following DNA damage (Figure 3.5B). These results indicate that inhibition of snoRNA24 leads to bypass of DNA damage induced-senescence by rewiring lipid metabolic pathways directly involved in the final steps of triglyceride production that feed into lipid droplets and eicosanoids synthesis. These findings indicate that regulation of snoRNA24 following DNA damage impinges on a very specific node of lipid metabolism leading to the accumulation of lipid stores, which has recently been associated with human cancers.

Loss of snoRNA24 cooperates with oncogenic N-ras to bypass senescence *in vivo* and results in the development of hepatocellular carcinoma

It is well known that different oncogenic insults activate the same cellular response pathways to counteract cellular transformation. One excellent example is the oncogene H-Ras^{V12} that triggers a cellular response similar to that observed upon DNA damage (Di Micco et al., 2006). Based on these observations we decided to further test whether inhibition of snoRNA24 cooperates with H-Ras^{V12} to bypass senescence. Similar to our observations using DNA damage, we also found that loss of snoRNA24 lead to bypass of oncogene induce senescence mediated by H-Ras^{V12} (Figure S3.5). Since inhibition of snoRNA24 cooperates with different types of oncogenic insults, such as Ras which is the most common oncogene across different human cancers, we analyzed if snoRNA24

expression was deregulated across different cancers. Surprisingly, by analyzing the expression of a large group of snoRNAs among different types of cancers, we found that snoRNA24 is the top most significantly downregulated snoRNA in liver cancer (Figure S3.1). Based on these results we next extended these findings *in vivo*, using a mouse model of liver senescence mediated by expression of oncogenic N-RasV12 (Figure 3.6A) (Kang et al., 2011). Upon activation of oncogenic N-RasV12 in mouse liver, we detected a dramatic increase in snoRNA24 levels (Figure 3.6B) as observed in primary fibroblasts upon H-Ras^{V12} activation. These results suggest that snoRNAs are dynamically regulated both in vitro and in vivo upon oncogenic insult. We next confirmed that expression of N-RasV12 in mouse liver promoted senescence by β-galactosidase staining and an additional marker for senescence, p21 (Figure 3.6C). Importantly, hydrodynamic tail vein delivery of LNA-24, which significantly reduced snoRNA24 levels in mouse liver, resulted in a bypass of senescence in this model compared to LNA-Scrbl treated mice (Figure 3.6C).

Our *in vitro* and *in vivo* findings demonstrate that inhibition of snoRNA24 cooperates with oncogenic signals to bypass senescence and suggests that loss of snoRNA24 may represent a 'second hit' and cooperate with oncogenic insult to promote cellular transformation. To test this possibility, we prolonged this study for an additional four months and observed that, in contrast to LNA-Scbl treated mice that have normal livers, inhibition of snoRNA24 cooperates with N-RasV12 resulting in the development of hepatocellular carcinoma (HCC) (Figure 3.6D). Histological analysis of tumor nodules revealed an increase in N-RasV12 expression, decrease expression of snoRNA24, and loss reticulin, a well-known marker of HCC (Figure 3.6E-H). Strikingly, tumor nodules derived from LNA-24 treated mice also display a dramatic increase in lipid stores and their

pathology resembles that of steatotic human HCC, a cancer variant characterized by an increase in fat accumulation (Figure 3.6G) (Yeh et al., 2015). Importantly, further analysis of micro dissected tumor nodules validated that the same lipid metabolic program identified *in vitro* also exists in vivo (Figure 3.6I). For example, there is a profound decrease in protein expression of lipid oxidation and increase of lipid synthesis genes, such as ACOT2 and ELOVL3 respectively, from tumor nodules of LNA-24 treated mice compared to LNA-Scbl treated mice expressing N-RasV12. Altogether, our findings suggest that loss of a single H/ACA snoRNA promotes a metabolic shift whereby increasing lipid synthesis and decreasing lipid oxidation contributes the development of liver cancer that resembles human HCC.

H/ACA snoRNA24 expression is decreased in human hepatocellular carcinoma

Our findings strongly suggest that snoRNA24 functions as a tumor suppressor by modulating site-specific pseudouridine modifications within the ribosome to promote a translation program to counteract cellular transformation. Given our findings that loss of function of snoRNA24 promotes the development of HCC in vivo, we next sought to determine whether snoRNA24 expression is deregulated in human HCC. We first analyzed snoRNA24 levels in a previously published dataset of 268 HCC tissues and 243 adjacent non-tumor tissue (Hao et al., 2011). Interestingly, we observed a significant decrease in the levels of snoRNA24 in HCC tissue compared to adjacent non-tumor tissue ($p<1.6E-26$) (Figure 3.7A). These findings identify that snoRNA24 is significantly reduced in human HCC tumors and provides a new link between snoRNA24, HCC, and lipid synthesis.

Figures

Figure 3.1. Dynamic and coordinated regulation of subsets of H/ACA snoRNAs upon DNA damage. H/ACA snoRNA expression levels guiding modifications on regions of (A) 18S and (B) 28S rRNA upon DNA damage (10 Gy gamma irradiation) in primary human skin fibroblasts. Coordinated regulation of snoRNAs guiding modifications on distinct clusters of the rRNA is observed upon ribosome 3D modeling on PyMOL. The expression of 63 H/ACA snoRNAs was measured by real-time qPCR and normalized to the abundance of small RNA RN7SK from at least three independent experiments. Color-coding of snoRNA expression ranges from +3 to −3 in $\log_2$ space relative to expression in non-irradiated cells.

Figure 3.2. Control of site-specific pseudouridine modifications within distinct regions of rRNA during DNA damage. Quantification of site-specific pseudouridine and uridine levels at (A) snoRNA24 target-residues on 18S rRNA 3 days following DNA damage and at (B) snoRNA17 target-residues on 28S rRNA in primary skin fibroblasts. Target rRNA residues were radiolabeled and levels of uridine and pseudouridine were separated and measured by thin layer chromatography (Karijolich et al., 2010). Graphs show quantifications of Ψ/U levels on TLC membranes from three independent experiments. Statistical analysis was performed using the unpaired Student's t test, $^{*}p < 0.05$.

Figure 3.3. DNA damage induced senescence is impaired upon decreased expression of a single H/ACA snoRNA, SNORA24. (A) Representative image of primary fibroblasts following DNA damage treated with LNA-scrbl or LNA-SNORNA24 and treated with β-

galactosidase to stain senescent cells. Graph shows percentage β-galactosidase-positive cells from three independent experiments. Statistical analysis was performed using the unpaired Student's t test, $^{*}p < 0.05$. (B) Colony forming assay of primary fibroblast following DNA damage and inhibition of snoRNA24. Statistical analysis was performed using the unpaired Student's t test, $^{*}p < 0.05$.

Figure 3.4. H/ACA snoRNA24 modulates distinct gene expression programs upon DNA damage. (A) Ribosome profiling analysis of genes regulated at the transcriptional (left) and translational (right) level upon gamma irradiation of primary fibroblasts treated with LNA-scbl and LNA-SNORA24 (FDR <0.001 and <0.01 respectively). Gene ontology analysis by DAVID of mRNAs regulated at the translational level (B) and the transcriptional level (C) treated with LNA-scbl and LNA-SNORA24 upon gamma irradiation ($p < 0.05$).

Figure 3.5. Deregulated lipid metabolism upon loss of snoRNA24 leads to bypass of senescence upon DNA damage. (A) Visualization of lipid droplet formation after Nile Red staining on primary fibroblast upon DNA damage and treated with LNA-scbl and LNA-SNORA24 (B) Cell cycle analysis of primary fibroblast treated with phospholipase C inhibitor and gamma irradiation after inhibition of snoRNA24. Bars represent mean +/-SD.

Figure 3.6. Loss of snoRNA24 cooperates with oncogenic N-RasV12 leading to the development of hepatocellular carcinoma. (A) Cartoon outlining experimental approach to test the requirement of snoRNA24 during senescence and liver cancer. (B) Regulation of snoRNA24 expression in liver after six days of N-RasV12 expression. (C) Staining for Nras,

p21, and SA-β-Gal (400X) were performed on liver sections or resected liver loves (SA-β-gal wholemount staining) 6 days after delivery of transposon constructs. (D) Downregulation of snoRNA24 cooperates with N-RasV12 to develop HCC. Shown are representative photographs of explanted livers (n = 20). (E) Expression of N-RasV12 or (F) snoRNA24 in microdisected tumor nodules. (G) H&E staining of tumor nodule. Arrows, fat droplets. (E) Reticulin staining. Arrows indicate the presence of reticulin in adjacent non-tumor tissue. Tumor nodule displays absence of reticulin stain. (F) Representative western blots of snoRNA24 lipid target gene expression in four independent tumors and tree independent control liver sections.

Figure 3.7. H/ACA snoRNA24 expression is decreased in human hepatocellular carcinoma. Expression of snoRNA24 in HCC specimens compared to adjacent non-tumor tissue. snoRNA24 expression was analyzed from a microarray dataset obtained from 257 HCC patients undergoing hepatectomy treatment (GSE25097).

Figure 3.1

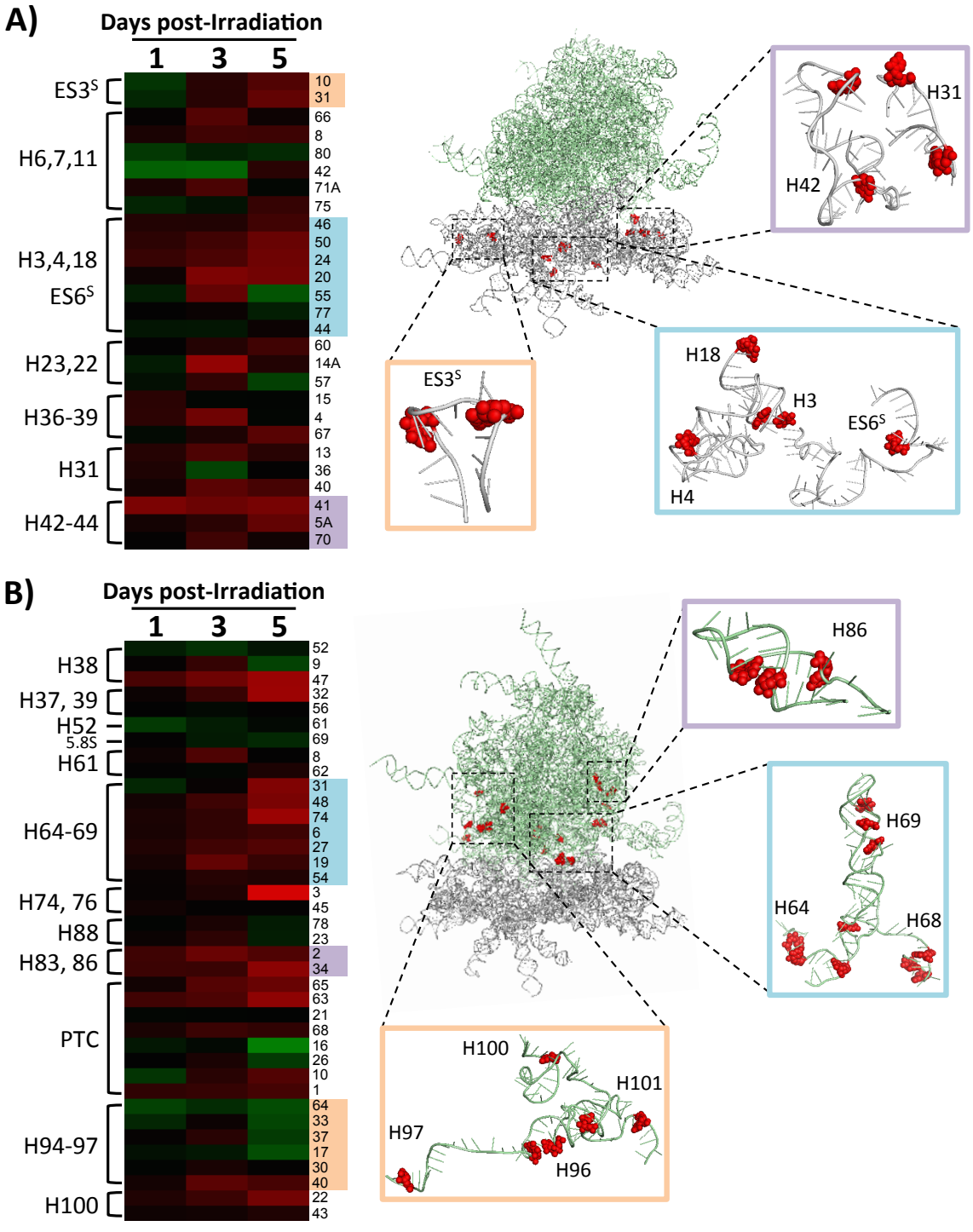
A)
Days post-Irradiation
1
3
5
ES3S
H6,7,11
H3,4,18
ES6S
H23,22
H36-39
H31
H42-44
10
31
66
8
80
42
71A
75
46
50
24
20
55
77
44
60
14A
57
15
4
67
13
36
40
41
5A
70
H31
H42
ES3S
H18
H3
ES6S
H4
B)
Days post-Irradiation
1
3
5
H38
H37, 39
H52
5.8S
H61
H64-69
H74, 76
H88
H83, 86
PTC
H94-97
H100
52
9
47
32
56
61
69
8
62
31
48
74
6
27
19
54
3
45
78
23
2
34
65
63
21
68
16
26
10
1
64
33
37
17
30
40
22
43
H86
H69
H64
H68
H100
H101
H97
H96

Figure 3.2

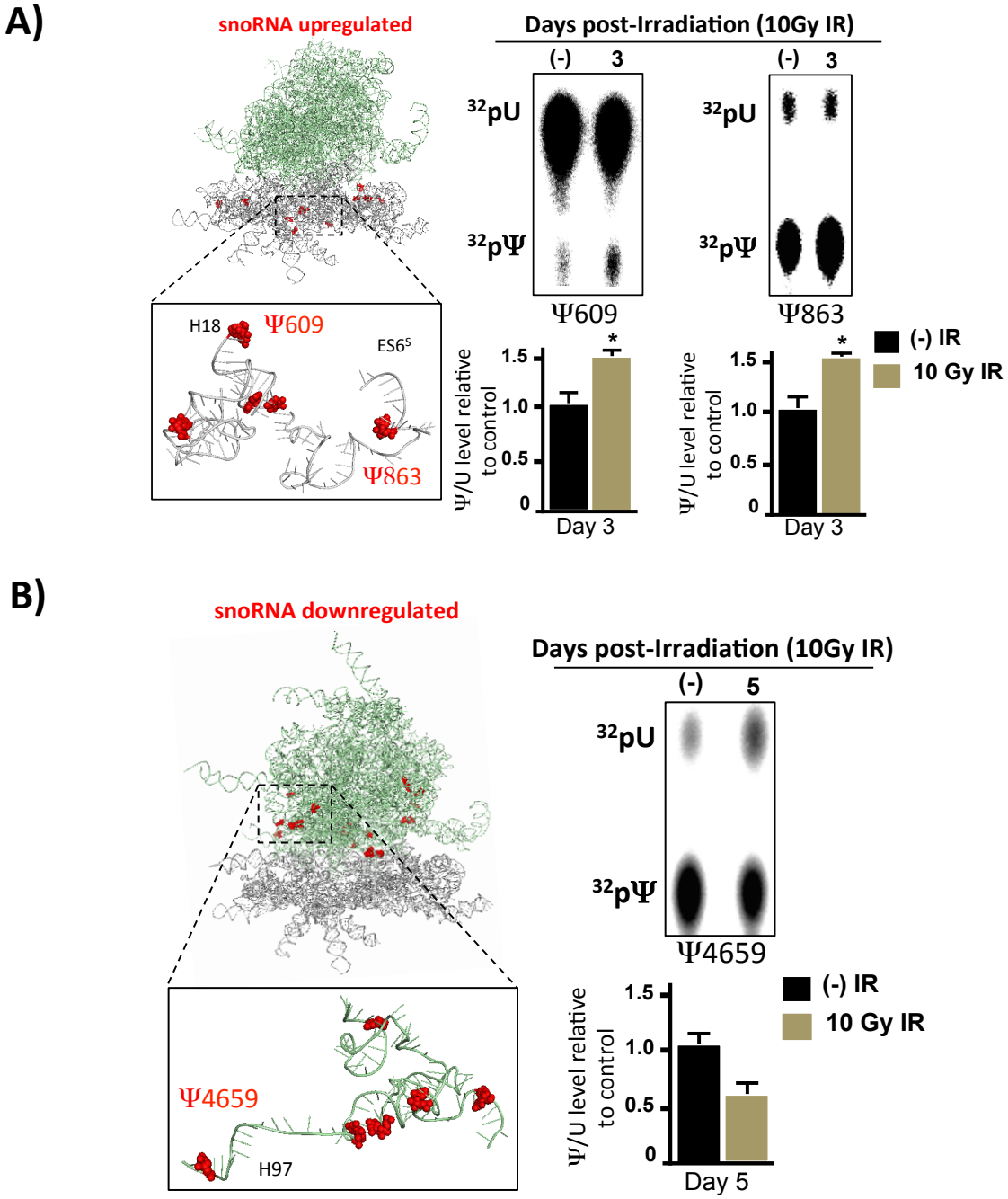
A)
snoRNA upregulated
H18
Ψ609
ES6S
Ψ863
Days post-Irradiation (10Gy IR)
(-)
3
32pU
32pΨ
Ψ609
Ψ863
Ψ/U level relative to control
1.5
1.0
0.5
0
Day 3
(-) IR
10 Gy IR
B)
snoRNA downregulated
Ψ4659
H97
Days post-Irradiation (10Gy IR)
(-)
5
32pU
32pΨ
Ψ4659
Ψ/U level relative to control
Day 5
(-) IR
10 Gy IR

Figure 3.3

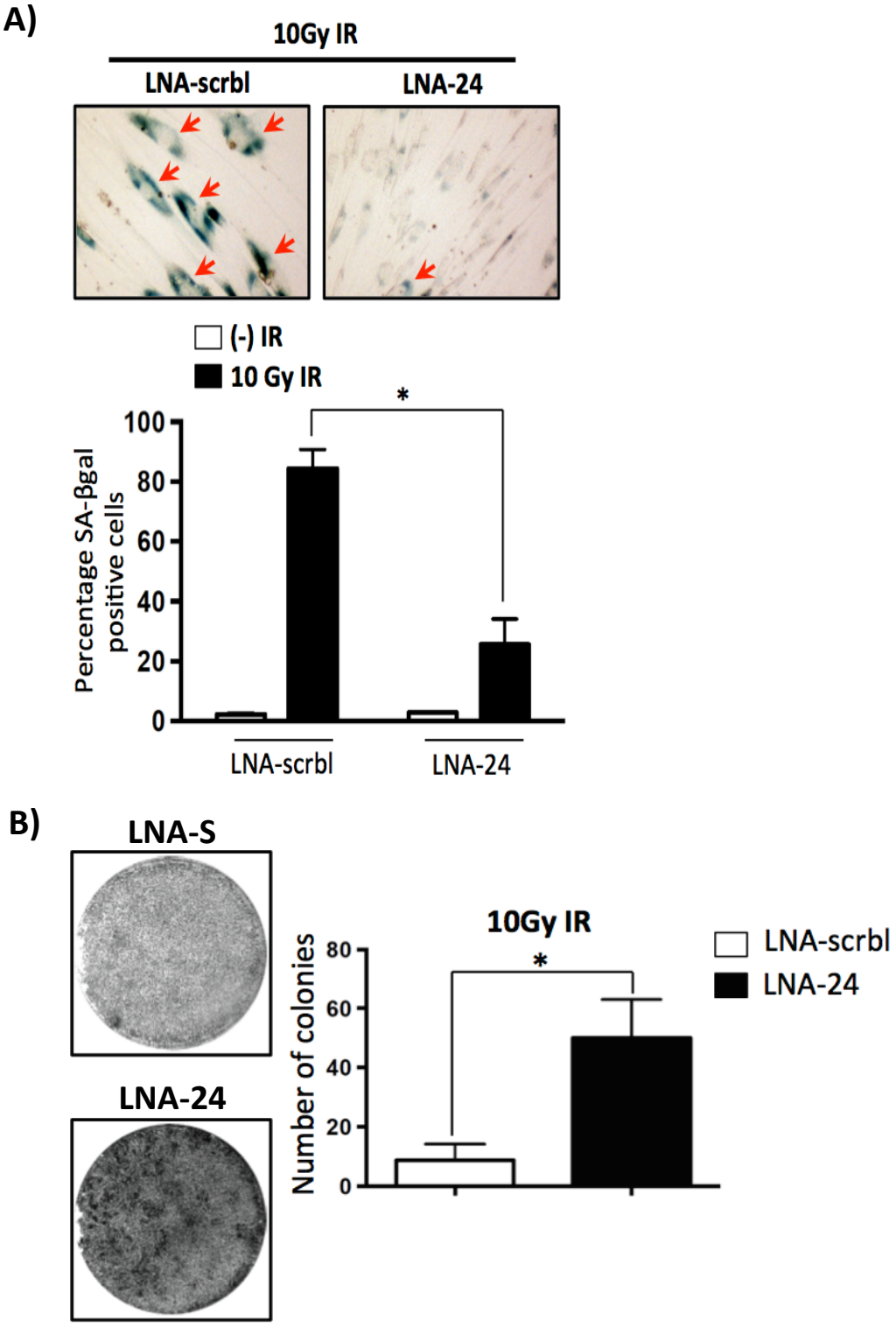
A)
10Gy IR
LNA-scrbl
LNA-24
(-) IR
10 Gy IR
*
Percentage SA-βgal positive cells
100
80
60
40
20
0
LNA-scrbl
LNA-24
B)
LNA-S
LNA-24
10Gy IR
*
Number of colonies
80
60
40
20
0
LNA-scrbl
LNA-24

Figure 3.4

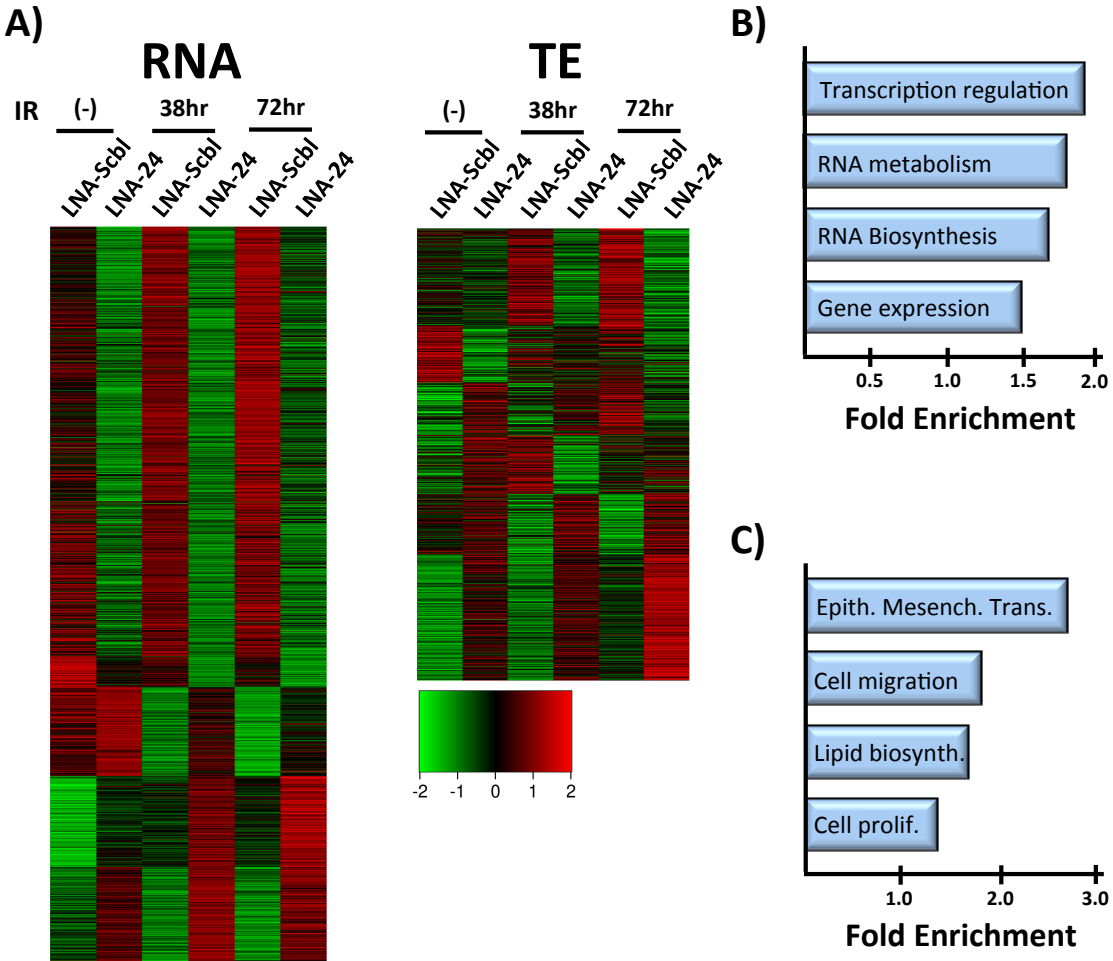
A)
RNA
TE
IR
(-)
38hr
72hr
LNA-Scbl
LNA-24
-1
0
1
-2
2
B)
Transcription regulation
RNA metabolism
RNA Biosynthesis
Gene expression
0.5
1.0
1.5
2.0
Fold Enrichment
C)
Epith. Mesench. Trans.
Cell migration
Lipid biosynth.
Cell prolif.
1.0
2.0
3.0
Fold Enrichment

Figure 3.5

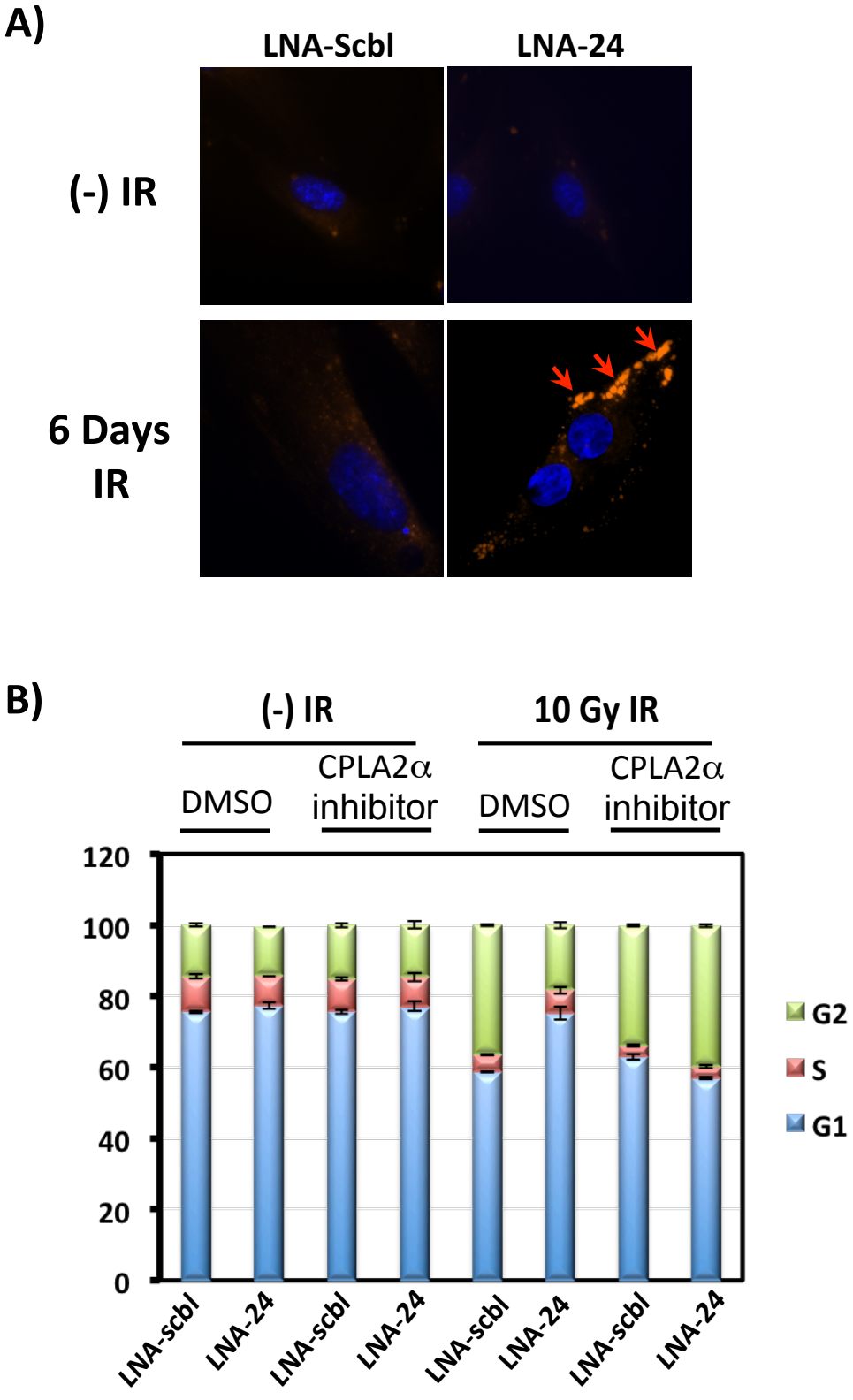
A)
LNA-Scbl
LNA-24
(-) IR
6 Days IR
B)
(-) IR
10 Gy IR
DMSO
CPLA2α inhibitor
DMSO
CPLA2α inhibitor
120
100
80
60
40
20
0
G2
S
G1
LNA-scbl
LNA-24
LNA-scbl
LNA-24
LNA-scbl
LNA-24
LNA-scbl
LNA-24

Figure 3.6

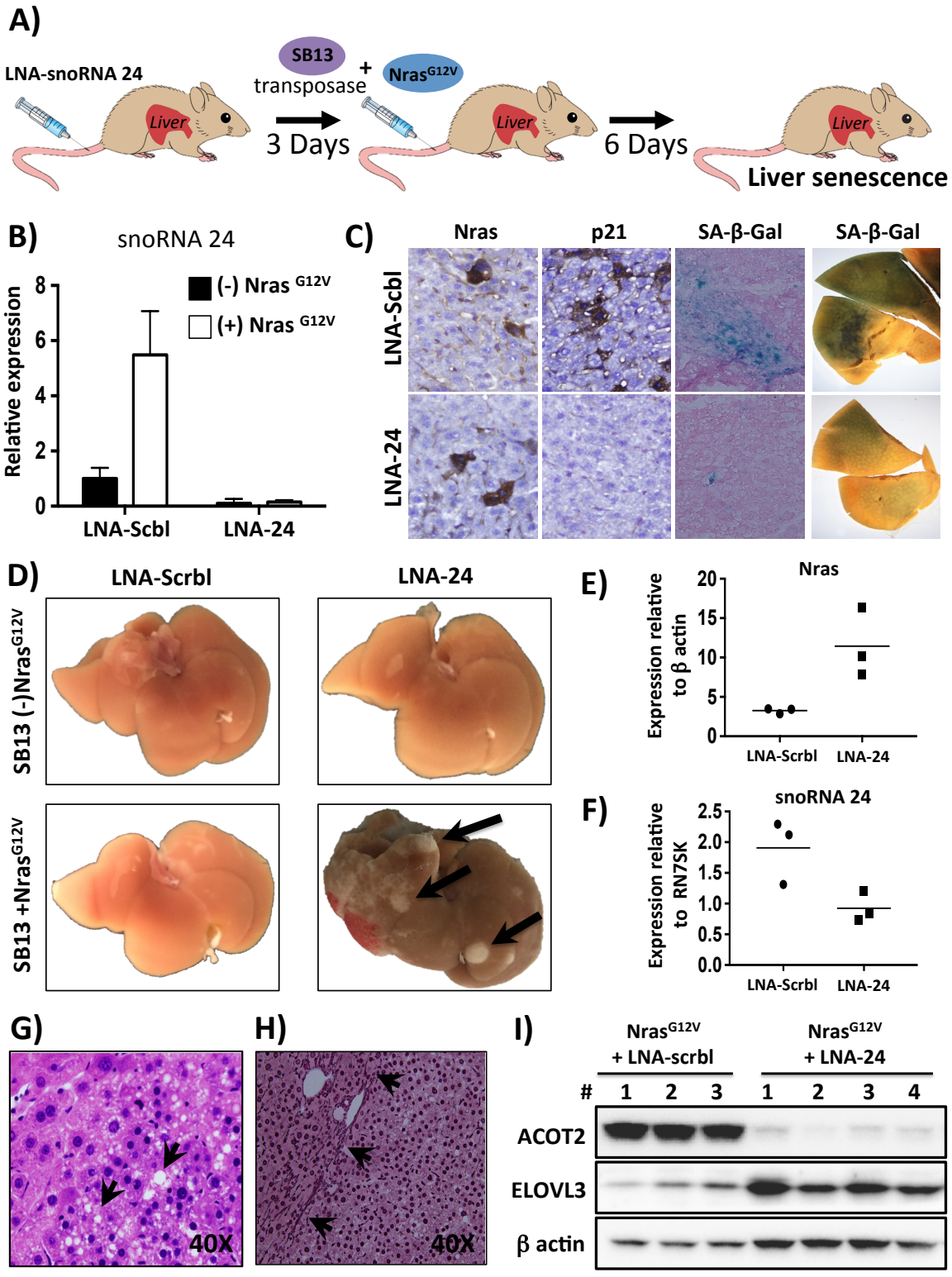
A)
LNA-snoRNA 24
Liver
SB13
transposase
+
Nras^G12V
3 Days
6 Days
Liver senescence
B)
snoRNA 24
(-) Nras G12V
(+) Nras G12V
Relative expression
LNA-Scbl
LNA-24
C)
Nras
p21
SA-β-Gal
SA-β-Gal
LNA-Scbl
LNA-24
D)
LNA-Scrbl
LNA-24
SB13 (-)Nras^G12V
SB13 +Nras^G12V
E)
Nras
Expression relative to β actin
LNA-Scrbl
LNA-24
F)
snoRNA 24
Expression relative to RN7SK
LNA-Scrbl
LNA-24
G)
40X
H)
40X
I)
Nras^G12V + LNA-scrbl
Nras^G12V + LNA-24
1 2 3 1 2 3 4
ACOT2
ELOVL3
β actin

Figure 3.7

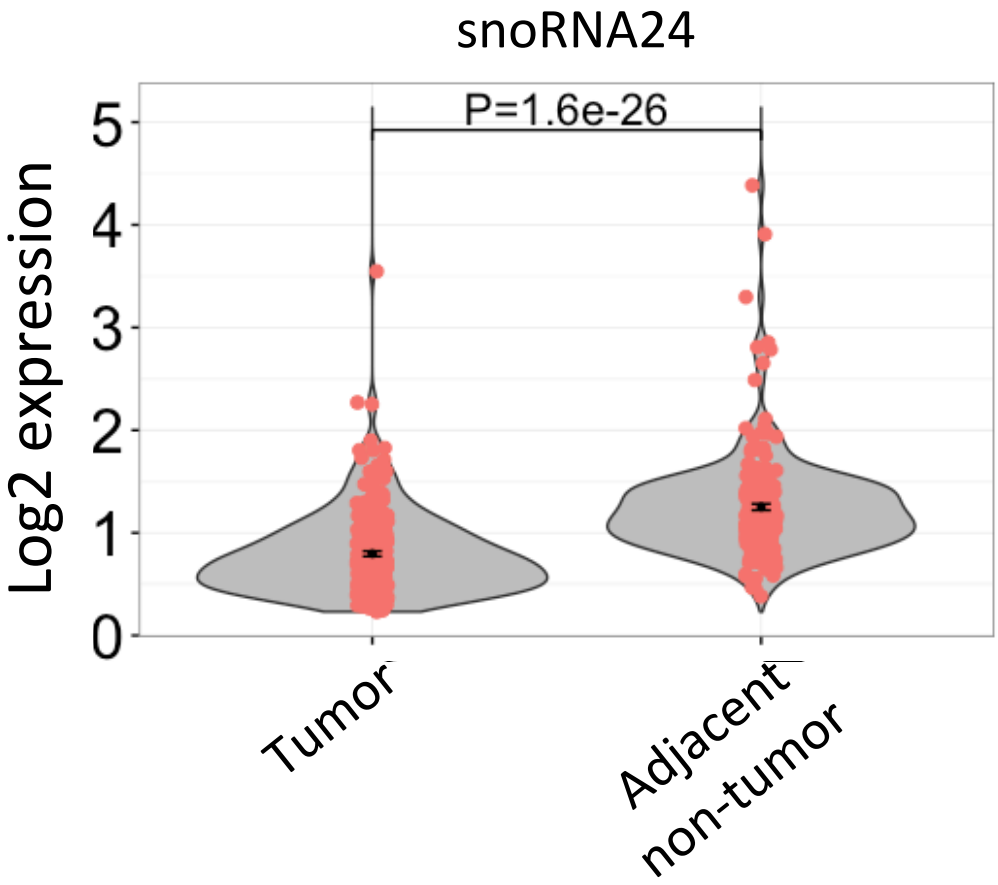
snoRNA24
P=1.6e-26
Log2 expression
0
1
2
3
4
5
Tumor
Adjacent non-tumor

Supplemental Figure 3.1. snoRNA24 is the most significantly downregulated snoRNA in liver cancer. Expression of several H/ACA snoRNAs obtained from different Gene Expression Omnibus cancer studies for liver (GSE25097), pancreatic (GSE28735), lung (GSE43458), colon (GSE20916), lymphoma (GSE22898), osteoblast (GSE12865), and breast. Color bar represents p value significance between tumor and adjacent non-tumor sampels.

Supplemental Figure 3.2. Downregulation of snoRNA24 results in a decrease of target pseudouridines and does not affect ribosome biogenesis. (A) Quantification of site-specific pseudouridine and uridine levels targeted by snoRNA24 (Ψ609 and Ψ863) and non-target sites (Ψ105, Ψ1731) following inhibition of snoRNA24 and DNA damage on primary fibroblast. Target rRNA residues were radiolabeled and levels of uridine and pseudouridine were separated and measured by thin layer chromatography (Karijolich et al., 2010). Graphs show quantifications of Ψ/U levels on TLC membranes from three independent experiments. Statistical analysis was performed using the unpaired student's t test, $^{*}p < 0.05$. (B) Separation and quantification of ribosome subunits by sucrose gradient analysis. Graph show quantification of area under the curve corresponding to ribosome subunits from three independent experiments.

Supplemental Figure 3.3. DNA damage induced senescence is impaired upon decreased expression of a single H/ACA snoRNA, SNORA24. (A) Representative image of osteosarcoma cell line U2OS following DNA damage treated with LNA-scrbl or LNA-SNORNA24 and treated with β-galactosidase to stain senescent cells. Graph shows

percentage β-galactosidase-positive cells from three independent experiments. Statistical analysis was performed using the unpaired Student's t test, $^{*}p < 0.05$. (B) Colony forming assay of U2OS cells following DNA damage and inhibition of snoRNA24. Statistical analysis was performed using the unpaired Student's t test, $^{*}p < 0.05$.

Supplemental Figure 3.4. DNA damage modulates distinct gene expression programs at the translational level. Gene ontology analysis by DAVID of mRNAs whose translation is (A) induced and (B) repressed upon gamma irradiation on primary fibroblast treated with LNA-Scbl ($p < 0.05$).

Supplemental Figure 3.5. Oncogene induced senescence is impaired upon decreased expression of snoRNA24. Colony forming assay of primary fibroblast following N-RasV12 expression and inhibition of snoRNA24. Statistical analysis was performed using the unpaired Student's t test, $^{*}p < 0.05$ from at least three independent experiments.

Figure S3.1

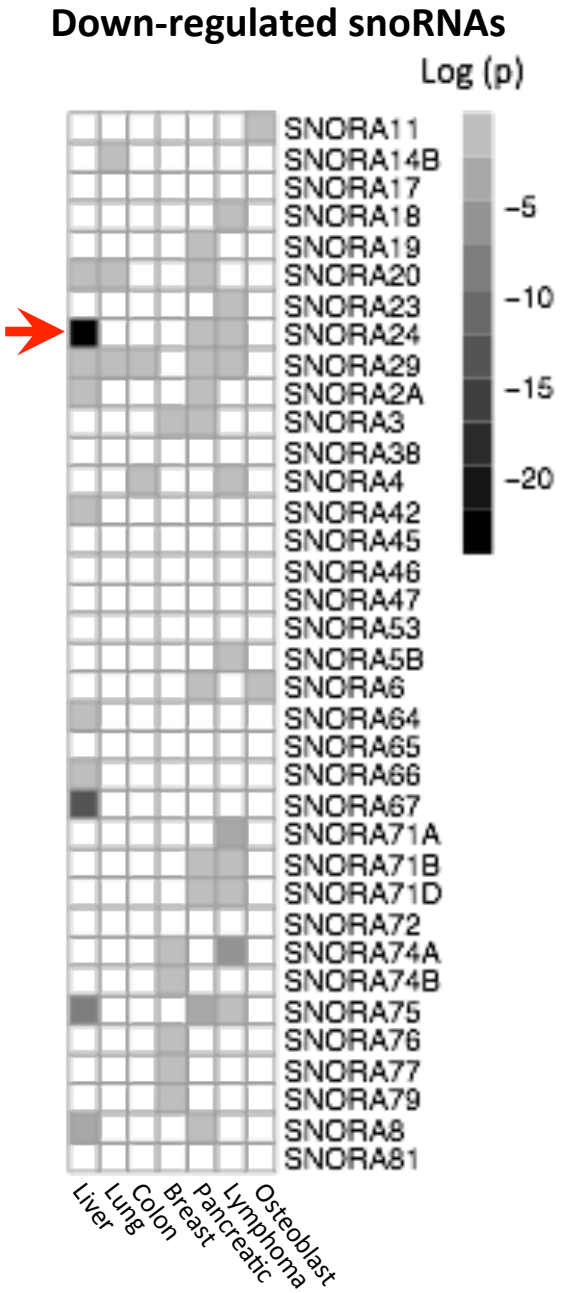
Down-regulated snoRNAs
Log (p)
-5
-10
-15
-20
SNORA11
SNORA14B
SNORA17
SNORA18
SNORA19
SNORA20
SNORA23
SNORA24
SNORA29
SNORA2A
SNORA3
SNORA38
SNORA4
SNORA42
SNORA45
SNORA46
SNORA47
SNORA53
SNORA5B
SNORA6
SNORA64
SNORA65
SNORA66
SNORA67
SNORA71A
SNORA71B
SNORA71D
SNORA72
SNORA74A
SNORA74B
SNORA75
SNORA76
SNORA77
SNORA79
SNORA8
SNORA81
Liver
Lung
Colon
Breast
Pancreatic
Lymphoma
Osteoblast

Figure S3.2

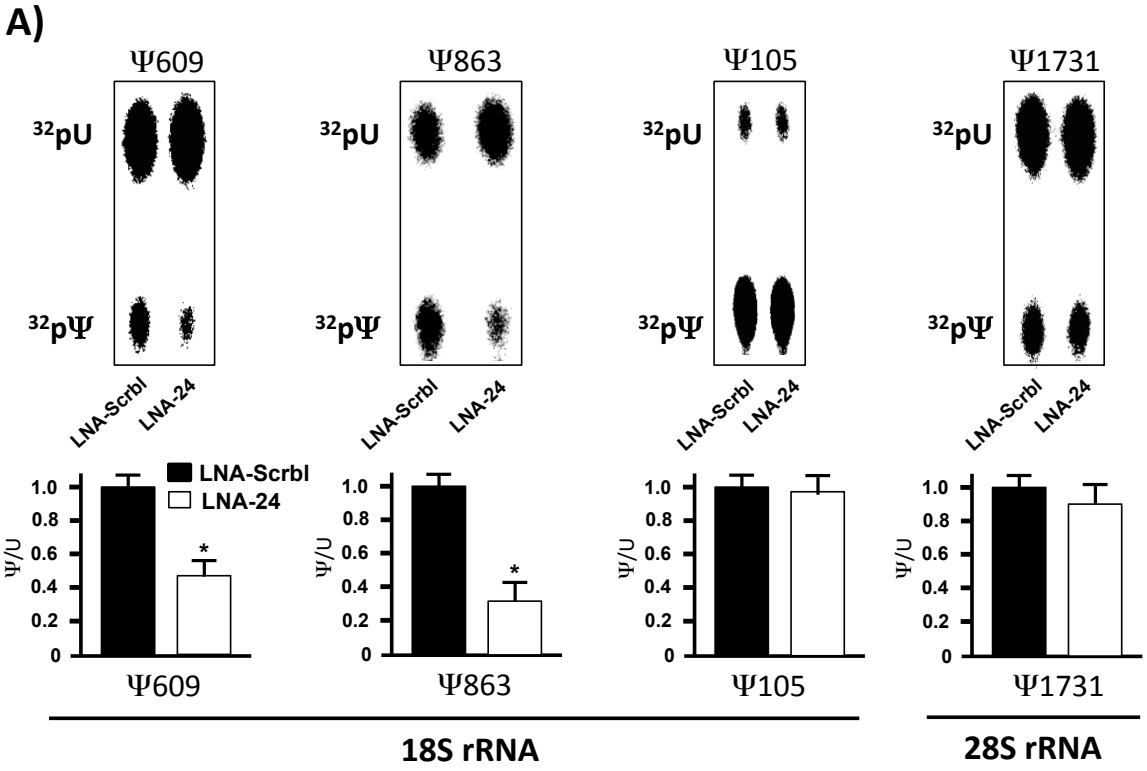
A)
Ψ609
Ψ863
Ψ105
Ψ1731
32pU
32pΨ
LNA-Scrbl
LNA-24
LNA-Scrbl
LNA-24
Ψ/U
1.0
0.8
0.6
0.4
0.2
0
*
Ψ609
Ψ863
Ψ105
Ψ1731
18S rRNA
28S rRNA

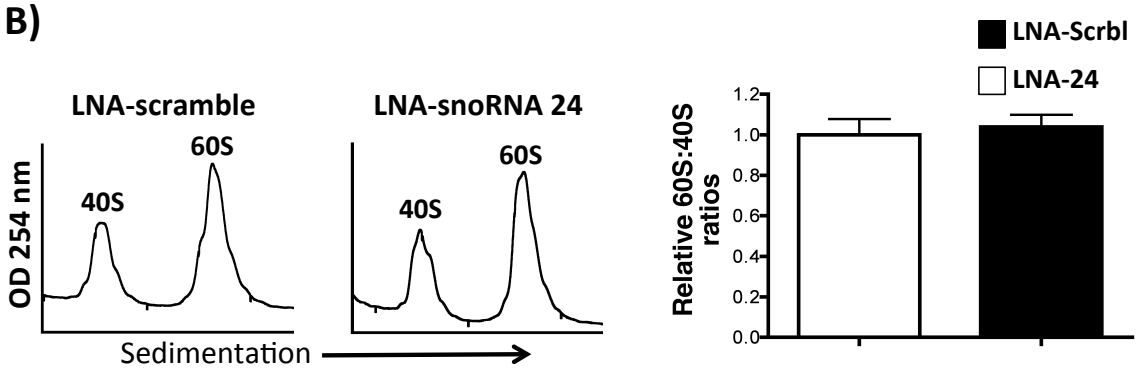
B)
LNA-scramble
LNA-snoRNA 24
60S
40S
OD 254 nm
Sedimentation
LNA-Scrbl
LNA-24
Relative 60S:40S ratios
1.2
1.0
0.8
0.6
0.4
0.2
0.0

Figure S3.3

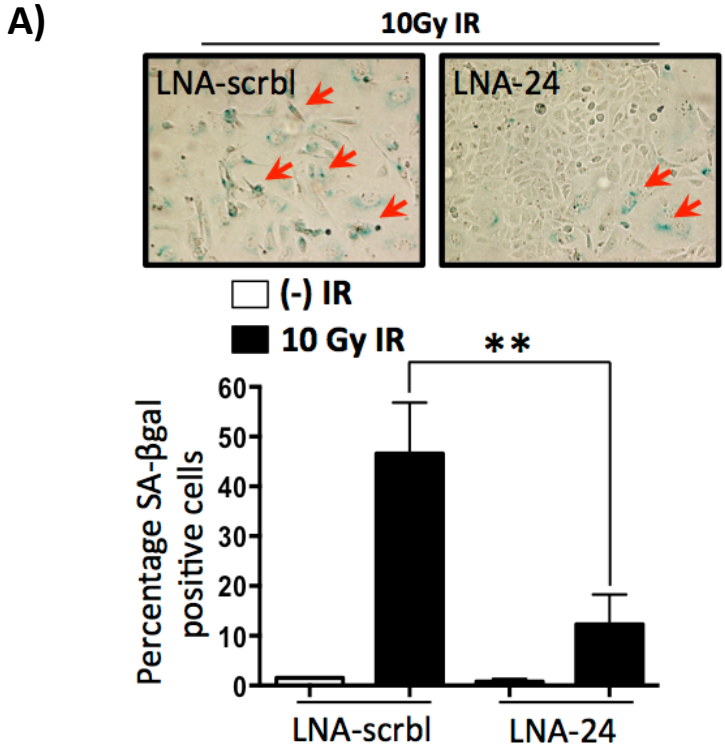
A)
10Gy IR
LNA-scrbl
LNA-24
(-) IR
10 Gy IR
**
Percentage SA-βgal positive cells
60
50
40
30
20
10
0
LNA-scrbl
LNA-24

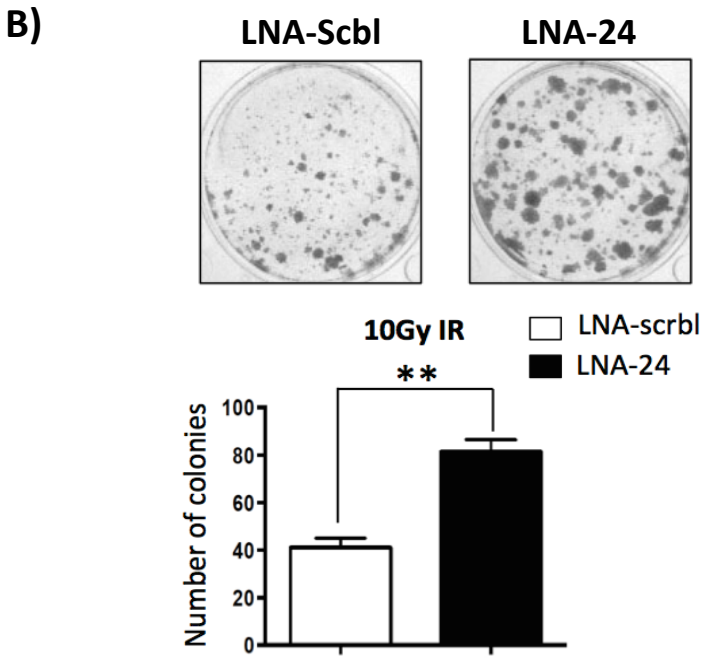
B)
LNA-Scbl
LNA-24
10Gy IR
LNA-scrbl
LNA-24
**
Number of colonies
100
80
60
40
20
0

Figure S3.4

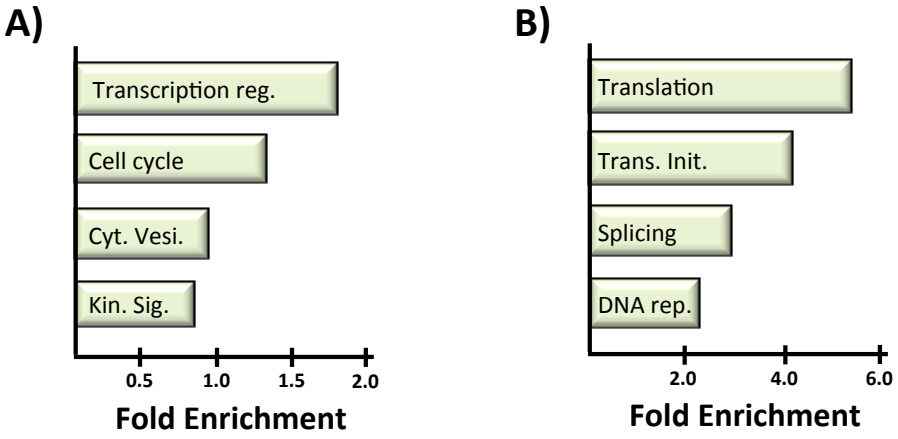
A)
Transcription reg.
Cell cycle
Cyt. Vesi.
Kin. Sig.
0.5
1.0
1.5
2.0
Fold Enrichment
B)
Translation
Trans. Init.
Splicing
DNA rep.
2.0
4.0
6.0
Fold Enrichment

Figure S3.5

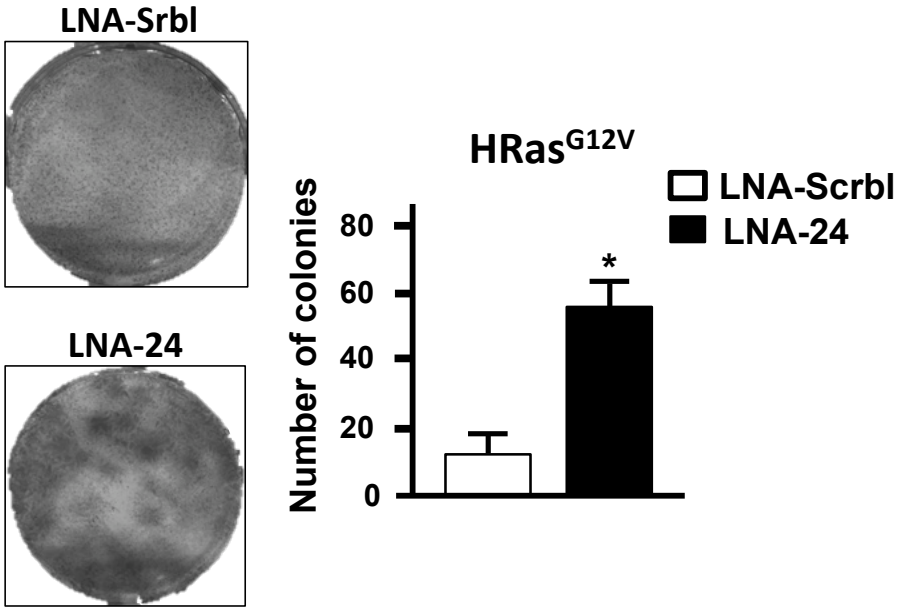
LNA-Srbl
LNA-24
HRas^{G12V}
LNA-Scrbl
LNA-24
Number of colonies
80
60
40
20
0
*

Materials and Methods

Mice

Expression of N-RasV12 in mouse liver was performed as described in (Kang et al, 2011) with minor modifications. Briefly, C57BL/6 female mice 8-12 weeks were injected with a 5:1 molar ratio of transposon (N-RasV12) to transposase (SB13) encoding plasmid (35ug total DNA) by hydrodynamic tailvain injection. Plasmid vectors were prepared using the Qiagen EndoFreeMaxi Kit. DNA was suspended in Normal Saline solution at a final volume of 10% of the animals body weight. Mice treated with locked nucleic acids (LNA-Scbl or LNA-snoRNA24) were injected with LNAs three days prior to hydrodynamic injection of N-RasV12 followed by LNA treatments every 10 days from the first injection. For determination of senescence mouse livers were harvested six days after N-RasV12 injections. Mice were maintained under pathogen-free conditions and all experiments were performed in compliance with guidelines approved by the institutional Animal Care and Use Committee of UCSF.

Cell culture

Primary human skin fibroblast (GM00730) passage 7 were obtained from Coriell Cell Repositories (Coriell Institution for Medical Research, Camden, NJ) and maintained in MEM as described (Bellodi et al., 2010a). Osteosarcoma U2OS cells were obtained from ATCC cell repositories and maintained in DMEM-high glucose, 10% FBS.

Western Blot, Immunohistochemistry, and qPCR Analysis

Western blot was performed using standard protocols and the following primary antibodies: ACOT2 (1:1,000; Proteintech), ELOVL3 (1:500; Proteintech), and β-actin (1: 5,000; Sigma). Immunohistochemistry analysis was performed on OCT embedded frozen tissue using standard protocols and the following primary antibodies: Nras (1:100; Santa Cruz), and p21 (1:100; Santa Cruz). Total RNA was isolated using TRIzol reagent (Invitrogen) and treated with Turbo DNA-free kit (Ambion). 1-2 μg of RNA was reverse transcribed using SuperScript II Reverse Transcriptase Kit (Invitrogen) and analysis was performed using iQ Sybr Green mix (Bio-Rad). The expression of H/ACA small RNAs was measured by real-time qPCR, relative to two type-matched control cells for each mutation, and normalized to the abundance of RN7SK small ncRNA from at least three independent experiments.

Ribosome Profiling Library Preparation, Sequencing, and Analysis of Ribosome Profiling Data

Next-generation sequencing libraries were prepared using the ARTseq Ribosome Profiling Kit (Epicentre) according to manufacturing instructions. Briefly, primary fibroblasts were treated with cycloheximide, lysed, and split into pools for isolating total mRNA and ribosome bound mRNA. Ribosome-protected mRNA fragments were isolated by column fractionation. Total mRNA was alkaline fragmented and size selected. Both samples were processed for small RNA library sequencing. Libraries from three biological replicates per condition were sequenced on an Illumina HiSeq 2000. Analysis of ribosome profiling data was performed according to (Stumpf et al., 2013). Sequencing reads were processed and

aligned to the human genome. Translation regulation was inferred using an errors-in-variables regression model.

Determination of Senescence

Determination of senescence in cells grown in culture was carried out as described in (Serrano et al, 1997) with minor modifications. Briefly, early passage primary fibroblasts were treated with 10Gy gamma irradiation or infected with H-RasV12 viral supernatants as described in (Bellodi et al, 2010). Cellular senescence was assayed after 15 days using a senescence detection kit (Calbiochem) according to manufacturer's instructions. The number of senescent SA-bgal-possitive cells was assessed using a Nikon TE2000E inverted microscope. Determination of senescence in liver sections or whole liver lobes was carried out as described in (Kang et al, 2011).

Isolation of Ribosome Subunits

Primary human fibroblasts were pelleted and lysed in 10mM Tris-HCl pH8, 140mM NaCl, 0.25% NP-40, 0.1% Triton-X 100, 50mM DTT and 640U/ml RNasin for 30min. Lysates were cleared by centrifugation for 5min at 10,000g and supernatants were loaded onto a 5-35% sucrose gradient. Samples were spun at 38,000rpm for 3hr at 4° in a Beckman L8-70M ultracentrifuge and then separated on an ISCO gradient fractionation system to evaluate ribosome subunits profile.

Cell cycle analysis

Single cell suspensions were washed with PBS and fixed with 70% ice-cold Ethanol. Cells were permeabilized with 0.1% Triton X-100 and treated with RNaseH and stained with propidium iodide to measure DNA content. Data was collected using a BD FACSCalibur flow cytometer. At least 10,000 events were recorder and analyzed using FlowJo software.

Colony Forming Assays

Cell proliferation was determined using crystal violet staining. In brief, cells were plated at 20,000 cells per 6 cm plate and cultured for 3 weeks. Cells were fixed using 70% ice-cold methanol, air dried, and the number of colonies was determined after staining with 0.5% crystal violet solution.

Site-Specific Pseudouridine Quantification on rRNA

Quantitation of single pseudouridine residues on rRNA was carried out according to (Karijolich et al., 2010) with minor modifications. Briefly, total RNA was isolated using Trizol reagent and 18S or 28S rRNA was purified by gel isolation. rRNA was hybridized to 2' O-methyl RNA-DNA chimera oligonucleotides complementary to specific pseudouridine residues:

Ψ609, CmAmgactUmGmCmCmUmCmCmAmAmUm;

Ψ863, UmAmttccUmAmGmCmUmGmCmGmGmAmCmCm;

Ψ105, GmAmtttaAmUmGmAmGmCmCmAmUmUmCm on 18S rRNA and

Ψ1731, CmAmttcgCmUmUmUmAmCmCmGmGmAmUm on 28S rRNA. RNA was digested with RNAseH to leave a 5' end at specific pseudouridine containing positions on rRNA and

radiolabeled using 150μCi of γ-^{32}P ATP and 10 units of T4 PNK followed by digestion with nuclease P1. Nucleosides were thenseparated by thin layer chromatography.

Lipid Droplet Staining

Cellular staining of lipid droplets was carried out according to (Listenberger and Brown, 2007) with minor modifications. Briefly, cells were fixed with 3% paraformaldehyde for 30min and stained with 1μg/ml of Nile Red (Molecular Probes) for 10min followed by Hoescht staining and mounted with ProLong Diamond Antifade (Molecular Probes) and visualized using a Zeiss Axiovision fluorescent microscope.

Acknowledgements

We thank members of the Ruggero lab for critical discussion. Special thanks to the UCSF Helen Diller Cancer Center Preclinical Therapeutics Core, in particular to Byron Hann and Donghui Wang, for their help in setting up our mouse studies. A.C. is in part supported by the UCSF HHMI GEMS fellowship and by the National Institutes of Health (NIH) R01DK098057. D.R. is a Leukemia and Lymphoma Society Scholar. M.B. is a Pew Scholar and Alfred P. Sloan Research Fellow.

Chapter 4: Conclusions and Future Directions

H/ACA Small RNA Dysfunctions in Disease Reveal Key Roles for Noncoding RNA Modifications in Hematopoietic Stem Cell Differentiation

There is a growing realization that the majority of the human genome previously thought to be "junk DNA" encodes for both short and long ncRNAs, which may instead exert important RNA-based cellular functions. However, the relative contribution of these RNAs to human disease is poorly understood. Our studies reveal that a large class of H/ACA small RNAs are found deregulated in human disease, displaying variable expression patterns that may dictate the number and the severity of disease features. With respect to H/ACA snoRNAs, deregulations in their expression patterns in X-DC directly produce site-specific defects in RNA modifications present on the ribosome, as revealed by state-of-the-art mass spectrometry. These findings provide a functional link between variations in expression patterns of H/ACA snoRNAs in disease and specific alterations in the array of nucleotide modifications present on the ribosome. Moreover, these studies suggest that heterogeneous pools of ribosomes harboring unique differences in modification patterns are present in X-DC patient cells. This heterogeneity in rRNA modifications may have important functional implications for expression of the X-DC patient genome at the post-transcription level and is consistent with previous studies revealing molecular impairments in accurate translational control in X-DC patient cells (Bellodi et al., 2010a; Yoon et al., 2006). Moreover, a specific subgroup of H/ACA snoRNAs is commonly reduced among all *DKC1* patient mutations. Intriguingly, these H/ACA snoRNAs guide modifications

that cluster primarily within two defined regions of the ribosome (Piekna-Przybylska et al., 2008), including expansion segment 6 (ES6) on 18S rRNA and domain II of 28S rRNA. These findings suggest that additional levels of specificity may coordinate the assembly of specific subsets of H/ACA snoRNPs required for modifications that cluster within functional regions of rRNA and are commonly deregulated in X-DC. Moreover, the mass spectrometry approach we have developed will now make it possible to test the intriguing possibility that different patterns of rRNA pseudouridylation may serve as a mechanism to modulate ribosome function in a cell-type and tissue specific manner.

Our study further reveals an important contribution of the pseudouridine synthase activity of dyskerin in hematopoiesis, which is critically impaired in X-DC patients (Dokal, 2000). This suggests a critical requirement for modifications of specific RNA species in accurate stem cell activity. This is further supported by the diminished expression of H/ACA snoRNAs, which require the catalytic activity of dyskerin. Thus, in addition to impaired telomere maintenance through reductions in TERC expression (Mitchell et al., 1999), heterogeneity in the expression and function of several additional H/ACA small RNAs may cause molecular defects that contribute to X-DC. The analysis of specific subsets of H/ACA small RNAs, such as those identified in our study, may be of great medical importance as novel prognostic markers, where the genetic basis of approximately 50% of DC patients remains unknown (Dokal, 2011). Further evidence for small RNAs in the pathogenesis of DC is highlighted by recent findings that the gene product of *C16orf57,* mutated in autosomal recessive DC and additional inherited diseases including poikiloderma with neutropenia, is required for the 3' end processing of spliceosomal U6 small nuclear RNA (Hilcenko et al., 2012; Mroczek et al., 2012; Walne et al., 2010).

Intriguingly, hypermethylation of several H/ACA snoRNA loci including snoRNA70C, which our findings reveal is deregulated in X-DC cells, have been reported in solid tumors (Ferreira et al., 2012). Thereby, small ncRNAs such as H/ACA snoRNAs may serve as important molecular markers for human health and should therefore be widely examined at the genomic and expression level in disease pathogenesis.

Our findings suggest that a common feature of human disease arising from perturbations in ncRNAs may be the selective pressure for specific core components of RNP complexes to invariably associate with a multitude of small RNAs, providing greater coordination between RNA-based cellular processes. For example, dyskerin's interactions with small H/ACA RNAs link the activity of a single protein to hundreds of RNAs involved in splicing, telomere activity, and ribosome function (Meier, 2006). Therefore, *DKC1* mutations simultaneously affect the expression and function of multiple classes of dyskerin-associated H/ACA small RNAs (Figure 1C), at the nexus of diverse RNA-based cellular processes. Thereby, mutations in genes encoding proteins such as dyskerin may reflect a particular vulnerability to the underlying biology of small RNAs, contributing to human disease. An outstanding question is the molecular nature of the extreme variability in the phenotypic spectrum of *DKC1* point mutations that range from severe birth defects, bone marrow failure, to cancer. Impaired modifications of distinct functional RNAs may represent an important, novel molecular mechanism underlying these specific pathological features.

Heterogeneity in Ribosomal RNA base modifications modulate lipid metabolic flux to maintain a tumor suppressive program

Historically, a large emphasis has been placed on investigating the contribution of protein coding genes towards cellular transformation. However, recently ncRNAs have gained much attention due to findings that several classes of ncRNAs are directly implicated in a growing list of human diseases including cancer (McMahon et al., 2015). An emerging class of small ncRNAs termed H/ACA snoRNAs that guide the site-specific isomerization of uridine to pseudouridine are deregulated in several cancers however, whether deregulation of H/ACA snoRNA function can directly play a role during the early stages of cellular transformation remains obscure. In this study, we unravel an unexpected coordinated regulation of specific subsets of H/ACA snoRNAs during the early stages of DNA damage-induced senescence that imparts site-specific changes in pseudouridine modifications present at distinct regions within the ribosome. Our study reveals for the first time that posttranscriptional rRNA modifications can be subject to regulation downstream of oncogenic signaling and demonstrate that site specific pseudouridine modifications are required to maintain the senescence program thus providing a new layer of ribosome-mediated control in safeguarding the genome against oncogenic insult.

One of the most striking findings from our study is that clusters of uridine residues within specific regions of rRNA are differentially pseudouridylated upon oncogenic insult. For decades, it has remained an outstanding question as to why specific uridine residues within rRNA are converted to pseudouridine. In eukaryotes, the selection of specific uridine residues is achieved by base pair complementary between guide H/ACA snoRNAs and the rRNA substrate and although pseudouridine residues are located within functionally

characterized regions of the ribosome, several pseudouridine residues are also located within functionally uncharacterized regions of the ribosome such as the so called rRNA expansion segments. Modeling H/ACA snoRNAs displaying co-regulated expression during senescence on the 3D structure of the ribosome reveals that Ψ modifications guided by these snoRNAs are clustered within defined regions of the ribosome. Alterations in pseudouridine levels within these regions of the ribosome could potentially influence rRNA flexibility, rRNA molecular interactions, or enhance ribosome rigidity upon oncogenic insult to promote an alternative mode of translation initiation. Previous studies from analysis of viral IRESs suggest that upon binding to IRES elements, ribosomes undergo a different conformational change that mimics changes caused by the binding of translation initiation factors (Spahn et al., 2001). Interestingly, one pseudouridine residue guided by snoRNA24, Ψ609 located within helix 18 of the small ribosomal subunit, has been shown to make direct contacts with the CrPV IRES element and also to directly interact with segments of mRNAs from 5' UTR of endogenous mRNAs (Schuler et al., 2006; Weingarten-Gabbay et al., 2016). These observations suggest that regulation of Ψ modifications within this region of the ribosome may influence translation initiation of mRNAs harboring cis-acting elements that may require direct contact with the ribosome to initiate translation. Modulating pseudouridine levels may therefore allow for ribosome-mediated regulation of specific gene expression programs upon oncogenic insult that is required to counteract cellular transformation. Indeed, our studies suggest that the regulation of snoRNA24 expression and function in RNA base modification within the ribosome is functionally important to maintain the senescence program by modulating lipid metabolism. An outstanding question that remains to be addressed is how does the chemical property of a

single pseudouridine residue influence RNA function? Although pseudouridine is thought to endow new properties to RNA such as influencing RNA stability, the precise function of pseudouridine on RNA have not been tested *in vivo*. Furthermore, our study opens up the possibility that regulation of rRNA pseudouridylation represents a new layer of post-transcriptional gene expression regulation mediated by the ribosome.

Mounting evidence suggests that ribosome harbors more than just 'housekeeping' functions within cells. In fact, an entire class of developmental disorders collectively referenced to as ribosomopathies have been described where the underlying molecular defects lies in ribosome biogenesis and function (Narla and Ebert, 2010). Emerging data demonstrate that subsets of H/ACA snoRNAs, implicated in Ψ modifications, are frequently down regulated in numerous cancers including hematological malignancies and solid cancers further supports a role for deregulation ribosome function in disease. For example, snoRNA24 is commonly found downregulated in hematological malignancies and in X-linked dyskeratosis congenita, a syndrome with high predisposition to cancer (Bellodi et al., 2013; McMahon et al., 2015). Our current findings, that snoRNA24 levels are significantly decreased in HCC specimens indicate that snoRNA24 may act as a tumor suppressor and loss of function of this snoRNA may be associated with cancer predisposition. Understanding whether HBV infection may also modulate snoRNA24 levels should be further investigated. Importantly, H/ACA snoRNAs other than snoRNA24 have also been reported to be deregulation in disease including altered expression of H/ACA snoRNAs, nucleotide deletions or substitutions with H/ACA snoRNAs and epigenetic alterations involving deletion and hypermethylation of distinct H/ACA snoRNA loci, all of which may alter the structure and hinder the ability of H/ACA snoRNAs to guide

modifications on rRNA (Bellodi et al., 2013; McMahon et al., 2015). Ultimately, our findings provide a greater understanding of how deregulation of H/ACA snoRNAs in disease may lead to cellular outcomes associated with increased cancer susceptibility and sheds new light on the role of an ancient RNA base modifications in modulating ribosome activity and cellular integrity.

References

Abramczyk, H., Surmacki, J., Kopec, M., Olejnik, A.K., Lubecka-Pietruszewska, K., and Fabianowska-Majewska, K. (2015). The role of lipid droplets and adipocytes in cancer. Raman imaging of cell cultures: MCF10A, MCF7, and MDA-MB-231 compared to adipocytes in cancerous human breast tissue. Analyst *140*, 2224-2235.

Aird, K.M., and Zhang, R. (2014). Metabolic alterations accompanying oncogene-induced senescence. Molecular & cellular oncology *1*, e963481.

Alawi, F., and Lee, M. (2007). DKC1 is an evolutionarily conserved c-Myc target. Faseb Journal *21*, A1155-A1155.

Alawi, F., and Lin, P. (2011). Dyskerin is Required for Tumor Cell Growth Through Mechanisms that are Independent of its Role in Telomerase and only Partially Related to its Function in Precursor rRNA Processing. Mol Carcinogen *50*, 334-345.

Alter, B.P., Baerlocher, G.M., Savage, S.A., Chanock, S.J., Weksler, B.B., Willner, J.P., Peters, J.A., Giri, N., and Lansdorp, P.M. (2007). Very short telomere length by flow fluorescence in situ hybridization identifies patients with dyskeratosis congenita. Blood *110*, 1439-1447.

Alter, B.P., Giri, N., Savage, S.A., Peters, J.A., Loud, J.T., Leathwood, L., Carr, A.G., Greene, M.H., and Rosenberg, P.S. (2010). Malignancies and survival patterns in the National Cancer Institute inherited bone marrow failure syndromes cohort study. British journal of haematology *150*, 179-188.

Alter, B.P., Giri, N., Savage, S.A., and Rosenberg, P.S. (2009). Cancer in dyskeratosis congenita. Blood *113*, 6549-6557.

Atzorn, V., Fragapane, P., and Kiss, T. (2004). U17/snR30 is a ubiquitous snoRNA with two conserved sequence motifs essential for 18S rRNA production. Molecular and cellular biology *24*, 1769-1778.

Bachellerie, J.P., and Cavaille, J. (1997). Guiding ribose methylation of rRNA. Trends in biochemical sciences *22*, 257-261.

Balakin, A.G., Smith, L., and Fournier, M.J. (1996). The RNA world of the nucleolus: two major families of small RNAs defined by different box elements with related functions. Cell *86*, 823-834.

Basu, A., Das, P., Chaudhuri, S., Bevilacqua, E., Andrews, J., Barik, S., Hatzoglou, M., Komar, A.A., and Mazumder, B. (2011). Requirement of rRNA methylation for 80S ribosome assembly on a cohort of cellular Internal Ribosome Entry Sites. Molecular and cellular biology.

Batista, L.F., Pech, M.F., Zhong, F.L., Nguyen, H.N., Xie, K.T., Zaug, A.J., Crary, S.M., Choi, J., Sebastiano, V., Cherry, A.*, et al.* (2011). Telomere shortening and loss of self-renewal in dyskeratosis congenita induced pluripotent stem cells. Nature *474*, 399-402.

Baudin-Baillieu, A., Fabret, C., Liang, X.H., Piekna-Przybylska, D., Fournier, M.J., and Rousset, J.P. (2009). Nucleotide modifications in three functionally important regions of the Saccharomyces cerevisiae ribosome affect translation accuracy. Nucleic acids research *37*, 7665-7677.

Baxter-Roshek, J.L., Petrov, A.N., and Dinman, J.D. (2007). Optimization of ribosome structure and function by rRNA base modification. PLoS One *2*, e174.

Bellodi, C., Kopmar, N., and Ruggero, D. (2010a). Deregulation of oncogene-induced senescence and p53 translational control in X-linked dyskeratosis congenita. EMBO J *29*, 1865-1876.

Bellodi, C., Krasnykh, O., Haynes, N., Theodoropoulou, M., Peng, G., Montanaro, L., and Ruggero, D. (2010b). Loss of function of the tumor suppressor DKC1 perturbs p27 translation control and contributes to pituitary tumorigenesis. Cancer Res *70*, 6026-6035.

Bellodi, C., McMahon, M., Contreras, A., Juliano, D., Kopmar, N., Nakamura, T., Maltby, D., Burlingame, A., Savage, S.A., Shimamura, A.*, et al.* (2013). H/ACA Small RNA Dysfunctions in Disease Reveal Key Roles for Noncoding RNA Modifications in Hematopoietic Stem Cell Differentiation. Cell Rep *3*, 1493-1502.

Beloribi-Djefaflia, S., Vasseur, S., and Guillaumond, F. (2016). Lipid metabolic reprogramming in cancer cells. Oncogenesis *5*.

Bortolin, M.L., Ganot, P., and Kiss, T. (1999). Elements essential for accumulation and function of small nucleolar RNAs directing site-specific pseudouridylation of ribosomal RNAs. The EMBO journal *18*, 457-469.

Bozza, P.T., and Viola, J.P.B. (2010). Lipid droplets in inflammation and cancer. Prostag Leukotr Ess *82*, 243-250.

Brecqueville, M., Rey, J., Devillier, R., Guille, A., Gillet, R., Adelaide, J., Gelsi-Boyer, V., Arnoulet, C., Chaffanet, M., Mozziconacci, M.J.*, et al.* (2014). Array comparative genomic hybridization and sequencing of 23 genes in 80 patients with myelofibrosis at chronic or acute phase. Haematologica *99*, 37-45.

Carlile, T.M., Rojas-Duran, M.F., Zinshteyn, B., Shin, H., Bartoli, K.M., and Gilbert, W.V. (2014). Pseudouridine profiling reveals regulated mRNA pseudouridylation in yeast and human cells. Nature *advance online publication*.

Castle, J.C., Armour, C.D., Lower, M., Haynor, D., Biery, M., Bouzek, H., Chen, R., Jackson, S., Johnson, J.M., Rohl, C.A.*, et al.* (2010). Digital genome-wide ncRNA expression, including SnoRNAs, across 11 human tissues using polyA-neutral amplification. PLoS One *5*, e11779.

Cavaille, J., Buiting, K., Kiefmann, M., Lalande, M., Brannan, C.I., Horsthemke, B., Bachellerie, J.P., Brosius, J., and Huttenhofer, A. (2000). Identification of brain-specific and imprinted small nucleolar RNA genes exhibiting an unusual genomic organization. P Natl Acad Sci USA *97*, 14311-14316.

Cerami, E., Gao, J., Dogrusoz, U., Gross, B.E., Sumer, S.O., Aksoy, B.A., Jacobsen, A., Byrne, C.J., Heuer, M.L., Larsson, E.*, et al.* (2012). The cBio cancer genomics portal: an open platform for exploring multidimensional cancer genomics data. Cancer Discov *2*, 401-404.

Charette, M., and Gray, M.W. (2000). Pseudouridine in RNA: what, where, how, and why. IUBMB Life *49*, 341-351.

Collado, M., and Serrano, M. (2010). Senescence in tumours: evidence from mice and humans. Nat Rev Cancer *10*, 51-57.

Darzacq, X., Jady, B.E., Verheggen, C., Kiss, A.M., Bertrand, E., and Kiss, T. (2002). Cajal body-specific small nuclear RNAs: a novel class of 2'-O-methylation and pseudouridylation guide RNAs. The EMBO journal *21*, 2746-2756.

Darzacq, X., Kittur, N., Roy, S., Shav-Tal, Y., Singer, R.H., and Meier, U.T. (2006). Stepwise RNP assembly at the site of H/ACA RNA transcription in human cells. Journal of Cell Biology *173*, 207-218.

Davis, F.F., and Allen, F.W. (1957). Ribonucleic acids from yeast which contain a fifth nucleotide. The Journal of biological chemistry *227*, 907-915.

de Gonzalo-Calvo, D., Lopez-Vilaro, L., Nasarre, L., Perez-Olabarria, M., Vazquez, T., Escuin, D., Badimon, L., Barnadas, A., Lerma, E., and Llorente-Cortes, V. (2015). Intratumor cholesteryl ester accumulation is associated with human breast cancer proliferation and aggressive potential: a molecular and clinicopathological study. Bmc Cancer *15*.

Debacq-Chainiaux, F., Erusalimsky, J.D., Campisi, J., and Toussaint, O. (2009). Protocols to detect senescence-associated beta-galactosidase (SA-betagal) activity, a biomarker of senescent cells in culture and in vivo. Nat Protoc *4*, 1798-1806.

Decatur, W.A., and Fournier, M.J. (2002). rRNA modifications and ribosome function. Trends in biochemical sciences *27*, 344-351.

Denman, R.B. (1993). Using RNAFOLD to predict the activity of small catalytic RNAs. Biotechniques *15*, 1090-1095.

di Fagagna, F.D. (2008). Living on a break: cellular senescence as a DNA-damage response. Nature Reviews Cancer *8*, 512-522.

Di Micco, R., Fumagalli, M., Cicalese, A., Piccinin, S., Gasparini, P., Luise, C., Schurra, C., Garre, M., Nuciforo, P.G., Bensimon, A.*, et al.* (2006). Oncogene-induced senescence is a DNA damage response triggered by DNA hyper-replication. Nature *444*, 638-642.

Dieci, G., Preti, M., and Montanini, B. (2009). Eukaryotic snoRNAs: a paradigm for gene expression flexibility. Genomics *94*, 83-88.

Dokal, I. (2000). Dyskeratosis congenita in all its forms. Br J Haematol *110*, 768-779.

Dokal, I. (2011). Dyskeratosis congenita. Hematology / the Education Program of the American Society of Hematology American Society of Hematology Education Program *2011*, 480-486.

Duan, J., Li, L., Lu, J., Wang, W., and Ye, K. (2009). Structural mechanism of substrate RNA recruitment in H/ACA RNA-guided pseudouridine synthase. Molecular cell *34*, 427-439.

Ender, C., Krek, A., Friedlander, M.R., Beitzinger, M., Weinmann, L., Chen, W., Pfeffer, S., Rajewsky, N., and Meister, G. (2008). A human snoRNA with microRNA-like functions. Molecular cell *32*, 519-528.

Esteller, M. (2011). Non-coding RNAs in human disease. Nat Rev Genet *12*, 861-874.

Fernandez, I.S., Ng, C.L., Kelley, A.C., Wu, G., Yu, Y.T., and Ramakrishnan, V. (2013). Unusual base pairing during the decoding of a stop codon by the ribosome. Nature *500*, 107-110.

Ferreira, H.J., Heyn, H., Moutinho, C., and Esteller, M. (2012). CpG island hypermethylation-associated silencing of small nucleolar RNAs in human cancer. RNA biology *9*, 881-890.

Filipowicz, W., and Pogacic, V. (2002). Biogenesis of small nucleolar ribonucleoproteins. Curr Opin Cell Biol *14*, 319-327.

Forbes, S.A., Bindal, N., Bamford, S., Cole, C., Kok, C.Y., Beare, D., Jia, M., Shepherd, R., Leung, K., Menzies, A.*, et al.* (2011). COSMIC: mining complete cancer genomes in the Catalogue of Somatic Mutations in Cancer. Nucleic acids research *39*, D945-950.

Ganot, P., Bortolin, M.L., and Kiss, T. (1997a). Site-specific pseudouridine formation in preribosomal RNA is guided by small nucleolar RNAs. Cell *89*, 799-809.

Ganot, P., Caizergues-Ferrer, M., and Kiss, T. (1997b). The family of box ACA small nucleolar RNAs is defined by an evolutionarily conserved secondary structure and ubiquitous sequence elements essential for RNA accumulation. Gene Dev *11*, 941-956.

Grozdanov, P.N., Roy, S., Kittur, N., and Meier, U.T. (2009). SHQ1 is required prior to NAF1 for assembly of H/ACA small nucleolar and telomerase RNPs. Rna-a Publication of the Rna Society *15*, 1188-1197.

Gu, A.D., Zhou, H., Yu, C.H., and Qu, L.H. (2005). A novel experimental approach for systematic identification of box H/ACA snoRNAs from eukaryotes. Nucleic acids research *33*, e194.

Gu, B.W., Bessler, M., and Mason, P.J. (2008). A pathogenic dyskerin mutation impairs proliferation and activates a DNA damage response independent of telomere length in mice. Proc Natl Acad Sci U S A *105*, 10173-10178.

Hamma, T., and Ferre-D'Amare, A.R. (2010). The box H/ACA ribonucleoprotein complex: interplay of RNA and protein structures in post-transcriptional RNA modification. The Journal of biological chemistry *285*, 805-809.

Hamma, T., Reichow, S.L., Varani, G., and Ferre-D'Amare, A.R. (2005). The Cbf5-Nop10 complex is a molecular bracket that organizes box H/ACA RNPs. Nat Struct Mol Biol *12*, 1101-1107.

Hao, K., Lamb, J., Zhang, C.S., Xie, T., Wang, K., Zhang, B., Chudin, E., Lee, N.P., Mao, M., Zhong, H.*, et al.* (2011). Clinicopathologic and gene expression parameters predict liver cancer prognosis. Bmc Cancer *11*.

Hashem, Y., Georges, A.D., Dhote, V., Langlois, R., Liao, H.Y., Grassucci, R.A., Hellen, C.U.T., Pestova, T.V., and Frank, J. (2013). Structure of the Mammalian Ribosomal 43S Preinitiation Complex Bound to the Scanning Factor DHX29. Cell *153*, 1108-1119.

He, J., Navarrete, S., Jasinski, M., Vulliamy, T., Dokal, I., Bessler, M., and Mason, P.J. (2002). Targeted disruption of Dkc1, the gene mutated in X-linked dyskeratosis congenita, causes embryonic lethality in mice. Oncogene *21*, 7740-7744.

Heiss, N.S., Knight, S.W., Vulliamy, T.J., Klauck, S.M., Wiemann, S., Mason, P.J., Poustka, A., and Dokal, I. (1998). X-linked dyskeratosis congenita is caused by mutations in a highly conserved gene with putative nucleolar functions. Nat Genet *19*, 32-38.

Hellen, C.U., and Sarnow, P. (2001). Internal ribosome entry sites in eukaryotic mRNA molecules. Genes Dev *15*, 1593-1612.

Hilcenko, C., Simpson, P.J., Finch, A.J., Bowler, F.R., Churcher, M.J., Jin, L., Packman, L.C., Shlien, A., Campbell, P., Kirwan, M.*, et al.* (2012). Aberrant 3' oligoadenylation of spliceosomal U6 small nuclear RNA in poikiloderma with neutropenia. Blood.

Holcik, M., and Sonenberg, N. (2005). Translational control in stress and apoptosis. Nat Rev Mol Cell Biol *6*, 318-327.

Jack, K., Bellodi, C., Landry, D.M., Niederer, R.O., Meskauskas, A., Musalgaonkar, S., Kopmar, N., Krasnykh, O., Dean, A.M., Thompson, S.R.*, et al.* (2011). rRNA Pseudouridylation Defects Affect Ribosomal Ligand Binding and Translational Fidelity from Yeast to Human Cells. Molecular cell *44*, 660-666.

Jady, B.E., Ketele, A., and Kiss, T. (2012). Human intron-encoded Alu RNAs are processed and packaged into Wdr79-associated nucleoplasmic box H/ACA RNPs. Gene Dev *26*, 1897-1910.

Jang, S.K., Krausslich, H.G., Nicklin, M.J., Duke, G.M., Palmenberg, A.C., and Wimmer, E. (1988). A segment of the 5' nontranslated region of encephalomyocarditis virus RNA directs internal entry of ribosomes during in vitro translation. Journal of virology *62*, 2636-2643.

Jiang, W., Middleton, K., Yoon, H.J., Fouquet, C., and Carbon, J. (1993). An essential yeast protein, CBF5p, binds in vitro to centromeres and microtubules. Molecular and cellular biology *13*, 4884-4893.

Kang, T.W., Yevsa, T., Woller, N., Hoenicke, L., Wuestefeld, T., Dauch, D., Hohmeyer, A., Gereke, M., Rudalska, R., Potapova, A.*, et al.* (2011). Senescence surveillance of pre-malignant hepatocytes limits liver cancer development. Nature *479*, 547-551.

Karijolich, J., Kantartzis, A., and Yu, Y.T. (2010). Quantitative Analysis of RNA Modifications. Methods Mol Biol *629*, 21-32.

Karijolich, J., and Yu, Y.T. (2011). Converting nonsense codons into sense codons by targeted pseudouridylation. Nature *474*, 395-398.

Kierzek, E., Malgowska, M., Lisowiec, J., Turner, D.H., Gdaniec, Z., and Kierzek, R. (2014). The contribution of pseudouridine to stabilities and structure of RNAs. Nucleic acids research *42*, 3492-3501.

King, T.H., Liu, B., McCully, R.R., and Fournier, M.J. (2003). Ribosome structure and activity are altered in cells lacking snoRNPs that form pseudouridines in the peptidyl transferase center. Molecular cell *11*, 425-435.

Kirwan, M., and Dokal, I. (2008). Dyskeratosis congenita: a genetic disorder of many faces. Clin Genet *73*, 103-112.

Kishore, S., Gruber, A.R., Jedlinski, D.J., Syed, A.P., Jorjani, H., and Zavolan, M. (2013). Insights into snoRNA biogenesis and processing from PAR-CLIP of snoRNA core proteins and small RNA sequencing. Genome Biology *14*.

Kiss, A.M., Jady, B.E., Bertrand, E., and Kiss, T. (2004). Human box H/ACA pseudouridylation guide RNA machinery. Mol Cell Biol *24*, 5797-5807.

Kiss, T. (2001). Small nucleolar RNA-guided post-transcriptional modification of cellular RNAs. The EMBO journal *20*, 3617-3622.

Kiss, T. (2002). Small nucleolar RNAs: an abundant group of noncoding RNAs with diverse cellular functions. Cell *109*, 145-148.

Kiss, T., Fayet, E., Jady, B.E., Richard, P., and Weber, M. (2006). Biogenesis and intranuclear trafficking of human box C/D and H/ACA RNPs. Cold Spring Harbor symposia on quantitative biology *71*, 407-417.

Kiss, T., and Filipowicz, W. (1995). Exonucleolytic processing of small nucleolar RNAs from pre-mRNA introns. Gene Dev *9*, 1411-1424.

Kiss-Laszlo, Z., Henry, Y., Bachellerie, J.P., Caizergues-Ferrer, M., and Kiss, T. (1996). Site-specific ribose methylation of preribosomal RNA: a novel function for small nucleolar RNAs. Cell *85*, 1077-1088.

Knight, S.W., Heiss, N.S., Vulliamy, T.J., Aalfs, C.M., McMahon, C., Richmond, P., Jones, A., Hennekam, R.C., Poustka, A., Mason, P.J.*, et al.* (1999). Unexplained aplastic anaemia, immunodeficiency, and cerebellar hypoplasia (Hoyeraal-Hreidarsson syndrome) due to mutations in the dyskeratosis congenita gene, DKC1. Br J Haematol *107*, 335-339.

Knight, S.W., Vulliamy, T.J., Morgan, B., Devriendt, K., Mason, P.J., and Dokal, I. (2001). Identification of novel DKC1 mutations in patients with dyskeratosis congenita: implications for pathophysiology and diagnosis. Hum Genet *108*, 299-303.

Lafontaine, D.L., Bousquet-Antonelli, C., Henry, Y., Caizergues-Ferrer, M., and Tollervey, D. (1998). The box H + ACA snoRNAs carry Cbf5p, the putative rRNA pseudouridine synthase. Gene Dev *12*, 527-537.

Lane, B.G., Ofengand, J., and Gray, M.W. (1995). Pseudouridine and O2'-methylated nucleosides. Significance of their selective occurrence in rRNA domains that function in ribosome-catalyzed synthesis of the peptide bonds in proteins. Biochimie *77*, 7-15.

Lawrence, M.S., Stojanov, P., Mermel, C.H., Robinson, J.T., Garraway, L.A., Golub, T.R., Meyerson, M., Gabriel, S.B., Lander, E.S., and Getz, G. (2014). Discovery and saturation analysis of cancer genes across 21 tumour types. Nature *505*, 495-501.

Lestrade, L., and Weber, M.J. (2006). snoRNA-LBME-db, a comprehensive database of human H/ACA and C/D box snoRNAs. Nucleic acids research *34*, D158-162.

Lewis, S.M., and Holcik, M. (2005). IRES in distress: translational regulation of the inhibitor of apoptosis proteins XIAP and HIAP2 during cell stress. Cell Death Differ *12*, 547-553.

Li, L., and Ye, K. (2006). Crystal structure of an H/ACA box ribonucleoprotein particle. Nature *443*, 302-307.

Liao, J.P., Yu, L., Mei, Y.P., Guarnera, M., Shen, J., Li, R.Y., Liu, Z.Q., and Jiang, F. (2010). Small nucleolar RNA signatures as biomarkers for non-small-cell lung cancer. Mol Cancer *9*.

Listenberger, L.L., and Brown, D.A. (2007). Fluorescent detection of lipid droplets and associated proteins. Curr Protoc Cell Biol *Chapter 24*, Unit 24 22.

Loayza-Puch, F., Drost, J., Rooijers, K., Lopes, R., Elkon, R., and Agami, R. (2013). p53 induces transcriptional and translational programs to suppress cell proliferation and growth. Genome Biology *14*.

Maden, B.E. (1990). The numerous modified nucleotides in eukaryotic ribosomal RNA. Prog Nucleic Acid Res Mol Biol *39*, 241-303.

Marcel, V., Ghayad, S.E., Belin, S., Therizols, G., Morel, A.P., Solano-Gonzalez, E., Vendrell, J.A., Hacot, S., Mertani, H.C., Albaret, M.A.*, et al.* (2013). p53 Acts as a Safeguard of Translational Control by Regulating Fibrillarin and rRNA Methylation in Cancer. Cancer Cell *24*, 318-330.

Martens-Uzunova, E.S., Jalava, S.E., Dits, N.F., van Leenders, G.J., Moller, S., Trapman, J., Bangma, C.H., Litman, T., Visakorpi, T., and Jenster, G. (2012). Diagnostic and prognostic signatures from the small non-coding RNA transcriptome in prostate cancer. Oncogene *31*, 978-991.

Matera, A.G., Terns, R.M., and Terns, M.P. (2007). Non-coding RNAs: lessons from the small nuclear and small nucleolar RNAs. Nature reviews Molecular cell biology *8*, 209-220.

Maxwell, E.S., and Fournier, M.J. (1995). The small nucleolar RNAs. Annual review of biochemistry *64*, 897-934.

McMahon, M., Bellodi, C., and Ruggero, D. (2013). The ‚ÄúFifth‚Äù RNA Nucleotide: A Role for Ribosomal RNA Pseudouridylation in Control of Gene Expression at the Translational Level. In Biophysical approaches to translational control of gene expression, J.D. Dinman, ed. (Springer New York), pp. 253-288.

McMahon, M., Contreras, A., and Ruggero, D. (2015). Small RNAs with big implications: new insights into H/ACA snoRNA function and their role in human disease. Wires Rna *6*, 173-189.

Mei, Y.P., Liao, J.P., Shen, J., Yu, L., Liu, B.L., Liu, L., Li, R.Y., Ji, L., Dorsey, S.G., Jiang, Z.R.*, et al.* (2012). Small nucleolar RNA 42 acts as an oncogene in lung tumorigenesis. Oncogene *31*, 2794-2804.

Meier, U.T. (2005). The many facets of H/ACA ribonucleoproteins. Chromosoma *114*, 1-14.

Meier, U.T. (2006). How a single protein complex accommodates many different H/ACA RNAs. Trends Biochem Sci *31*, 311-315.

Mitchell, J.R., Wood, E., and Collins, K. (1999). A telomerase component is defective in the human disease dyskeratosis congenita. Nature *402*, 551-555.

Montanaro, L. (2010). Dyskerin and cancer: more than telomerase. The defect in mRNA translation helps in explaining how a proliferative defect leads to cancer. The Journal of pathology *222*, 345-349.

Montanaro, L., Brigotti, M., Clohessy, J., Barbieri, S., Ceccarelli, C., Santini, D., Taffurelli, M., Calienni, M., Teruya-Feldstein, J., Trere, D.*, et al.* (2006). Dyskerin expression influences the level of ribosomal RNA pseudo-uridylation and telomerase RNA component in human breast cancer. J Pathol *210*, 10-18.

Montanaro, L., Calienni, M., Bertoni, S., Rocchi, L., Sansone, P., Storci, G., Santini, D., Ceccarelli, C., Taffurelli, M., Carnicelli, D., *et al.* (2010a). Novel dyskerin-mediated mechanism of p53 inactivation through defective mRNA translation. Cancer research *70*, 4767-4777.

Montanaro, L., Calienni, M., Bertoni, S., Rocchi, L., Sansone, P., Storci, G., Santini, D., Ceccarelli, C., Taffurelli, M., Carnicelli, D., *et al.* (2010b). Novel dyskerin-mediated mechanism of p53 inactivation through defective mRNA translation. Cancer Res *70*, 4767-4777.

Morrissey, J.P., and Tollervey, D. (1993). Yeast snR30 is a small nucleolar RNA required for 18S rRNA synthesis. Molecular and cellular biology *13*, 2469-2477.

Mroczek, S., Krwawicz, J., Kutner, J., Lazniewski, M., Kucinski, I., Ginalski, K., and Dziembowski, A. (2012). C16orf57, a gene mutated in poikiloderma with neutropenia, encodes a putative phosphodiesterase responsible for the U6 snRNA 3' end modification. Gene Dev *26*, 1911-1925.

Narla, A., and Ebert, B.L. (2010). Ribosomopathies: human disorders of ribosome dysfunction. Blood *115*, 3196-3205.

Newby, M.I., and Greenbaum, N.L. (2002). Investigation of Overhauser effects between pseudouridine and water protons in RNA helices. P Natl Acad Sci USA *99*, 12697-12702.

Newton, K., Petfalski, E., Tollervey, D., and Caceres, J.F. (2003). Fibrillarin is essential for early development and required for accumulation of an intron-encoded small nucleolar RNA in the mouse. Molecular and cellular biology *23*, 8519-8527.

Ni, J., Tien, A.L., and Fournier, M.J. (1997). Small nucleolar RNAs direct site-specific synthesis of pseudouridine in ribosomal RNA. Cell *89*, 565-573.

Ofengand, J. (2002). Ribosomal RNA pseudouridines and pseudouridine synthases. FEBS letters *514*, 17-25.

Pelletier, J., and Sonenberg, N. (1988). Internal initiation of translation of eukaryotic mRNA directed by a sequence derived from poliovirus RNA. Nature *334*, 320-325.

Perez-Mancera, P.A., Young, A.R.J., and Narita, M. (2014). Inside and out: the activities of senescence in cancer. Nature Reviews Cancer *14*, 547-558.

Piekna-Przybylska, D., Decatur, W.A., and Fournier, M.J. (2008). The 3D rRNA modification maps database: with interactive tools for ribosome analysis. Nucleic acids research *36*, D178-183.

Quijano, C., Cao, L., Fergusson, M.M., Romero, H., Liu, J., Gutkind, S., Rovira, I.I., Mohney, R.P., Karoly, E.D., and Finkel, T. (2012). Oncogene-induced senescence results in marked metabolic and bioenergetic alterations. Cell Cycle *11*, 1383-1392.

Rashid, R., Liang, B., Baker, D.L., Youssef, O.A., He, Y., Phipps, K., Terns, R.M., Terns, M.P., and Li, H. (2006). Crystal structure of a Cbf5-Nop10-Gar1 complex and implications in RNA-guided pseudouridylation and dyskeratosis congenita. Molecular cell *21*, 249-260.

Reichow, S.L., Hamma, T., Ferre-D'Amare, A.R., and Varani, G. (2007). The structure and function of small nucleolar ribonucleoproteins. Nucleic acids research *35*, 1452-1464.

Richard, P., Kiss, A.M., Darzacq, X., and Kiss, T. (2006). Cotranscriptional recognition of human intronic box H/ACA snoRNAs occurs in a splicing-independent manner. Molecular and cellular biology *26*, 2540-2549.

Ronchetti, D., Mosca, L., Cutrona, G., Tuana, G., Gentile, M., Fabris, S., Agnelli, L., Ciceri, G., Matis, S., Massucco, C.*, et al.* (2013). Small nucleolar RNAs as new biomarkers in chronic lymphocytic leukemia. Bmc Med Genomics *6*.

Ronchetti, D., Todoerti, K., Tuana, G., Agnelli, L., Mosca, L., Lionetti, M., Fabris, S., Colapietro, P., Miozzo, M., Ferrarini, M.*, et al.* (2012). The expression pattern of small nucleolar and small Cajal body-specific RNAs characterizes distinct molecular subtypes of multiple myeloma. Blood Cancer J *2*, e96.

Salowsky, R., Heiss, N.S., Benner, A., Wittig, R., and Poustka, A. (2002). Basal transcription activity of the dyskeratosis congenita gene is mediated by Sp1 and Sp3 and a patient mutation in a Sp1 binding site is associated with decreased promoter activity. Gene *293*, 9-19.

Santos, C.R., and Schulze, A. (2012). Lipid metabolism in cancer. Febs Journal *279*, 2610-2623.

Schattner, P., Barberan-Soler, S., and Lowe, T.M. (2006). A computational screen for mammalian pseudouridylation guide H/ACA RNAs. RNA *12*, 15-25.

Schubert, T., Pusch, M.C., Diermeier, S., Benes, V., Kremmer, E., Imhof, A., and Langst, G. (2012). Df31 protein and snoRNAs maintain accessible higher-order structures of chromatin. Molecular cell *48*, 434-444.

Schuler, M., Connell, S.R., Lescoute, A., Giesebrecht, J., Dabrowski, M., Schroeer, B., Mielke, T., Penczek, P.A., Westhof, E., and Spahn, C.M.T. (2006). Structure of the ribosome-bound cricket paralysis virus IRES RNA. Nat Struct Mol Biol *13*, 1092-1096.

Schwartz, S., Bernstein, D.A., Mumbach, M.R., Jovanovic, M., Herbst, R.H., Le√≥n-Ricardo, B.X., Engreitz, J.M., Guttman, M., Satija, R., Lander, E.S.*, et al.* Transcriptome-wide Mapping Reveals Widespread Dynamic-Regulated Pseudouridylation of ncRNA and mRNA. Cell.

Scott, M.S., Avolio, F., Ono, M., Lamond, A.I., and Barton, G.J. (2009). Human miRNA precursors with box H/ACA snoRNA features. PLoS Comput Biol *5*, e1000507.

Sims, R.J., Rojas, L.A., Beck, D., Bonasio, R., Schuller, R., Drury, W.J., Eick, D., and Reinberg, D. (2011). The C-Terminal Domain of RNA Polymerase II Is Modified by Site-Specific Methylation. Science *332*, 99-103.

Spahn, C.M., Kieft, J.S., Grassucci, R.A., Penczek, P.A., Zhou, K., Doudna, J.A., and Frank, J. (2001). Hepatitis C virus IRES RNA-induced changes in the conformation of the 40s ribosomal subunit. Science *291*, 1959-1962.

Stumpf, C.R., Moreno, M.V., Olshen, A.B., Taylor, B.S., and Ruggero, D. (2013). The Translational Landscape of the Mammalian Cell Cycle. Molecular Cell *52*, 574-582.

Sumita, M., Desaulniers, J.P., Chang, Y.C., Chui, H.M., Clos, L., 2nd, and Chow, C.S. (2005). Effects of nucleotide substitution and modification on the stability and structure of helix 69 from 28S rRNA. RNA *11*, 1420-1429.

Taft, R.J., Glazov, E.A., Lassmann, T., Hayashizaki, Y., Carninci, P., and Mattick, J.S. (2009). Small RNAs derived from snoRNAs. RNA *15*, 1233-1240.

Taft, R.J., Pang, K.C., Mercer, T.R., Dinger, M., and Mattick, J.S. (2010). Non-coding RNAs: regulators of disease. The Journal of pathology *220*, 126-139.

Taylor, B.S., Schultz, N., Hieronymus, H., Gopalan, A., Xiao, Y., Carver, B.S., Arora, V.K., Kaushik, P., Cerami, E., Reva, B*., et al.* (2010). Integrative genomic profiling of human prostate cancer. Cancer Cell *18*, 11-22.

Teittinen, K.J., Laiho, A., Uusimaki, A., Pursiheimo, J.P., Gyenesei, A., and Lohi, O. (2012). Expression of small nucleolar RNAs in leukemic cells. Cell Oncol (Dordr).

Terns, M., and Terns, R. (2006). Noncoding RNAs of the H/ACA family. Cold Spring Harbor symposia on quantitative biology *71*, 395-405.

Terns, M.P., and Terns, R.M. (2002). Small nucleolar RNAs: versatile trans-acting molecules of ancient evolutionary origin. Gene Expr *10*, 17-39.

Tollervey, D., Lehtonen, H., Carmo-Fonseca, M., and Hurt, E.C. (1991). The small nucleolar RNP protein NOP1 (fibrillarin) is required for pre-rRNA processing in yeast. The EMBO journal *10*, 573-583.

Tyc, K., and Steitz, J.A. (1989). U3, U8 and U13 comprise a new class of mammalian snRNPs localized in the cell nucleolus. The EMBO journal *8*, 3113-3119.

Valleron, W., Laprevotte, E., Gautier, E.F., Quelen, C., Demur, C., Delabesse, E., Agirre, X., Prosper, F., Kiss, T., and Brousset, P. (2012a). Specific small nucleolar RNA expression profiles in acute leukemia. Leukemia : official journal of the Leukemia Society of America, Leukemia Research Fund, UK *26*, 2052-2060.

Valleron, W., Ysebaert, L., Berquet, L., Fataccioli, V., Quelen, C., Martin, A., Parrens, M., Lamant, L., de Leval, L., Gisselbrecht, C.*, et al.* (2012b). Small nucleolar RNA expression profiling identifies potential prognostic markers in peripheral T-cell lymphoma. Blood *120*, 3997-4005.

van Riggelen, J., Yetil, A., and Felsher, D.W. (2010). MYC as a regulator of ribosome biogenesis and protein synthesis. Nature Reviews Cancer *10*, 301-309.

Vitali, P., Royo, H., Seitz, H., Bachellerie, J.P., Huttenhofer, A., and Cavaille, J. (2003). Identification of 13 novel human modification guide RNAs. Nucleic acids research *31*, 6543-6551.

Vulliamy, T., Beswick, R., Kirwan, M., Marrone, A., Digweed, M., Walne, A., and Dokal, I. (2008). Mutations in the telomerase component NHP2 cause the premature ageing syndrome dyskeratosis congenita. Proc Natl Acad Sci U S A *105*, 8073-8078.

Walbott, H., Machado-Pinilla, R., Liger, D., Blaud, M., Rety, S., Grozdanov, P.N., Godin, K., van Tilbeurgh, H., Varani, G., Meier, U.T.*, et al.* (2011). The H/ACA RNP assembly factor SHQ1 functions as an RNA mimic. Gene Dev *25*, 2398-2408.

Walne, A.J., Vulliamy, T., Beswick, R., Kirwan, M., and Dokal, I. (2010). Mutations in C16orf57 and normal-length telomeres unify a subset of patients with dyskeratosis congenita, poikiloderma with neutropenia and Rothmund-Thomson syndrome. Human molecular genetics *19*, 4453-4461.

Walne, A.J., Vulliamy, T., Marrone, A., Beswick, R., Kirwan, M., Masunari, Y., Al-Qurashi, F.H., Aljurf, M., and Dokal, I. (2007). Genetic heterogeneity in autosomal recessive dyskeratosis congenita with one subtype due to mutations in the telomerase-associated protein NOP10. Human Molecular Genetics *16*, 1619-1629.

Watkins, N.J., and Bohnsack, M.T. (2012). The box C/D and H/ACA snoRNPs: key players in the modification, processing and the dynamic folding of ribosomal RNA. Wiley Interdiscip Rev RNA *3*, 397-414.

Watkins, N.J., Gottschalk, A., Neubauer, G., Kastner, B., Fabrizio, P., Mann, M., and Luhrmann, R. (1998). Cbf5p, a potential pseudouridine synthase, and Nhp2p, a putative RNA-binding protein, are present together with Gar1p in all H BOX/ACA-motif snoRNPs and constitute a common bipartite structure. RNA *4*, 1549-1568.

Watkins, N.J., Segault, V., Charpentier, B., Nottrott, S., Fabrizio, P., Bachi, A., Wilm, M., Rosbash, M., Branlant, C., and Luhrmann, R. (2000). A common core RNP structure shared between the small nucleoar box C/D RNPs and the spliceosomal U4 snRNP. Cell *103*, 457-466.

Weingarten-Gabbay, S., Elias-Kirma, S., Nir, R., Gritsenko, A.A., Stern-Ginossar, N., Yakhini, Z., Weinberger, A., and Segal, E. (2016). Systematic discovery of cap-independent translation sequences in human and viral genomes. Science *351*, 240-U144.

Williams, G.T., and Farzaneh, F. (2012). Are snoRNAs and snoRNA host genes new players in cancer? Nature reviews Cancer *12*, 84-88.

Xue, S.F., and Barna, M. (2012). Specialized ribosomes: a new frontier in gene regulation and organismal biology. Nat Rev Mol Cell Bio *13*, 355-369.

Yarian, C.S., Basti, M.M., Cain, R.J., Ansari, G., Guenther, R.H., Sochacka, E., Czerwinska, G., Malkiewicz, A., and Agris, P.F. (1999). Structural and functional roles of the N1- and N3-protons of psi at tRNA's position 39. Nucleic acids research *27*, 3543-3549.

Yeh, M.M., Liu, Y.J., and Torbenson, M. (2015). Steatohepatitic variant of hepatocellular carcinoma in the absence of metabolic syndrome or background steatosis: a clinical, pathological, and genetic study. Hum Pathol *46*, 1769-1775.

Yip, S., Butterfield, Y.S., Morozova, O., Chittaranjan, S., Blough, M.D., An, J., Birol, I., Chesnelong, C., Chiu, R., Chuah, E.*, et al.* (2012). Concurrent CIC mutations, IDH mutations, and 1p/19q loss distinguish oligodendrogliomas from other cancers. The Journal of pathology *226*, 7-16.

Yoon, A., Peng, G., Brandenburger, Y., Zollo, O., Xu, W., Rego, E., and Ruggero, D. (2006). Impaired control of IRES-mediated translation in X-linked dyskeratosis congenita. Science *312*, 902-906.

Yue, S.H., Li, J.J., Lee, S.Y., Lee, H.J., Shao, T., Song, B., Cheng, L., Masterson, T.A., Liu, X.Q., Ratliff, T.L.*, et al.* (2014). Cholesteryl Ester Accumulation Induced by PTEN Loss and PI3K/AKT Activation Underlies Human Prostate Cancer Aggressiveness. Cell Metab *19*, 393-406.

Zebarjadian, Y., King, T., Fournier, M.J., Clarke, L., and Carbon, J. (1999). Point mutations in yeast CBF5 can abolish in vivo pseudouridylation of rRNA. Molecular and cellular biology *19*, 7461-7472.

Zhong, F., Savage, S.A., Shkreli, M., Giri, N., Jessop, L., Myers, T., Chen, R., Alter, B.P., and Artandi, S.E. (2011). Disruption of telomerase trafficking by TCAB1 mutation causes dyskeratosis congenita. Gene Dev *25*, 11-16.

Publishing Agreement

It is the policy of the University to encourage the distribution of all theses, dissertations, and manuscripts. Copies of all UCSF theses, dissertations, and manuscripts will be routed to the library via the Graduate Division. The library will make all theses, dissertations, and manuscripts accessible to the public and will preserve these to the best of their abilities, in perpetuity.

I hereby grant permission to the Graduate Division of the University of California, San Francisco to release copies of my thesis, dissertation, or manuscript to the Campus Library to provide access and preservation, in whole or in part, in perpetuity.

Author Signature 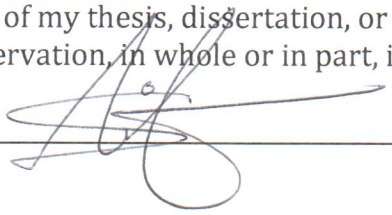 Date 12-27-16